Proceedings of the Mini-Workshop

Few-Quark Problems

Bled, Slovenia, July 8–15, 2000

Edited by

Bojan Golli[1,2]
Mitja Rosina[1,2]
Simon Širca[1,3]

[1] *University of Ljubljana,* [2] *J. Stefan Institute*
[3] *Massachusetts Institute of Technology*

The Mini-Workshop *Few-Quark Problems*

was organized by

Jožef Stefan Institute, Ljubljana

Department of Physics, Faculty of Mathematics and Physics, University of Ljubljana

and sponsored by

Ministry of Science and Technology of Slovenia

Ministry of Education and Sport of Slovenia

Department of Physics, Faculty of Mathematics and Physics, University of Ljubljana

Society of Mathematicians, Physicists and Astronomers of Slovenia

Organizing Committee

Mitja Rosina
Bojan Golli
Simon Širca

List of participants

Enrique Ruiz Arriola, Granada, `earriola@ugr.es`
Michael Birse, Manchester, `mike.birse@man.ac.uk`
Wojciech Broniowski, Krakow, `broniows@solaris.ifj.edu.pl`
Thomas Cohen, Maryland, `cohen@physics.umd.edu`
Manuel Fiolhais, Coimbra, `tmanuel@hydra.ci.uc.pt`
Yoshikazu Fujiwara, Kyoto, `fujiwara@ruby.scphys.kyoto-u.ac.jp`
Leonid Glozman, Graz, `lyg@physik.kfunigraz.ac.at`
Michio Kohno, Kitakyushu, `kohno@kyu-dent.ac.jp`
Vladimir Kukulin, Moscow, `kukulin@nucl-th.npi.msu.su`
Judith McGovern, Manchester, `judith.mcgovern@man.ac.uk`
Dubravko Klabučar, Zagreb, `klabucar@phy.hr`
Steven Moszkowski, Los Angeles, `stevemos@ucla.edu`
Zoltan Papp, Debrecen, `pz@indigo.atomki.hu`
Willibald Plessas, Graz, `plessas@bkfug.kfunigraz.ac.at`
Jean Marc Richard, Grenoble, `jean-marc.richard@isn.in2p3.fr`
Georges Ripka, Saclay, `ripka@amoco.saclay.cea.fr`
Floarea Stancu, Liege, `fstancu@ulg.ac.be`
Bojan Golli, Ljubljana, `bojan.golli@ijs.si`
Damjan Janc, Ljubljana, `domen.car@siol.net`
Mitja Rosina, Ljubljana, `mitja.rosina@ijs.si`

Electronic edition

`http://www-f1.ijs.si/Bled2000/`

Contents

Preface

The encouragement for the mini-workshops at Bled came from the fruitful and friendly encounter at the first, 1987 workshop *Mesonic Degrees of Freedom in Hadrons* held at Bled and in Ljubljana, and from the successes of other mini-workshops organized at Bled so far. We intend to organize Workshops of a similar character every year.

It is now for the fourth time that a small group of enthusiasts met in this renowned holiday resort to clarify several open problems of common interest. The topics of this meeting ranged from few-quark problems, baryon spectra, dimesons, baryon-baryon interactions, decaying states to solitons and hadronic matter. The participants enjoyed a focused, intense discussion and critical confrontation of their results and ideas in a friendly atmosphere. Every participant had up to one hour time for his exposition which could be interrupted by questions and remarks, plus half an hour of general discussion. The advantage of such mini-workshops is the ease with which the participants sincerely acknowledge not only the successes, but also the weak points and open problems in their research.

The mini-workshop took place in Villa Plemelj, bequeathed to the Society of Mathematicians, Physicists and Astronomers by the renowned Slovenian mathematician Josip Plemelj. The beautiful environment of Lake Bled helped a lot to the cheerful atmosphere and optimism in the presentations; however, the inclement weather contributed to the patience for long afternoon free discussions.

We encouraged the participants to submit a four-page (A4) version of their presentation or comments for the Proceedings which were initially intended to appear in the electronic form only, but the participants liked the idea of a printed version too. Two participants, however, brought their talk with them to Bled and as a reward it is included unabridged. We did our best and will hopefully soon see these proceedings grow into a full-fledged serial publication.

Ljubljana, November 2000   *M. Rosina*
                                                                 B. Golli
                                                                 S. Širca

Previous workshops organized at Bled

▷ What Comes beyond the Standard Model (June 29–July 9, 1998)
▷ Hadrons as Solitons (July 6-17, 1999)
▷ What Comes beyond the Standard Model (July 22–31, 1999)
▷ Few-Quark Problems (July 8-15, 2000)
▷ What Comes beyond the Standard Model (July 17–31, 2000)
▷ Statistical Mechanics of Complex Systems (August 27–September 2, 2000)

Published proceedings

▷ Proceedings to the international workshop on *What comes beyond the standard model*, Eds. N. Mankoč Borštnik, H. B. Nielsen, C. Froggatt, Bled, Slovenia, June 29–July 9, 1998 (Bled Workshops in Physics, Vol. 0, No. 1), published in 1999.

Chiral Perturbation Theory and Unitarization*

Enrique Ruiz Arriola[1]**, A. Gómez Nicola[2], J. Nieves[1] and J. R. Peláez[2]

[1] Departamento de Física Moderna, Universidad de Granada, E-18071 Granada, Spain
[2] Departamento de Física Teórica Universidad Complutense, 28040 Madrid, Spain

Abstract. We review our recent work on unitarization and chiral perturbation theory both in the $\pi\pi$ and the πN sectors. We pay particular attention to the Bethe-Salpeter and Inverse Amplitude unitarization methods and their recent applications to $\pi\pi$ and πN scattering.

1 Introduction

Chiral Perturbation Theory (ChPT) is a practical and widely accepted effective field theory to deal with low energy processes in hadronic physics. [1–3]. The essential point stressed in this approach is that the low energy physics does not depend on the details of the short distance dynamics, but rather on some bulk properties effectively encoded in the low energy parameters. This point of view has been implicitly adopted in practice in everyday quantum physics; well separated energy and distance scales can be studied independently of each other. The effective field theory approach also makes such a natural idea into a workable and systematic computational scheme.

The great advantage of ChPT is that the expansion parameter can be clearly identified *a priori* (see e.g. Ref. [3]) when carrying out systematic calculations of mass splittings, form factors and scattering amplitudes. However, the connection to the underlying QCD dynamics becomes obscure since the problem is naturally formulated in terms of the relevant hadronic low energy degrees of freedom with no explicit reference to the fundamental quarks and gluons. In addition, in some cases (see below) a possible drawback is the lack of numerical convergence of such an expansion when confronted to experimental data, a problem that gets worse as the energy of the process increases. Recent analysis provide good examples of both rapid convergence and slow convergence in ChPT. In the $\pi\pi$ sector the situation to two loops [4] seems to be very good for the scattering lengths. Here, the expansion parameter is $m_\pi^2/(4\pi f_\pi)^2 = 0.01$ ($m_\pi = 139.6$MeV the physical mass of the charged pion) and the coefficients of the expansion are of order unity. For instance, to two loops (third order in the expansion parameter) the expansion of the s-wave of the isospin $I = 0$ channel reads [5]

$$a_{00} m_\pi = \underbrace{0.156}_{tree} + \underbrace{0.043 \pm 0.003}_{1\,loop} + \underbrace{0.015 \pm 0.003}_{2\,loops} + \cdots \tag{1}$$

---

* Talk delivered by Enrique Ruiz Arriola
** E-mail: earriola@ugr.es

where the theoretical errors are described in [5]. Thus the expansion up to two loops is both convergent $a^{(n)} >> a^{(n+1)}$ and predictive $\Delta a^{(n)} << a^{(n+1)}$, $\Delta a^{(n)} << a^{(n)}$. The *prediction* of ChPT of s-wave scattering lengths a_{IJ} in the isospin $I = 0$ and $I = 2$ channels yields [5]

$$a_{00}m_\pi = +0.214 \pm 0.005 \quad (\exp. +0.26 \pm 0.05)$$
$$a_{20}m_\pi = -0.420 \pm 0.010 \quad (\exp. -0.28 \pm 0.12) \tag{2}$$

The theoretical predictions for these observables are an order of magnitude more accurate than the corresponding experimental numbers. Note that in hadronic physics we are usually dealing with the opposite situation, confronting accurate measurements to inaccurate theoretical model calculations. On the contrary, for πN scattering, for ChPT in the heavy baryon formulation the expansion is less rapidly converging than in the $\pi\pi$ case, since NLO corrections become comparable to the LO ones. For instance in the P_{33}-channel the expansion up to third order, after a fit to the threshold properties, reads [6]

$$a_{33}^1 m_\pi^3 = \underbrace{35.3}_{\text{1st order}} + \underbrace{47.95}_{\text{2nd order}} - \underbrace{1.49}_{\text{3rd order}} + \cdots = 81.8 \pm 0.9 \quad (\exp. 80.3 \pm 0.6) \tag{3}$$

Here first order means $1/f_\pi^2$, second order $1/f_\pi^2 M_N$ and third order $1/f_\pi^4$ and $1/f_\pi^2 M_N^2$. Despite these caveats, there is no doubt that the effective field theory approach provides a general framework where one can either verify or falsify, not only bulk properties of the underlying dynamics, but also the dynamics of all models sharing the same general symmetries of QCD.

Finally, let us remark that the perturbative nature of the chiral expansion makes the generation of pole singularities, either bound states or resonances, impossible from the very beginning unless they are already present at lowest order in the expansion. There are no bound states in the $\pi\pi$ and πN systems, but the ρ and the Δ resonances are outstanding features of these reactions dominating the corresponding cross sections at the C.M. energies $\sqrt{s} = m_\rho = 770\text{MeV}$ and $\sqrt{s} = m_\Delta = 1232\text{MeV}$ respectively.

2   The role played by unitarity

Exact Unitarity plays a crucial role in the description of resonances. However, ChPT only satisfies unitarity perturbatively. Nevertheless, there are many ways to restore exact unitarity out of perturbative information, i.e.: the K-matrix method Ref. [7], the Inverse Amplitude Method (IAM) Ref. [8,9], the Bethe-Salpeter Equation (BSE) Ref. [11,12], the N/D method Ref. [10], etc. (See e.g. Ref. [13] for a recent review), which are closely related to one another.

Some of these Unitarization methods have been very successful describing experimental data in the intermediate energy region including the resonant behavior. Despite this success the main drawback is that this approach is not as systematic as standard ChPT, for instance in the estimation of the order of the neglected corrections. In this work we report on our most recent works related to
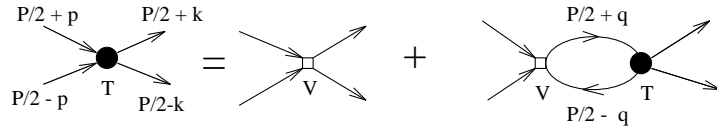
Fig. 1. Diagrammatic representation of the BSE equation. It is also sketched the used kinematics.

unitarization, both in the $\pi\pi$ and πN sectors, where we have obtained intermediate energy *predictions* using the chiral parameters and their error bars obtained from standard ChPT applied at low energies. This means in practice transporting the possible correlations among the fitting parameters obtained from a fit where the phase shifts are assumed to be gauss-distributed in an uncorrelated way.

3 Results in the $\pi\pi$ sector

The ChPT expansion displays a very good convergence in the meson-meson sector. As a consequence the unitarization methods have been very successful in extending the ChPT applicability to higher energies. In particular, within a coupled channel IAM formalism, it has been possible to describe all the meson-meson scattering data, even the resonant behavior, below 1.2 GeV [9], but without including explicitly any resonance field. These works have already been extensively described in the literature and here we will concentrate in the most recent works of two of the authors on the $\pi\pi$ sector, dealing with the Bethe-Salpeter equation, which has the nice advantage of allowing us to identify the diagrams which are resumed.

Indeed, any unitarization method performs, in some way or another, an infinite sum of perturbative contributions. At first sight, this may seem arbitrary, but some constraints have to be imposed on the unitarization method to comply with the spirit of the perturbative expansion we want to enforce. In the BSE approach the natural objects to be expanded are the *potential* and the *propagators*. The BSE as it has been used in Refs. [11,12] reads (See Fig. 1)

$$T_P^I(p,k) = V_P^I(p,k) + i\int \frac{d^4q}{(2\pi)^4} T_P^I(q,k)\Delta(q_+)\Delta(q_-)V_P^I(p,q) \tag{4}$$

where $q_\pm = (P/2\pm q)$ and $T_P^I(p,k)$ and $V_P^I(p,k)$ are the total scattering amplitude[1] and potential for the channel with total isospin $I = 0,1,2$. and then the projection over each partial wave J in the CM frame, $T_{IJ}(s)$, is given by

$$T_{IJ}(s) = \frac{1}{2}\int_{-1}^{+1} P_J(\cos\theta)\,T_P^I(p,k)\,d(\cos\theta) = \frac{i8\pi s}{\lambda^{\frac{1}{2}}(s,m^2,m^2)}\left[e^{2i\delta_{IJ}(s)} - 1\right] \tag{5}$$

---

[1] The normalization of the amplitude T is determined by its relation with the differential cross section in the CM system of the two identical mesons and it is given by $d\sigma/d\Omega = |T_P(p,k)|^2/64\pi^2 s$, where $s = P^2$. The phase of the amplitude T is such that the optical theorem reads $\text{Im}\,T_P(p,p) = -\sigma_{\text{tot}}(s^2 - 4s\,m^2)^{1/2}$, with σ_{tot} the total cross section. The contribution to the amputated Feynman diagram is $(-iT_P(p,k))$ in Fig. 1.

where θ is the angle between $\mathbf{p}$ and $\mathbf{k}$ in the CM frame, P_J the Legendre polynomials and $\lambda(x, y, z) = x^2 + y^2 + z^2 - 2xy - 2xz - 2yz$. Notice that in our normalization the unitarity limit implies $|T_{IJ}(s)| < 16\pi s / \lambda^{1/2}(s, m^2, m^2)$.

The solution of the BSE at lowest order, i.e., taking the free propagators for the mesons and the potential as the tree level amplitude can be obtained after algebraic manipulations described in detail in Refs. [11,12], renormalization and matching to the Taylor expansion up to second order in $s - 4m^2$ of the one loop chiral perturbation theory result. We only quote here the result for the ρ channel:

$$T_{11}^{-1}(s) = -\bar{I}_0(s) + \frac{1}{16\pi^2}\left[2(\bar{l}_2 - \bar{l}_1) + \frac{97}{60}\right] \tag{6}$$

$$+ \frac{1}{s - 4m^2}\left\{\frac{m^2}{4\pi^2}\left[2(\bar{l}_2 - \bar{l}_1) + 3\bar{l}_4 - \frac{65}{24}\right] - 6f^2\right\} \tag{7}$$

where the unitarity integral $\bar{I}_0(s)$ reads

$$\bar{I}_0(s) \equiv I_0(s) - I_0(4m^2) = \frac{1}{(4\pi)^2}\sqrt{1 - \frac{4m^2}{s}}\log\frac{\sqrt{1 - \frac{4m^2}{s}} + 1}{\sqrt{1 - \frac{4m^2}{s}} - 1} \tag{8}$$

Here the complex phase of the argument of the log is taken in the interval $[-\pi, \pi[$. Similar expressions hold for the scalar-isoscalar (σ) and the scalar-isotensor channels. Notice that in this, so-called *off-shell* scheme, the left hand cut is replaced at lowest order by a pole in the region $s \ll 0$. For the low energy coefficients $\bar{l}_{1,2,3,4}$ we take the values

set **A** : $\bar{l}_1 = -0.62 \pm 0.94,\ \bar{l}_2 = 6.28 \pm 0.48,\ \bar{l}_3 = 2.9 \pm 2.4,\ \bar{l}_4 = 4.4 \pm 0.3$

set **B** : $\bar{l}_1 = -1.7\ \pm 1.0\ ,\ \bar{l}_2 = 6.1\ \pm 0.5\ ,\ \bar{l}_3 = 2.9 \pm 2.4,\ \bar{l}_4 = 4.4 \pm 0.3$ (9)

In both sets $\bar{l}_3$ and $\bar{l}_4$ have been determined from the $SU(3)$ mass formulae and the scalar radius as suggested in [1] and in [14], respectively. On the other hand the values of $\bar{l}_{1,2}$ come from the analysis of Ref. [15] of the data on K_{l4}−decays (set **A**) and from the combined study of K_{l4}−decays and $\pi\pi$ with some unitarization procedure (set **B**) performed in Ref. [16]. The results for the ρ channel are shown in Fig. 2.

As discussed in Ref. [12] it is also possible to take into account the left hand cut in the so-called *on-shell* scheme where it can be shown that after renormalization the on-shell unitarized amplitude acquires the following form

$$T_{IJ}(s)^{-1} + \bar{I}_0(s) - V_{IJ}(s)^{-1} = T_{IJ}(s_0)^{-1} + \bar{I}_0(s_0) - V_{IJ}(s_0)^{-1} = -C_{IJ} \tag{10}$$

where C_{IJ} should be a constant, independent of s and the subtraction point s_0, and chosen to have a well defined limit when $m \to 0$ and $1/f \to 0$. $V_{IJ}(s)$ is the *on-shell*-potential and has the important property of being real for $0 < s < 16m^2$, and presenting cuts in the four pion threshold and the left hand cut caused by the unitarity cuts in the t and u channels. The potential can be determined by matching the amplitude to the ChPT amplitude in a perturbative expansion. This method provides a way of generating a unitarized amplitude directly in terms of the low
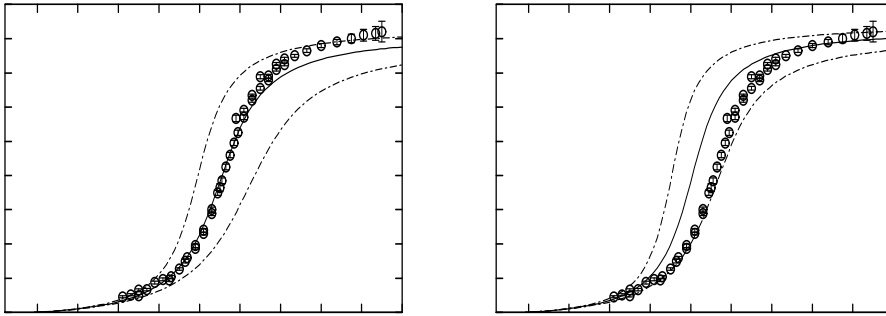
Fig. 2. $I = J = 1$ $\pi\pi$ phase shifts as a function of the total CM energy $\sqrt{s}$ for both sets of $\bar{l}$'s given in Eq. (9). Left (right) figures have been obtained with the set **A** (**B**) of parameters. Solid lines are the predictions of the off-shell BSE approach, at lowest order, for the different IJ−channels. Dashed lines are the 68% confidence limits. Circles stand for the experimental analysis of Refs. [17] and [18].

energy coefficients $\bar{l}_{1,2,3,4}$ and their errors. In this *on-shell* scheme a successful description of both $\pi\pi$ scattering data as well as the electromagnetic pion form factor, in agreement with Watson's theorem, becomes possible yielding a very accurate determination of some low energy parameters. The procedure to do this becomes a bit involved and we refer to Ref. [12] for further details. We should also say that the one-loop unitarized amplitudes generate the complete ChPT result and *some* of the two and higher loop results. The comparison of the generated two-loop contribution of threshold parameters with those obtained from the full two loop calculation is quantitatively satisfactory within uncertainties.

4   Results in the πN sector

The methods and results found in the $\pi\pi$ system are very encouraging, suggesting the extension to the πN system. However, ChPT does not work in the πN sector as nicely as it does in the $\pi\pi$ sector. As we will see, the low convergence rate of the chiral expansion makes it difficult to match standard amplitudes to unitarized ones in a numerically sensible manner. After an initial attempt within the relativistic formulation [19], it was proposed to treat the baryon as a heavy particle well below the nucleon production threshold [20]. The resulting Heavy Baryon Chiral Perturbation Theory (HBChPT) provides a consistent framework for the one nucleon sector, particularly in πN scattering [6]. The proposal of Ref. [21] adopting the original relativistic formalism but with a clever renormalization scheme seems rather promising but unfortunately the phenomenological applications to πN scattering have not been worked out yet.

4.1   The IAM method in π-N scattering

The inverse amplitude method (IAM) is a unitarization method where the inverse amplitude, and not the amplitude, is expanded, i.e., if we have the perturbative

expansion for the partial wave amplitude $f(\omega)$,

$$f(\omega) = f_1(\omega) + f_2(\omega) + f_3(\omega) + \ldots \tag{11}$$

with $\omega = \sqrt{q^2 + m_\pi^2}$ and q the C.M. momentum, then one considers the expansion

$$\frac{1}{f(\omega)} = \frac{1}{f_1(\omega)} - \frac{f_2(\omega) + f_3(\omega)}{[f_1(\omega)]^2} + \frac{f_2(\omega)^2}{[f_1(\omega)]^3} + \ldots \tag{12}$$

The IAM fulfills exact unitarity, $\mathrm{Im} f(\omega)^{-1} = -q$ and reproduces the perturbative expansion to the desired order.

   This method has been applied for πN scattering [22] to unitarize the HBChPT results of Ref. [6] to third order. In this context, it is worth pointing out that the use of a similar unitarization method, together with very simple phenomenological models, was already successfully undertaken in the 70's (see [23] and references therein). Nonetheless, a systematic application within an effective Lagrangian approach was not carried out. In [22] the phase shifts for the partial waves up to the inelastic thresholds have been fitted, obtaining the right pole for the $\Delta(1232)$ in the P_{33} channel. In that work, it has been pointed out that to get the best accuracy with data, one needs chiral parameters of unnatural size, very different from those of perturbative HBChPT. This is most likely related to the slow convergence rate of the expansion. However, it must be stressed that one can still reproduce the $\Delta(1232)$ with second order parameters compatible with the hypothesis of resonance saturation [32]. In a subsequent work [24] we have proposed an improved IAM method based on a reordering of the HBChPT series. The encouraging results for the Δ-channel have also been extended to the remaining low partial waves [25], as it can be seen in Fig. 3. In this case, the size of the chiral parameters is natural and the χ^2 per d.o.f is considerably better than the IAM applied to plain HBChPT.

4.2   BSE method and the Δ-resonance

Recently [26], we have used the BSE to HBChPT at lowest order in the chiral expansion and have looked at the P_{33} channel. We have found a dispersive solution which needs four subtraction constants,

$$f^{3/2}_{3/2,1}(\omega)^{-1} = -\frac{24\pi}{(\omega^2 - m^2)} \left\{ \frac{-f^2 \omega}{2g_A^2} + P(\omega) + (\omega^2 - m^2)\bar{J}_0(\omega)/6 \right\}$$

$$P(\omega) = m^3 \left(c_0 + c_1(\frac{\omega}{m} - 1) + c_2(\frac{\omega}{m} - 1)^2 + c_3(\frac{\omega}{m} - 1)^3 \right) \tag{13}$$

where the unitarity integral is given by

$$\bar{J}_0(\omega) \equiv J_0(\omega) - J_0(m) = -\frac{\sqrt{\omega^2 - m^2}}{4\pi^2}\{\mathrm{arcosh}\frac{\omega}{m} - i\pi\}; \qquad \omega > m \tag{14}$$

The χ^2 fit yields the following numerical values for the parameters:

$$c_0^{\mathrm{fit}} = 0.045 \pm 0.021\,, \quad c_1^{\mathrm{fit}} = 0.29 \pm 0.08\,, \quad c_2^{\mathrm{fit}} = -0.17 \pm 0.09\,, \quad c_3^{\mathrm{fit}} = 0.16 \pm 0.03$$
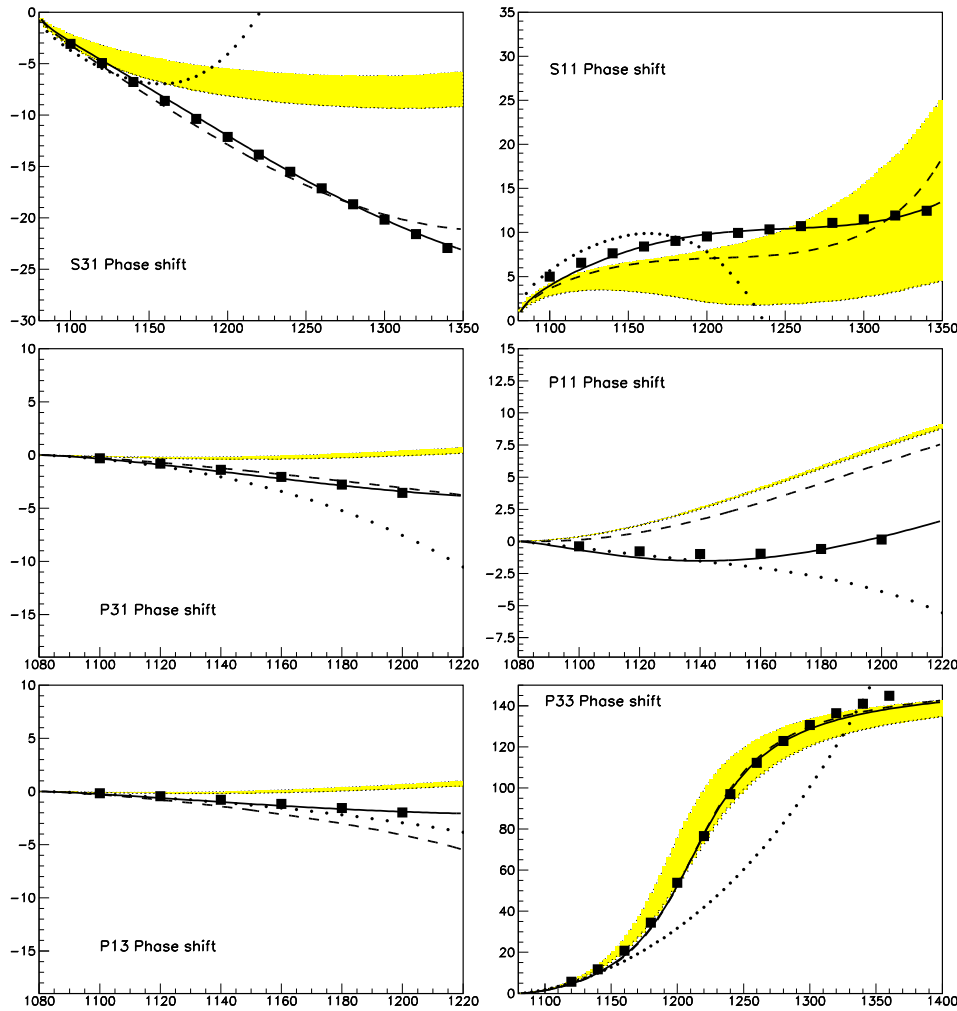
Fig. 3. Phase shifts in the IAM method as a function of the C.M. energy $\sqrt{s}$. The shaded area corresponds to the result of propagating the errors of the chiral parameters obtained from low-energy data (see Ref. [25]). This illustrates the uncertainties due to the choice of different parameter sets from the literature. The dotted line is the extrapolated HBChPT result. The continuous line is an unconstrained IAM *fis* to the data, whereas for the dashed line the fit has been constrained to the resonance saturation hypothesis.

with $\chi^2/\text{d.o.f.} = 0.2$. However, if we match the coefficients with those stemming from HBChPT we would get instead the following numerical values:

$$c_0^{th} = 0.001 \pm 0.003 \,, \ c_1^{th} = 0.038 \pm 0.006 \,, \ c_2^{th} = 0.064 \pm 0.005 \,, \ c_3^{th} = 0.036 \pm 0.002$$

The discrepancy is, again, attributed to the low convergence rate of the expansion. The results for the P_{33} phase shift both for the fit and the MonteCarlo propagated errors of the HBChPT matched amplitudes have been depicted in Fig. 4
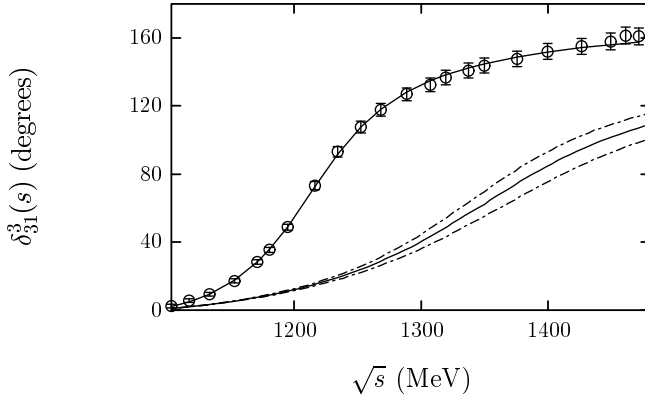
Fig. 4. P_{33} phase shifts as a function of the total CM energy $\sqrt{s}$. The upper solid line represents a χ^2-fit of the parameters, $c_{0,1,2,3}$ to the data of Ref. [31] (circles). Best fit parameters are denoted $c^{fit}_{0,1,2,3}$ in the main text. The lower lines stand for the results obtained with the parameters deduced from HBChPT and denoted $c^{th}_{0,1,2,3}$. Central values lead to the solid line, whereas the errors on $c^{th}_{0,1,2,3}$ lead to the dash-dotted lines.

4.3 πN scattering and the $N^*(1535)$ resonance

One of the greatest advantages of both the IAM and the BSE methods is that the generalization to include coupled channels is rather straightforward. For the IAM case we refer to [9] for more details. As for the BSE, two of the authors [30] have dealt with the problem in the S_{11} channel, at $\sqrt{s}$ up to $1800 GeV$ using the full relativistic, rather than the heavy baryon formulation used in Ref. [27] for the s-wave and extended in Ref. [28] to account for p-wave effects. For these energies there are four open channels, namely $\pi N, \eta N, K\Sigma$ and $K\Lambda$, so that the BSE becomes a 4×4 matrix equation for the $I = 1/2$, $J = 1/2$ and $L = 0$ partial wave. Additional complications arise due to the Dirac spinor structure of the nucleon, but the BSE can be analytically solved after using the above mentioned off-shell renormalization scheme. It turns out [30] that to lowest order in the potential and the propagators, one needs 12 unknown parameters, which should be used to fit experimental data. Several features make the fitting procedure a bit cumbersome. In the first place, there is no conventional analysis in the relativistic version of ChPT for this process and thus no clear constraints can be imposed on the unknown parameters. Secondly, the channel $\pi N \rightarrow \pi\pi N$ is not included in our calculation. Therefore one should not expect perfect agreement with experiment, particularly in the elastic channel since it is known that $10 - 20\%$ of the N^* resonance decay width goes into $\pi\pi N$. On the other hand, one cannot deduce from here how important is the $\pi\pi N$ channel in the η production channel, $\pi N \rightarrow \eta N$. Actually, in Ref. [29] it has been suggested that the bulk of the process may be explained without appealing to the three body intermediate state $\pi\pi N$. The work of Ref. [29] would correspond in our nomenclature to the on-shell lowest order BSE approximation, which by our own experience describes well the bulk of the data. With the BSE we have provided a further improvement at low energies

by including higher order corrections. In the absence of a canonical low energy analysis it seems wiser to proceed using the off-shell renormalization scheme. In Fig. 5 we present a possible 12 parameter fit which accounts both for the elastic low and intermediate energy region and the lowest production channels. The failure to describe data around the N^* resonance is expected, since as we have already mentioned the $\pi\pi N$ channel must be included. Our results seem to confirm the assumption made in Ref. [29] regarding the unimportance of the three body channel in describing the coupling of the N^* resonance to ηN.
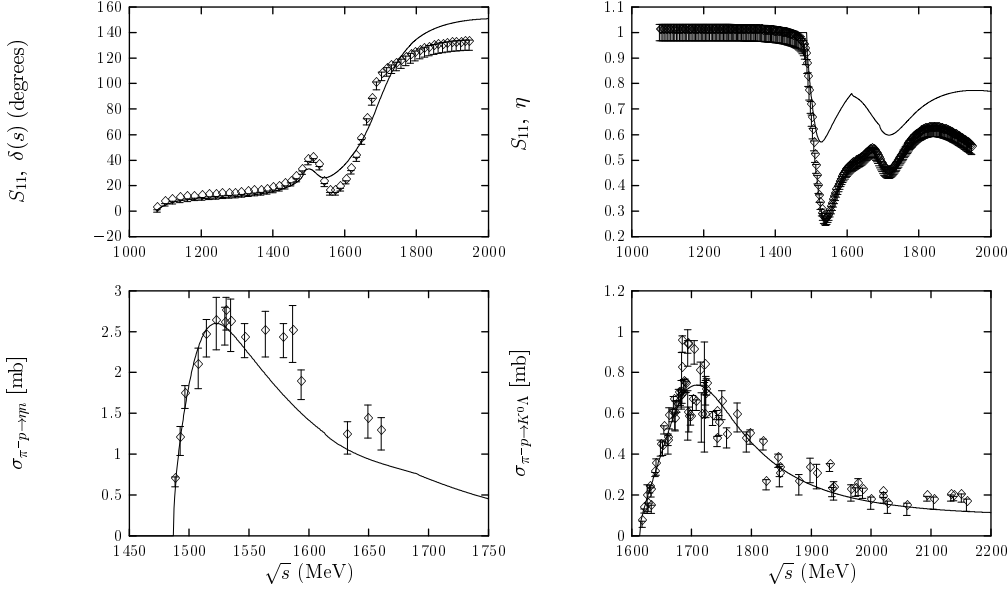
Fig. 5. πN scattering BSE results as a function of C.M. energy $\sqrt{s}$. Upper left figure: S_{11} phase shifts. Upper right figure: inelasticity in the πN channel. Lower left figure: $\pi N \to \eta N$ cross section. Lower right figure: $\pi N \to K\Lambda$ cross section. Data from Ref. [31]. (See Ref. [30] for further details.)

5   Conclusions and Outlook

The results presented here show the success and provide further support for unitarization methods complemented with standard chiral perturbation theory, particularly in the case when resonances are present. But unitarization by itself is not a guarantee of success; the unitarization method has to be carefully chosen so that it provides a systematic convergent and predictive expansion, as we have discussed above. In order to describe the data in the intermediate energy region the chiral parameters can then be obtained from

- Either a direct χ^2 fit of the order by order unitarized amplitude and the corresponding low energy parameters. The upper energy limit is determined by imposing an acceptable description $\chi^2/\text{DOF} \sim 1$.

- Or from a low energy determination of the low energy parameters with errors by performing a χ^2-fit of the standard ChPT amplitude until $\chi^2/DOF \sim 1$, and subsequent MonteCarlo error propagation of the unitarized amplitude.

Differences in the low energy parameters within several methods should be compatible within errors, as long as the Chiral expansion has a good convergence. But, unfortunately this is not always the case. Clearly, the πN sector is not only more cumbersome theoretically than the $\pi\pi$ sector but also more troublesome from a numerical point of view. Standard ChPT to a given order can be seen as a particular choice which sets higher order terms to zero in order to comply with exact crossing but breaking exact unitarity. The unitarization of a the ChPT amplitude is also another choice of higher order terms designed to reproduce exact unitarity but breaking exact crossing symmetry. Given our inability to write a closed analytic expression for an amplitude in a chiral expansion which simultaneously fulfills both exact crossing and unitarity we have preferred exact unitarity. This is justified a posteriori by the successful description of data in the intermediate energy region, which indeed suggests a larger convergence radius of the chiral expansion.

Acknowledgments

References

1. J. Gasser and H. Leutwyler, Ann. of Phys., NY **158** (1984) 142.
2. H. Leutwyler, Ann. of Phys. NY **235** (1994) 165.
3. For reviews see e.g., A. Pich, Rept. Prog. Phys. **58** (1995) 563 and G. Ecker, Prog. Part. Nucl. Phys. **35** (1995) 1 for the meson sector, V. Bernard, N. Kaiser and U.-G. Meißner, Int. J. Mod. Phys. **E4** (1995) 193 for the baryon-meson system.
4. M. Knecht, B. Moussallam, J. Stern and N. H. Fuchs, Nucl. Phys. B **457** (1995) 513, Nucl. Phys. B **471** (1996) 445; J. Bijnens, G. Colangelo, G. Ecker J. Gasser and M. E. Sainio, Phys. Lett. B **374** (1996) 210, Nucl. Phys. B **508** (1997) 263.
5. J. Nieves and E. Ruiz Arriola, Eur. Jour. Phys. A **8** (2000) 377, G. Amoros, J. Bijnens and P. Talavera, Nucl. Phys. B **585** (2000) 293.
6. M. Mojzis, Eur. Phys. Jour. C **2** (1998) 181. N. Fettes, U.-G. Meißner and S. Steininger, Nucl. Phys. A **640** (1998) 199.
7. A. D. Martin and T.D. Spearman, *Elementary Particle Theory* (Wiley, New York ,1970) p. 348. S.N. Gupta, *Quantum Electrodynamics* (Gordon and Breach, New York,1981), p. 191.
8. T. N. Truong, Phys. Rev. Lett. 661 (1988) 2526; Phys. Rev. Lett. 67 (1991) 2260. A. Dobado, M.J. Herrero and T. N. Truong, Phys. Lett. B235 (1990) 134. A. Dobado and J. R. Peláez, Phys. Rev. D47 (1993) 4883; Phys. Rev. D56 (1997)3057.
9. J.A. Oller, E. Oset and J.R. Peláez, Phys. Rev. Lett. 80(1998) 3452;Phys. Rev. D59(1999) 074001. F. Guerrero and J.A. Oller, Nucl. Phys. B537 (1999) 3057.
10. J.A. Oller and E. Oset, Phys. Rev. D60: 074023,1999.

11. J. Nieves and E. Ruiz Arriola, Phys. Lett. B **455** (1999) 30.
12. J. Nieves and E. Ruiz Arriola, Nucl. Phys. A **679** (2000) 57.
13. J.A. Oller, E. Oset and A. Ramos, Prog. Part. Nucl. Phys. **45** (2000) 157.
14. J. Bijnens, G. Colangelo and P. Talavera, JHEP **9805** (1998) 014.
15. C. Riggenbach, J.F. Donoghue, J. Gasser, B.R. Holstein, Phys. Rev. D **43** (1991) 127.
16. J. Bijnens, G. Colangelo and J. Gasser, Nucl. Phys. B **427** (1994) 427.
17. S. D. Protopopescu *et. al.,* Phys. Rev. D **7** (1973) 1279.
18. P. Estabrooks and A. D. Martin, Nucl. Phys. B **79** (1974) 301.
19. J. Gasser, M.E. Sainio and A. Svarc, Nucl. Phys. B **307** (1988) 779.
20. E. Jenkins and A. V. Manohar, Phys. Lett. B **255** (1991) 558. V. Bernard, N. Kaiser, J. Kambor and U. -G. Meißner, Nucl. Phys. B **388** (1992) 315.
21. T. Becher and H. Leutwyler, Eur. Phys. Jour. C **9** (1999) 643.
22. A. Gómez Nicola and J.R. Peláez, Phys. Rev. D **62** (2000) 017502.
23. J.L. Basdevant, Fort. der Phys. 20 (1972) 283.
24. J. Nieves and E. Ruiz Arriola, hep-ph/0001013
25. A. Gómez Nicola, J. Nieves, J.R. Peláez and E. Ruiz Arriola, Phys. Lett. B **486** (2000) 77.
26. J. Nieves and E. Ruiz Arriola, Phys. Rev. D in print, hep-ph/0008034.
27. N. Kaiser, P.B. Siegel and W. Weise, Phys. Lett. B **362** (1995) 23.
28. J. Caro, N. Kaiser, S. Wetzel and W. Weise, Nucl. Phys. A **672** (2000) 249.
29. J.C. Nacher, A. Parreno, E. Oset, A. Ramos, M. Oka, Nucl. Phys. A **678** (2000) 187.
30. J. Nieves and E. Ruiz Arriola, work in progress.
31. R.A. Arndt, I.I. Strakovsky, R.L. Workman, and M.M. Pavan, Phys. Rev. C **52**, 2120 (1995). R.A. Arndt, *et. al.,* nucl-th/9807087. SAID online-program (Virginia Tech Partial–Wave Analysis Facility). Latest update, http://said.phys.vt.edu.
32. V. Bernard, N. Kaiser and U. -G. Meißner, Phys. Lett. B309 (1993) 421; Phys. Rev. C52 (1995) 2185; Phys. Lett. B389 (1996) 144; Nucl. Phys. A615 (1997) 483;

Nucleons or diquarks: Competition between clustering and color superconductivity in quark matter

Michael C. Birse[*]

Theoretical Physics Group, Department of Physics and Astronomy, University of Manchester, Manchester M13 9PL, United Kingdom

Baryonic matter at high densities could be very different from matter in ordinary nuclei: manifest chiral symmetry might be restored, baryons might dissolve into a fluid of free quarks, and quark pairs might condense to form a colour superconductor. Do these changes occur at sharp phase transitions or smooth cross-overs? How many phase transitions are there? At what densities do they occur? So far lattice QCD has provided no answers to these questions and we must rely on models to explore the possible behaviour of strongly interacting matter at high densities.

The possibility of colour superconductivity has recently attracted considerable attention following suggestions by Wilczek, Shuryak and others that strongly attractive quark-quark forces could lead to such a state with a large gap, of the order of 100 MeV. (For reviews of this idea, see [1,2].) In recent work [3], we have examined the competition between this pairing of quarks and the three-quark clustering responsible for forming baryons at low densities. We have used a generalized Nambu–Jona-Lasinio model, which provides a quark-quark interaction which is similar to that in the instanton-liquid model often used in studies of colour superconductivity. Since there is no simple analogue of the BCS state for composite fermions, we have gone back to a Cooper-type treatment, looking for the instabilities of a Fermi gas of quarks.

The model includes interactions that generate bound diquarks states in both scalar and axial diquark channels. The energies of these are found by solving the quark-quark Bethe-Salpeter equations, which are straightforward algebraic equations in this kind of model. The relativistic Faddeev equations for the nucleon and Δ are constructed using the methods of Refs. [4,5] and, in particular, [6]. These are integral equations which we solve iteratively using the method of Malfleit and Tjon [7].

A sharp 3-momentum cut-off of about 600 MeV was used to regulate the contact interaction since this is easy to combine with the effects of the Fermi sea. However it should be noted that this choice is not covariant. The couplings in the scalar and axial diquark channels are chosen to give the observed N and Δ masses in vacuum. For a parameter set which gives a quark mass of 450 MeV, the scalar and axial diquarks have masses of 635 MeV and 700 MeV.

[*] E-mail: mike.birse@man.ac.uk

At finite density, the quark mass is reduced and vanishes at the chiral phase transition, which occurs at a Fermi momentum of about 370 MeV for the parameter sets we use. (For comparison, nuclear-matter density corresponds to $k_F = 270$ MeV.) In addition, Pauli blocking provides a lower cut-off on the momenta of the quarks in the Bethe-Salpeter and Faddeev equations.

We find that the nucleon remains bound with respect to the quark-diquark threshold only up to nuclear matter density. Morover, except for densities below about a quarter of that of nuclear matter, we find that it is energetically much more favorable to form three diquarks rather than two nucleons. Hence in models of this type, quark matter is more unstable against pairing (leading to a colour superconductor) than it is against three-quark clustering, even at the density of nuclear matter.

Clearly something important is missing from models of this type: confinement. We need to examine whether extending the model to include confinement at low densities also affects behaviour at high densities. Indeed, is it possible to get a realistic phase diagram without confinement?

References

1. K. Rajagopal, Nucl. Phys. **A661** (1999) 150 [hep-ph/9908360].
2. T. Schäfer, nucl-th/9911017.
3. S. Pepin, M. C. Birse, J. A. McGovern and N. R. Walet, Phys. Rev. **C61** (2000) 055209 [hep-ph/9912475].
4. A. Buck, R. Alkofer and H. Reinhardt, Phys. Lett. B **286**, 29 (1992).
5. S. Huang and J. Tjon, Phys. Rev. C **49**, 1702 (1994).
6. N. Ishii, W. Bentz and K. Yazaki, Nucl. Phys. **A587**, 617 (1995).
7. R. A. Malfliet and J. A. Tjon, Nucl. Phys. **A127**, 161 (1969).

Distinct Hagedorn temperatures from particle spectra: a higher one for mesons, a lower one for baryons

Wojciech Broniowski[*]

The H. Niewodniczański Institute of Nuclear Physics, PL-31342 Cracow, Poland[**]

Abstract. We analyze experimental particle spectra and show that the Hagedorn temperature is significantly larger for mesons than for baryons. The effect can be explained within dual string models: excitations of three strings in the baryon produce "faster" combinatorics than a single string in the meson, hence lead to a more rapid growth of baryons than mesons. Predictions of other approaches for the gross features of particle spectra are also discussed.

This research is being carried out in collaboration with Wojciech Florkowski and Piotr Żenczykowski from INP, Cracow.

1 Introduction

The famous Hagedorn hypothesis [1–3], dating back to pre-chromodynamic times of the sixties, states that at asymptotically large masses, m, the density of hadronic resonance states, $\rho(m)$, grows exponentially:

$$\rho(m) \sim \exp\left(\frac{m}{T_H}\right) \tag{1}$$

The Hagedorn temperature, T_H, is a scale controlling the exponential growth of the spectrum. Although the Hagedorn hypothesis has sound thermodynamical consequences (one cannot heat-up a hadronic system above this temperature), T_H should not be immediately associated with thermodynamics. In this talk we are concerned with the spectrum of particles *per se*, as read off form the Particle Data Tables [4]. In this context the "temperature" T_H is just a parameter in Eq. (1).

Ever since hypothesis (1) was posed, it has been believed that there is one universal Hagedorn temperature for all hadrons. *Presently available experimental data show that this is not the case*, as has been pointed out by W. Florkowski and WB in Refs. [5,6].

---

[*] E-mail: broniows@solaris.ifj.edu.pl
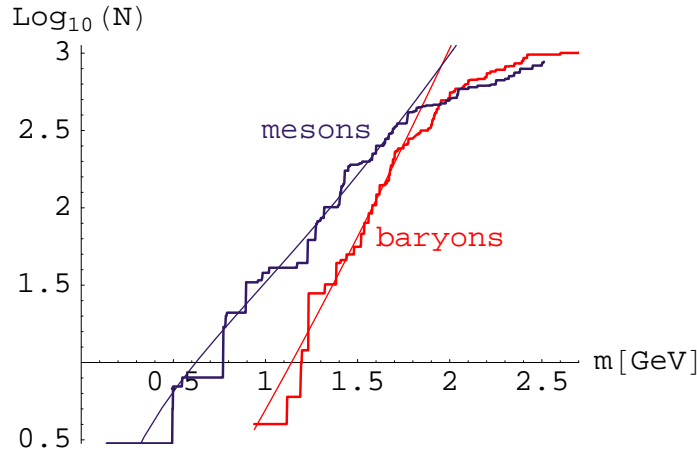
Fig. 1. Cumulants of meson and baryon spectra, and the Hagedorn-like fit with Eqs. (4,5), plotted as functions of mass.

This talk has two parts: experimental and theoretical. In the experimental part (Sec. 2) we show how well the Hagedorn hypothesis works even for very low masses, and point out the key observation that *the mesonic temperature is significantly larger from the baryonic temperature*. In the theoretical part (Sec. 3) we argue that the only framework (known to us) which is capable of producing the observed behavior in a natural way are the Dual String Models [7]. In Sec. 4 we discuss other approaches and more speculative ideas.

2   Experiment

2.1   Experimental spectra of mesons and baryons

In Fig. 1 we compare the *cumulants* of the spectrum [4], defined as the number of states with mass lower than m. The experimental curve is

$$N_{exp}(m) = \sum_i g_i \Theta(m - m_i), \tag{2}$$

where $g_i = (2J_i + 1)(2I_i + 1)$ is the spin-isospin degeneracy of the ith state, and m_i is its mass. The theoretical curve corresponds to

$$N_{theor}(m) = \int_0^m \rho_{theor}(m')dm', \tag{3}$$

where

$$\rho_{theor}(m) = f(m)\exp(m/T), \tag{4}$$

with $f(m)$ denoting a slowly-varying function. A typical choice [3,8], used in the plot of Fig. 1, is

$$f(m) = A/(m^2 + (500\text{MeV})^2)^{5/4}. \tag{5}$$

Formula	m_0 MeV	T_{mes} MeV	T_{bar} MeV	σ^2_{mes}	σ^2_{bar}
$\frac{A}{(m^2+m_0^2)^{5/4}}\exp(\frac{m}{T})$	500	195	141	0.016	0.015
- - -	1000	228	152	0.014	0.015
- - -	250	177	136	0.025	0.015
$\frac{A}{(m+m_0)^{5/2}}\exp(\frac{m}{T})$	1000	223	154	0.015	0.015
$A\exp(\frac{m}{T})$		311	186	0.014	0.015
$\frac{A}{m}I_2(\frac{m}{T})$		249	157	0.014	0.015

Table 1. Various Hagedorn-like fits. Rows 1-4 use formulas of Ref. [2], row 5 uses a simple exponent, and row 6 uses the scalar string model of Ref. [10]. The last two column display the mean suared deviation for the meson and baryon case, respectively.

Parameters T_H and A are obtained with the least-square fit to $\log N_{theor}$, made over the range up to $m = 1.8$GeV, and skipping the lightest particle in the set. Other choices of $f(m)$ give fits of similar quality (see Fig. 2). A striking feature of Fig. 1 is the linearity of $\log N$ starting at very low m, and extending till $m \sim$ 1.8GeV. Clearly, this shows that (1) is valid in the range of available data.[1] However, the slopes in Fig. 1 are *different* for mesons and baryons. For the assumed $f(m)$ of Eq. (5) we get

$$T_{meson} = 195\text{MeV}, \quad T_{baryon} = 141\text{MeV}. \tag{6}$$

This means that $T_{meson} > T_{baryon}$, and the inequality is substantial! Although it has been known to researchers in the field of hadron spectroscopy that the baryons multiply more rapidly than mesons [9], to our knowledge this fact has not been presented as vividly as in Fig. 1. To emphasize the strength of the effect we note that in order to make the meson line parallel to the baryon line, we would have to aggregate ~ 500 additional meson states up to $m = 1.8$MeV as compared to the present number of ~ 400.

2.2   Are we asymptotic?

An important question is whether the presently available range of masses is asymptotic in view of Eq. (1). The answer is *no*! This is how we can look at this question quantitatively. Consider the generic form of the spectrum of Eq. (4). We can rewrite it as

$$f(m)e^{m/T} = e^{\log f(m)+m/T} \simeq e^{\log[f(\overline{m})+f'(\overline{m})\Delta m]+(\overline{m}+\Delta m)/T} =$$
$$\text{const } e^{\left(\frac{1}{T}+\frac{f'(\overline{m})}{f(\overline{m})}\right)\Delta m} = \text{const } e^{\frac{\Delta m}{T_{eff}}},$$

where $m = \overline{m} + \Delta m$, and in the range of data $\overline{m} \sim 1$GeV. We have defined T_{eff} as the *effective* Hagedorn temperature in the (non-asymptotic) region around $\overline{m}$. The

[1] Above 1.8GeV the data seems to be sparse and we should wait for this region to be explored by future experiments.
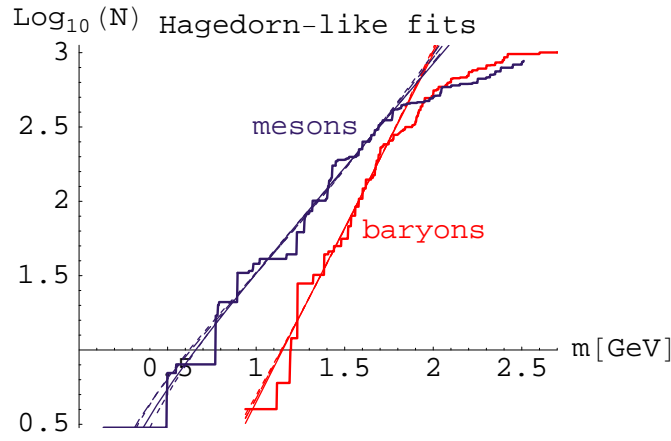
Fig. 2. Various Hagedorn-like fits, made according to formulas of Table 1.

value of T_{eff} follows directly from the data. We have, according to Eq. (7),

$$\frac{1}{T} = \frac{1}{T_{\text{eff.}}} - \frac{f'(\overline{m})}{f(\overline{m})}. \tag{7}$$

The following statements are obvious:

- since $f'(\overline{m}) < 0$, $T < T_{\text{eff}}$,
- only at $m \rightarrow \infty$ we have $T = T_{\text{eff}}$. In the region of data we find significant differences between T and T_{eff}.

Here is a numerical example. Consider

$$f(m) = \frac{A}{(m^2 + m_0^2)^{5/4}}, \tag{8}$$

which leads to

$$\frac{1}{T} = \frac{1}{T_{\text{eff.}}} + \frac{5}{2} \frac{\overline{m}}{(\overline{m}^2 + m_0^2)} \tag{9}$$

Now we take $m_0 = 0.5\text{GeV}$ and $\overline{m} = 1\text{GeV}$ and find

for mesons: $T_{\text{eff}} = 311\text{MeV}$, $T = 192\text{MeV}$ (exact fit: 195MeV)
for baryons: $T_{\text{eff}} = 186\text{MeV}$, $T = 136\text{MeV}$ (exact fit: 141MeV)

We conclude that only in the asymptotic region, $m >> m_0$, the choice of $f(m)$ is not important. In the region of presently-available data $f(m)$ matters very much for the extracted values of the Hagedorn temperature. This simply means that we need a *theory* in order to make quantitative statements!

The numerical parameters obtained from various choices of the function $f(m)$ are collected in Table 1. Figure 2 shows the fits corresponding to the rows 1, 4, 5 and 6 of Table 1. Note the fits are very close to each other and the theoretical curves are virtually indistinguishable in the region of data. In view of the above discussion it makes little sense to treat the Hagedorn temperature as an absolute parameter and to quote its value without specifying the model that yields the function $f(m)$.
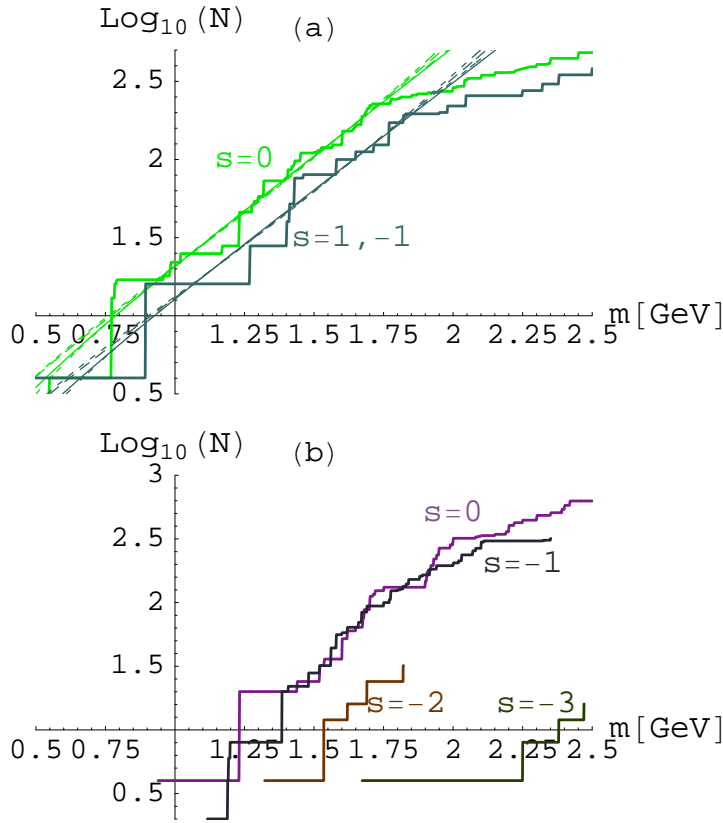
Fig. 3. Strange vs. non-strange mesons (a), and baryons (b).

2.3   Flavor universality

In Fig. 3 we show the cumulants of particle spectra of a given value of strangeness. We can clearly see that the slopes in the figure do not depend on strangeness. The meson plot includes various Hagedorn fits of Fig. 2. The two sets of lines are displaced in the m variable by roughly 150MeV, which is the difference of the masses on the strange and non-strange quarks. The conclusion here is that the addition of the strange quark mass has no effect on the rate of growth of the number of states with m. Certainly, we are rediscovering the $SU(3)$ flavor symmetry here!

2.4   Plot in the exponential variable

We end the experimental part of this talk by showing the same information as in Fig. 1, but instead of using logarithmic units on the vertical axes, we take exponential units on the horizontal axis. More precisely, we take the fit to the spectrum with of the form with the simple exponent (row 5 in Table 1), which leads to the cumulant $N(m) = AT(\exp(m/T) - 1)$, where the values of A and T result from the least-square fit. Next, we define the variable $y = AT(\exp(m/T) - 1)$ and plot the cumulants as functions of y. Note that the A and T parameters are different
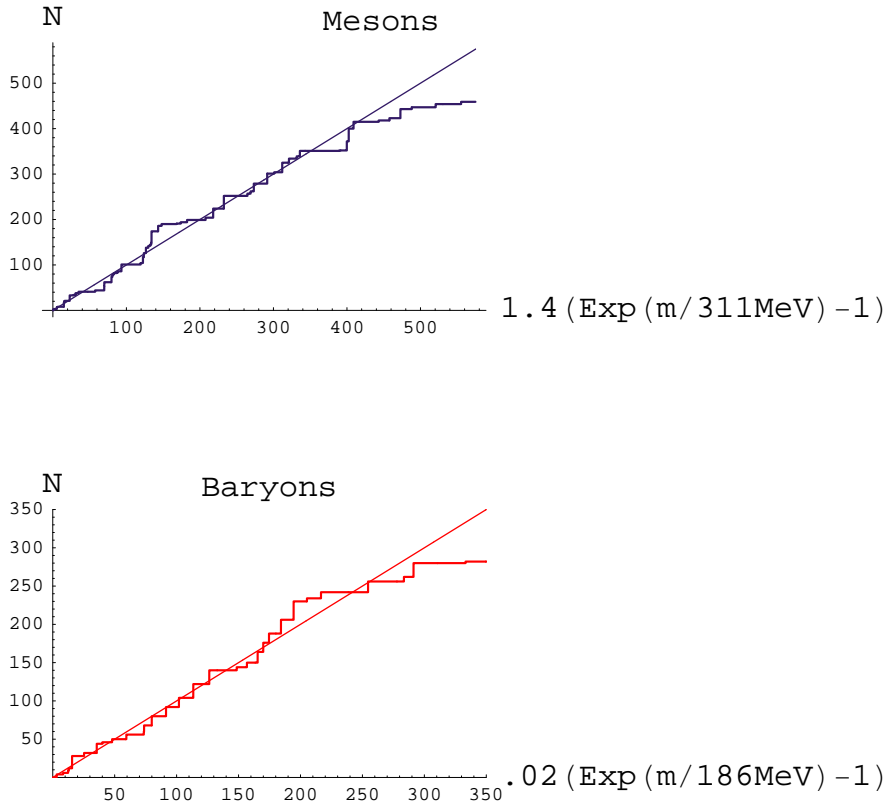
Fig. 4. Cumulants of the meson and baryon spectra plotted in exponential variables.

for mesons and baryons. Again, the linearity of data in the figure is striking. It starts at basically $m = 0$, and extends to $m \sim 1.8\text{GeV}$. The advantage of the plot in Fig. 4 to that of Fig. 1 is that now the steps in the experimental cumulant are of a similar size independently of m.

We conclude this section by stating that the exponential growth of hadronic spectra in the region of m up to about 1.8GeV, with $T_{\text{mes}} > T_{\text{bar}}$, is an *experimental fact*.

3   Theory

We are faced with two basic theoretical questions:

1. *Why is the spectrum of resonances exponential?*
2. *Why do mesons and baryons behave so differently?*

Concerning the first question, let us stress that it is not at all easy to get an exponentially rising spectrum of resonances. Take the simplistic harmonic-oscillator model, whose density of states grows as m^{d-1}, with d denoting the number of

dimensions. For mesons there is one relative coordinate, hence $\rho \sim m^2$, whereas the two relative coordinates in the baryon give $\rho \sim m^5$. Weaker-growing potentials lead to a faster growth of the number of states, but fall short of the behavior (1). We know of three approaches yielding behavior (1), both involving combinatorics of infinitely-many degrees of freedom. These are the *Statistical Bootstrap Model* [1–3,11], Bag Models [12–14], and Dual String Models [7]. The first two, however, lead to the same rate of growth for the mesons and baryons. Statistical Bootstrap Models are discussed in Sec. 3.1. In Bag Models [12–14] the exponential growth of the spectrum is associated with the melting out of the vacuum around the bag when the hadron is being excited. Since the scales in the Bag Model are practically the same for the meson and the baryon (the size scales as the number of constituents to the power 1/4), the Bag Models are not capable of answering question 2. On the other hand, the *Dual String Models* [7] is offer a natural explanation of questions 1 and 2. This has already been pointed out in Ref. [6].

3.1   Statistical Bootstrap Models

Statistical bootstrap models [1,3,11] form particles from clusters of particles, and employ the principle of self-similarity. The simplest, "generic", bootstrap equation has the form

$$\rho(m) = \delta(m - m_0) + \sum_{n=2}^{\infty} \frac{1}{n!} \int_0^{\infty} dm_1...dm_n \times \delta(m - \sum_{i=1}^{n} m_i)\rho(m_1)...\rho(m_n), \quad (10)$$

where $\rho(m)$ is the particle spectrum (here, for a moment, mesons and baryons are not distinguished). Equation (10) can be nicely solved with help of Laplace transforms [1,3,15], yielding the asymptotic solution $\rho(m) \sim \exp(m/T)$, with $T = m_0/\log(-\log \frac{4}{e})$. More complicated bootstrap equations involve integration over momenta, more degrees of freedom, different combinatorial factors [3], however, irrespectively of these details, they always lead to an exponentially growing spectrum. It can be shown, following *e.g.* the steps of Ref. [16], that the model leads to equal Hagedorn temperatures for mesons and for baryons. This is quite obvious. Since baryons are formed by attaching mesons to the "input" baryon, the baryon spectrum grows at exactly the same rate as the meson spectrum. Specific calculations confirm this simple observation. Thus the bootstrap idea *is not capable* of explaining the different behavior of mesons and baryons in Fig. 1.

3.2   Dual String models

The *Dual String models* [7] also date back to pre-QCD times. Their greatest success is a natural explanation of the Regge trajectories – a basic experimental fact which remain a serious problem for other approaches. Similarly to the bootstrap models, the Dual String Models lead to exponentially-growing spectra, but they do give the demanded effect of $T_{meson} > T_{baryon}$, at least at asymptotic masses [6].
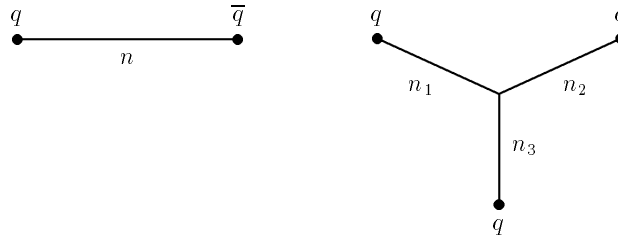
Fig. 5. Meson and baryon string configurations.

Let us analyze mesons first. The particle spectrum is generated by the harmonic-oscillator operator describing vibrations of the string,

$$N = \sum_{k=1}^{\infty} \sum_{\mu=1}^{D} k a_{k,\mu}^{\dagger} a_{k,\mu}, \tag{11}$$

where k labels the modes and μ labels additional degeneracy, related to the number of dimensions [7]. Eigenvalues of N are composed in order to get the square of mass of the meson, according to the Regge formula

$$\alpha' m^2 - \alpha_0 = n, \tag{12}$$

where $\alpha' \sim 1\text{GeV}^{-2}$ is the Regge slope, and $\alpha_0 \approx 0$ is the intercept. Here is an example: take $n = 5$. The value 5 can be formed by taking the $k = 5$ eigenvalue of N (this is the leading Regge trajectory, with a maximum angular momentum), but we can also obtain the same m^2 by exciting one $k = 4$ and one $k = 1$ mode, alternatively $k = 3$ and $k = 2$ modes, and so on. The number of possibilities corresponds to partitioning the number 5 into natural components: 5, 4+1, 3+2, 3+1+1, 2+2+1, 2+1+1+1, 1+1+1+1+1. Here we have 7 possibilities, but the number of partitions grows very fast with n. Partitions with more than one component describe the sub-leading Regge trajectories. With D degrees of freedom each component can come in D different species. Let us denote the number of partitions in our problem as $P_D(n)$. For large n the asymptotic formula for *partitio numerorum* leads to the exponential spectrum according to the formula [17,7].

$$\rho(m) = 2\alpha' m P_D(n), \quad P_D(n) \simeq \sqrt{\frac{1}{2n}} \left(\frac{D}{24n} \right)^{\frac{D+1}{4}} \exp\left(2\pi \sqrt{\frac{Dn}{6}} \right), \tag{13}$$

where $n = \alpha' m^2$. We can now read-off the mesonic Hagedorn temperature:

$$T_{\text{meson}} = \frac{1}{2\pi} \sqrt{\frac{6}{D\alpha'}}. \tag{14}$$

Now the baryons: the "Mercedes-Benz" string configuration for the baryon is shown in Fig. 5. The three strings vibrate *independently*, and the corresponding vibration operators, N, add up. Consequently, their eigenvalues n_1, n_2, and n_3
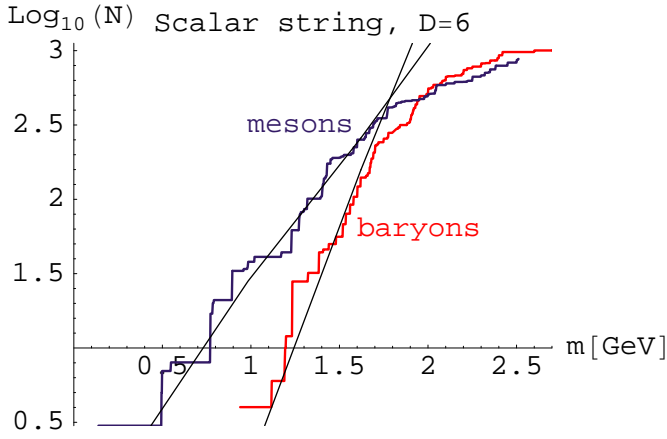
Fig. 6. Predicions of the scalar string model of Ref. [10], with $D = 6$.

add up. Thus we simply have a partition problem with 3 times more degrees of freedom than in the meson. The replacement $D \to 3D$ in (13) leads immediately to

$$T_{baryon} = \frac{1}{2\pi}\sqrt{\frac{2}{D\alpha'}}, \tag{15}$$

such that

$$T_{meson}/T_{baryon} = \sqrt{3}. \tag{16}$$

We stress that the presented picture is fully consistent with the Regge phenomenology. The leading Regge trajectory for baryons is generated by the excitation of a single string, *i.e.* two out of three numbers n_i vanish (this is the quark-diquark configuration). The subleading trajectories for baryons come in a much larger degeneracy than for mesons, due to more combinatorial possibilities. The slopes of the meson and baryon trajectories are universal, and given by α'. We stress that the "number-of-strings" mechanism described above is asymptotic. Thus, there is a problem in applying string models to the experimentally accessible range of m. This range is not asymptotic enough to use Eq. (13). From the Regge formula (12) we find immediately that for m in the range $1 - 2$GeV the values of n lie between 1 and 4, hence n is not large enough to justify the form (13).

One can do better by using an improved asymptotic formula, derived in Ref. [10]. The results obtained in the scalar string model [10] are displayed in Fig. 6. Here the formula for the meson spectrum is

$$\rho_{mes}(m) = 36 \times \rho_{scalar}(m), \quad \rho_{scalar}(m) = \frac{2\alpha'}{(4\pi\alpha' m T_{mes})^\nu} m I_\nu\left(\frac{m}{T_{mes}}\right), \tag{17}$$

where I_2 is a modified Bessel function, T_{mes} is the meson Hagedorn temperature (the *only* adjustable parameter here), and $\nu = 1 + D/2$, with D denoting the number of transverse dimensions. The factor of $36 = 6 \times 6$ is just the spin-flavor degeneracy of the $\bar{q}q$ configuration [10]. For the baryons we fold the three scalar-string densities, $\rho_{scalar}(m)$. We use 56 (rather than 36) copies of the string, which
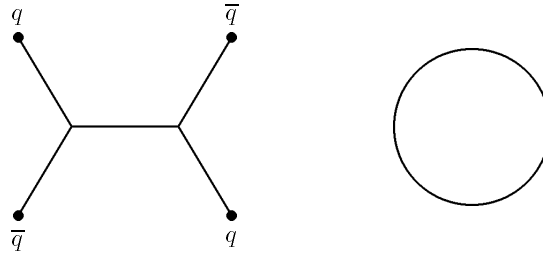
Fig. 7. $\overline{q}q\overline{q}q$ and glueball configurations.

is the degeneracy of the baryon multiplet in the ground state. We notice good agreement with data in Fig. 6, for $D = 6$. Note that both curves are fitted with only one parameter, T_{mes}. For lower values of D one can fit the mesons equally well, but too many baryon states are predicted.

3.3 Exotics as dual strings

During this workshop we have heard many talks on hadron exotics. If an exotic is a multi-string configuration, *e.g.* as in Fig. 7, then the corresponding spectrum will grow exponentially with the Hagedorn temperature inversely proportional to the square root of the number of strings. For instance, $T_{q\overline{q}q\overline{q}} = \frac{1}{\sqrt{5}}T_{meson}$. This is reminiscent of the effect described in Ref. [18]. For the glueballs, described by the closed string in Fig. (7), we get $T_G = T_{meson}$.

Thus, according to the string model, the $q\overline{q}q\overline{q}$ grow more rapidly than non-exotic mesons and baryons, and glueballs grow at the same rate as mesons.

4 Other approaches

In the remaining part of this talk we will, in a sense, work against our results presented in previous sections, where have we argued that the plots of Fig. 1 are linear, and offered an explanation of the difference between the mesonic and baryonic Hagedorn temperatures within the Dual String Models.

What if the experimental plots of Fig. 1 are not really linear, and the effect of bending down of the curves at higher masses is physical, rather than due to incomplete experiments? Below we will show alternative descriptions which do not comply to Eq. (1), but nevertheless reproduce the present data at least as good as the Hagedorn-like fits.

4.1 Compound hadrons

In the statistical model of nuclear reactions one uses the *compound-nucleus model* [19,20]. In this model the density of states grows at large excitation energies, E^*, according to the formula

$$\rho(E) \sim (E^*)^{-5/4} e^{a\sqrt{E^*}}, \tag{18}$$
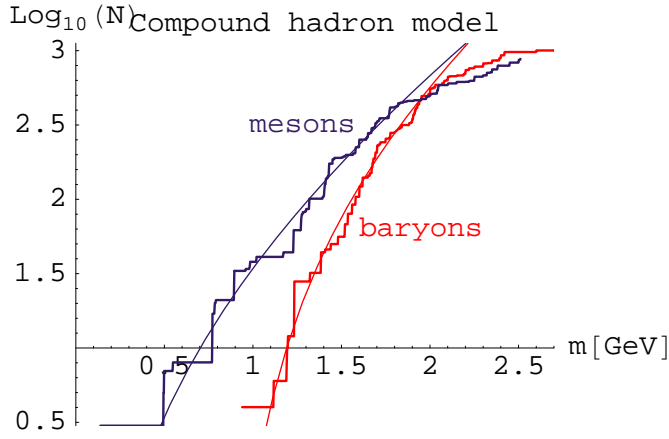
Fig. 8. Fits of the Compound Hadron Model, Eq. (19).

where a is a constant. Formula (18) can be derived within the Fermi gas model [20]. More generally, it can be derived in a model where the single-particle orbits are *equally spaced*. One then considers $1p1h$, $2p2h$, $3p3h$, *etc.*, excitations and counts the number of states at a given excitation energy, E^*. Amusingly, this leads [21] to the partitio numerorum formula (13), but now the number n has the interpretation $n = E^*/\Delta E$, with ΔE denoting the level spacing.

We now use the following Compound-Hadron-Model formula for the mass spectra:

$$\rho(m) = \frac{A\Theta(m - m_0) \exp\left(2\pi\sqrt{\frac{(m - m_0)}{6\Delta E}}\right)}{\left((m - m_0)^2 + (0.5\text{GeV})^2\right)^{5/8}}, \tag{19}$$

where A is a constant, m_0 is the ground-state mass, and ΔE is the average level spacing. The constant 0.5GeV in the denominator has been introduced *ad hoc*, similarly as in Eq. (5), in order for the formula to make sense at $m \to m_0$. Asymptotically, the power of m multiplying the exponent is $-5/4$, as in Eq. (18).

The underlying physical picture behind compound hadrons is as follows: hadrons are bound objects of constituents (quarks, gluons, pions). The Fock space contains a ground state, and excitations on top of it. In the case of the compound nucleus these elementary excitations are $1p1h$, $2p2h$, $3p3h$, *etc.* states. In the case of hadrons they are formed of $q\bar{q}$ and gluon excitations, *e.g.* for mesons we have $q\bar{q}, q\bar{q}g, qq\bar{q}\bar{q}, q\bar{q}gg$, *etc.* We can form the excitation energy (hadron mass) by differently composing elementary excitations. This bring us to the above-described combinatorial problem [21]. It seems reasonable to take zero ground-state energy for mesons, $m_0^{\text{mes}} = 0$, since they are excitations on top of the vacuum. For baryons we take $m_0^{\text{bar}} = 900\text{MeV}$, which is the mass of the nucleon. The quantity ΔE is treated as a model parameter and is fitted to data.

The results of the compound-hadron-model fit, Eq. (19), are shown in Fig. 8. The curves are slightly bent down, compared to the Hagedorn-like fits of Figs. 1,2, which is caused by the square root in the exponent of Eq. (19). But the fits
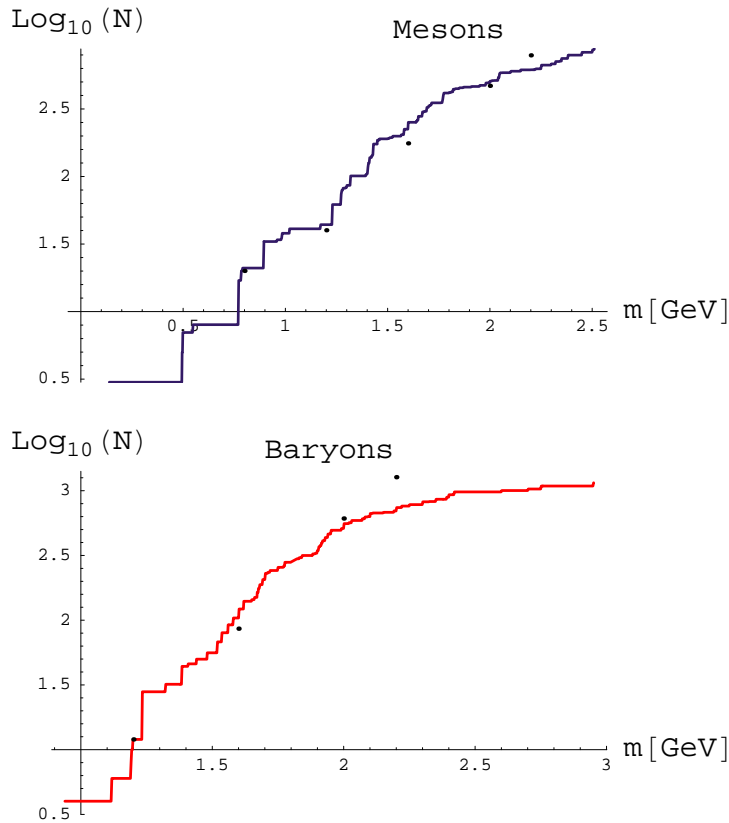
Fig. 9. Experimental cumulants and the predicions of the quark model of Ref. [22,23], as counted in Ref. [9], indicated by dots.

are at least as good, or even better when the fit region is extended to $m = 2\text{GeV}$. Numerically, the least-square fit for m up to 1.8GeV gives $\Delta E^{mes} = 100\text{MeV}$ for mesons, and $\Delta E^{bar} = 106\text{MeV}$ for baryons. The proximity of these numbers shows that the scales for mesons and baryons are similar, as should be the case.

The obtained values for ΔE^{mes} mean that the corresponding n at $m = 1.8\text{GeV}$ is around 18 for mesons and 9 for baryons. Such values of n are sufficiently large to justify the use of the asymptotic formulas.

4.2   Combinatorial saturation and the light-flavor-desert hypothesis

There is a possibility of an interesting effect we wish to point out. It is natural to expect that a bound hadronic system has an upper limit for the excitation energy. It is helpful to think here of bags of finite depth. Thus, in constructing the single-particle Fock space for bound objects we should have a limited number of quanta to our disposal. If such a limit is put into the Compound Hadron Model, it will result in a maximum number of states that can possibly be formed out of light quarks [5]. We can call it the *"light-flavor-desert hypothesis"*: above a certain mass there are no more light-flavor resonances. Certainly, this is tangential to

the conventional wisdom that the Regge trajectories should continue indefinitely. Note, however, that infinite Regge trajectories have recently been challenged by Brisudová, Burakovsky and Goldman, who claim that they should stop around $m \sim 2.7 \text{GeV}$. Amusingly, this is consistent with the presently-available data. The cumulants if Fig. 1 flatten-out in that region.

4.3   Quark models

Many talk in this workshop were devoted to variants of the quark model. Here we present the result of counting of states in the model of Refs. [22,23], as made by Freund and Rosner [9].

When we look at Fig. 9, we again see good agreement in the predicted and experimental number of states. This is not at all surprising, since the quark model is designed to fit the data "state by state" in the low-mass regime. As for other approaches, spectra at higher m would be needed to verify the predictions.

5   Final remarks

There are many fundamental questions which should be cleared when more experimental data on hadron resonances are available: Is the Hagedorn hypothesis of exponentially-growing spectra indeed correct, or is the growth weaker at higher masses? Do the Regge trajectories continue for ever, or stop? Consequently, is there a light-flavor desert above a certain mass? Are there exotic states, if so, at what rate do they grow?... Certainly, the spectrum above 2GeV may reveal many answers and help us to verify various models and approaches.

However, even the presently-available spectrum allows for interesting speculations. Recall the remarks made here by Leonid Glozman, concerning the parity doublets in the N and Δ spectra above 2GeV [24]. Almost all states in that region can be paired, and such a regularity suggests that the data in that region may be complete! This, in turn, indicates that the bending down of the cumulants in Fig. 1 may be a physical, rather than experimental effect.

Another important aspect, not touched in this talk, are the thermodynamical implications of the presence of two distinct Hagedorn temperatures for the phenomenology of heavy-ion collisions, transition to quark-gluon plasma, *etc.* This will be discussed in [21].

References

1. R. Hagedorn, Suppl. Nuovo Cim. 3 (1965) 147
2. R. Hagedorn, CERN preprint No. CERN 71-12 (1971), and references therein
3. R. Hagedorn, CERN preprint No. CERN-TH.7190/94 (1994), and references therein
4. Particle Data Group, Eur. Phys. J. C 3 (1998) 1

5. W. Broniowski and W. Florkowski, INP Cracow preprint No. 1843/PH (2000), `hep-ph//0004104`

6. W. Broniowski, talk presented at *Meson 2000*, 19-23 May 2000, Cracow, `hep-ph//0006020`

7. in Dual Theory, Vol. 1 of Physics Reports reprint book series, edited by M. Jacob (North Holland, Amsterdam, 1974)

8. R. Hagedorn and J. Ranft, Suppl. Nuovo Cim. 6 (1968) 169

9. G. O. Freund and J. L. Rosner, Phys. Rev. Lett. 68 (1992) 765

10. K. R. Dienes and J.-R. Cudell, Phys. Rev. Lett. 72 (1994) 187

11. S. Frautschi, Phys. Rev. **D** 3 (1971) 2821

12. A. Chodos, R. L. Jaffe, K. Johnson, C. B. Thorn, and V. F. Weisskopf, Phys. Rev. **D** 9 (1974) 3471

13. J. Kapusta, Nucl. Phys. **B** 196 (1982) 1

14. R. Gagnon and L. Marleau, Phys. Rev. **D** 35 (1987) 910

15. J. Yellin, Nucl. Phys. **B** 52 (1973) 583

16. W. Nahm, Nucl. Phys. **B** 45 (1972) 525

17. G. H. Hardy and S. S. Ramanujan, Proc. London Math. Soc. 17 (1918) 76

18. J.-R. Cudell and K. R. Dienes, Phys. Rev. Lett. 69 (1992) 1324

19. E. Vogt, in Advances in Nuclear Physics, edited by M. Baranger and E. Vogt (Plenum Press, New York, 1968), Vol. 1, p. 261

20. A. Bohr and B. R. Mottelson, Nuclear Structure (Benjamin, Reading, Massachussetts, 1969), Vol. 1

21. W. Broniowski, W. Florkowski, and P. Żenczykowski, to be published

22. S. Godfrey and N. Isgur, Phys. Rev. **D** 32 (1985) 189

23. S. Capstick and N. Isgur, Phys. Rev. **D** 34 (1986) 2809

24. L. Y. Glozman, Nucl. Phys. **B** 475 (2000) 329

Heavy Baryons, Solitons and Large N_c QCD or A New Emergent Symmetry of QCD

Thomas D. Cohen[*]

Department of Physics, University of Maryland, College Park, 20742-4111, USA.

In this talk I describe some recent work with C. K. Chow on heavy baryons—
i.e. baryons with a single heavy quark. In the combined heavy quark and large
N_c limits of QCD a simple physical picture emerges of such states. The system is
well described by the collective motion of the light quark and gluon degrees of
freedom against the heavy quark. This can be shown by studying commutators of
collective operators with the QCD Hamiltonian in the context of a power count-
ing scheme in which both the heavy quark and the nucleon mass is treated as
heavy. The power counting parameter is λ where $\lambda \sim \Lambda/M_Q,\, , \, 1/N_c$. Collective
excitations have an energy which scale as $\lambda^{1/2}$ and hence all become degener-
ate with the ground state in this combined limit—this indicates the emergence
of a new symmetry. This new symmetry is contracted O(8) and is the spectrum
generating algebra for the three dimensional harmonic oscillator. One can exploit
this symmetry to make model independent predictions of excited state masses,
electro-magnetic and weak transitions of these states up to a fixed order in the
expansion. Unfortunately, the expansion turns out to be in $\lambda^{1/2}$ rather than λ so
the predictive power of this expansion is not clear. However at next-to-leading
order the expansion has only two parameters and several observables (of which
only one has presently been measured) so that the possibility of getting semi-
quantitative information from this expansion is quite real.

[*] E-mail: cohen@physics.umd.edu

A Realistic Description of Nucleon-Nucleon and Hyperon-Nucleon Interactions in the SU_6 Quark Model[*]

Yoshikazu Fujiwara[1][**], M. Kohno[2], C. Nakamoto[3] and Y. Suzuki[4]

[1] Department of Physics, Kyoto University, Kyoto 606-8502, Japan
[2] Physics Division, Kyushu Dental College, Kitakyushu 803-8580, Japan
[3] Suzuka National College of Technology, Suzuka 510-0294, Japan
[4] Department of Physics, Niigata University, Niigata 950-2181, Japan

Abstract. The SU_6 quark model for the NN and YN interactions, developed by the Kyoto-Niigata group, is upgraded to incorporate some effects of scalar and vector mesons exchanged between quarks. The phase-shift agreement in the NN sector at the non-relativistic energies up to $T_{lab} = 350$ MeV is greatly improved. The essential feature of the ΛN-ΣN coupling is qualitatively similar to that obtained from the previous models. The G-matrix calculation of the ΛN-ΣN coupled-channel system shows that the Σ single-particle potential is repulsive in ordinary nuclear matter. The single-particle spin-orbit strength for the Λ particle is found to be very small, in comparison with that of the nucleons.

The quark-model study of the nucleon-nucleon (NN) and hyperon-nucleon (YN) interactions is motivated to gain a natural and accurate understanding of the fundamental strong interaction, in which the quark-gluon degree of freedom is believed to be the most economical ingredient to describe the short-range part of the interaction, while the medium- and long-range parts are dominated by the meson-exchange processes. We have recently achieved a simultaneous and realistic description of the NN and YN interactions in the resonating-group (RGM) formalism of the spin-flavor SU_6 quark model. [1–3] In this approach the effective quark-quark interaction is built by combining a phenomenological quark-confining potential and the colored version of the Fermi-Breit (FB) interaction with minimum effective meson-exchange potentials (EMEP) of scalar and pseudo-scalar meson nonets directly coupled to quarks. The flavor symmetry breaking for the YN system is explicitly introduced through the quark-mass dependence of the Hamiltonian. An advantage of introducing the EMEP at the quark level lies in the stringent relationship of the flavor dependence appearing in the various NN and YN interaction pieces. In this way we can utilize our rich knowledge of the NN interaction to minimize the ambiguity of model parameters, which is crucial since the present experimental data for the YN interaction are still very scarce.

---

[*] Talk delivered by Yoshikazu Fujiwara
[**] E-mail: fujiwara@ruby.scphys.kyoto-u.ac.jp

In this report we upgrade our model to incorporate vector mesons and the momentum-dependent Bryan-Scott terms, and compare the NN and YN observables with the existing experimental data. This model is dubbed fss2 since it is based on our previous model FSS [2,3] The agreement to the phase-shift parameters in the NN sector is greatly improved. The model fss2 shares the good reproduction of the YN scattering data and the essential features of the ΛN-ΣN coupling with our previous models [1–3]. The single-particle (s.p.) potentials of N, Λ and Σ are predicted through the G-matrix calculation, which employs the quark-exchange kernel explicitly. [4] The strength of the s.p. spin-orbit potential is also examined by using these G-matrices. [5] These applications of fss2 are discussed by Kohno in the present symposium.

A new version of our quark model is generated from the Hamiltonian which consists of some extra pieces of interaction generated from the scalar (S), pseudoscalar (PS) and vector (V) meson-exchange potentials acting between quarks:

$$H = \sum_{i=1}^{6} \left(m_i c^2 + \frac{\mathbf{p}_i^2}{2m_i} \right) + \sum_{i<j}^{6} \left(U_{ij}^{Cf} + U_{ij}^{FB} + \sum_{\beta} U_{ij}^{S\beta} + \sum_{\beta} U_{ij}^{PS\beta} + \sum_{\beta} U_{ij}^{V\beta} \right) .$$

It is important to include the momentum-dependent Bryan-Scott term in the S- and V-meson contributions, in order to ensure the correct asymptotic behavior of the s.p. potentials in high-momentum region. [6] We have calculated $U_N(q_1)$ by using the so-called $t^{eff}\rho$ prescription and made sure that it turns into repulsive beyond the incident momentum $q_1 \sim 6$ fm^{-1}, while our old model FSS is too attractive, having the minimum value ~ -70 MeV around $q_1 \sim 10$ fm^{-1}. Another important feature of fss2 is the introduction of vector mesons for improving the fit to the phase-shift parameters in the NN sector. Since the dominant effect of the ω-meson repulsion and the LS components of ρ, ω and K* mesons are already accounted for by the FB interaction, only the quadratic LS (QLS) component of the octet mesons is expected to play an important role to cancel partially the strong one-pion tensor force. Further details of the model fss2 is given in [7]. The model parameters are determined by fitting the most recent result of the phase shift analysis, SP99 [8], for the np scattering with the partial waves $J \leq 2$ and the incident energies $T_{lab} \leq 350$ MeV, under the constraint of the deuteron binding energy and the $^1S_0$ NN scattering length, as well as the low-energy YN total cross sections. The deuteron D-state probability of fss2 is 5.5 %, which is slightly smaller than 5.88 % in FSS [2].

Figure 1 shows some important low-partial wave NN phase-shift parameters, compared with the experiment SP99. The previous result by FSS is also shown with the dotted curves. The $^3D_2$ phase shift is greatly improved by the QLS component. The good accuracy of the NN phase-shift parameters continues up to $T_{lab} \sim 600$ MeV, where the inelasticity of the S-matrix becomes appreciable.

The total cross sections of the NN and YN scattering predicted by fss2 are compared with the available experimental data in Fig. 2. The "total" cross sections for the scattering of charged particles (i.e., pp, Σ^+p and Σ^-p systems) are calculated by integrating the differential cross sections over $\cos\theta_{min} = 0.5 \sim \cos\theta_{max} = -0.5$. The solid curves indicate the result in the particle basis, while the dashed
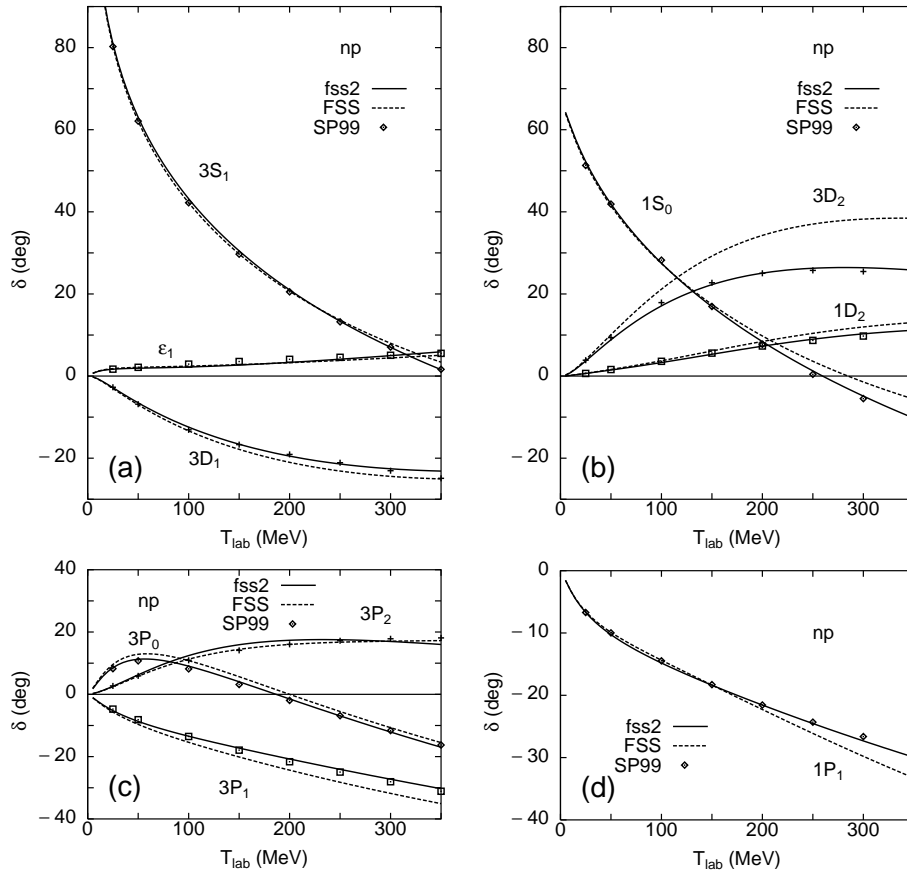
Fig. 1. Comparison of np phase shifts with the phase-shift analysis SP99 by Arndt *et al.* The dotted curves are by FSS.

curves in the isospin basis. In the latter case, the effects of the charge symmetry breaking, such as the Coulomb effect and the small difference of the threshold energies for $\Sigma^- p$ and $\Sigma^0 n$ channels, are neglected. The empirical total cross sections for the np and pp systems include the inelastic cross sections. This is the reason why our result with no inelasticity underestimate these total cross sections above the pion threshold. If we properly compare the total elastic cross sections with an appropriate angular range, we find that the agreement with the experiment is excellently good up to $T_{lab} = 800$ MeV. We find that the cusp structure of the Λp total cross sections at the ΣN threshold is enhanced by the effect of the P-wave ΛN-ΣN coupling due to the antisymmetric spin-orbit force ($LS^{(-)}$ force), which is a new feature of the YN interaction as the scattering of non-identical particles.
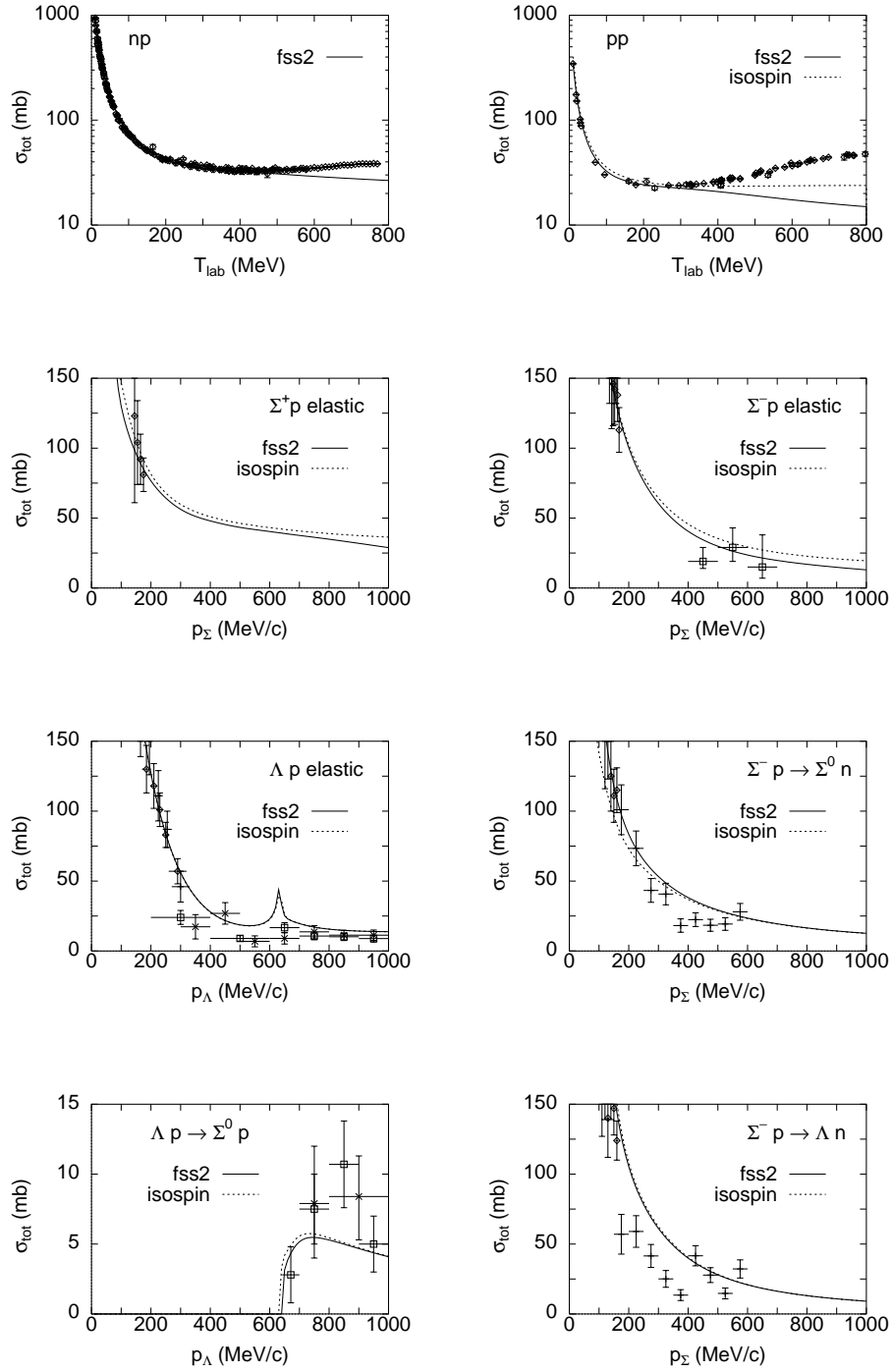
Fig. 2. Calculated NN and YN total cross sections compared with the available experimental data.

In the present model fss2, the $\Sigma N(I = 1/2)$ $^3P_1$ resonance still stays at the ΣN channel, which is similar to the situation in RGM-H [2]. As to the ΛN-ΣN coupling in the positive-parity states, the present $^3S_1$-$^3D_1$ tensor coupling by the one-pion tensor force is rather close to that in RGM-F [1]. The Σ^-p inelastic capture ratio at rest is $r_R = 0.442$ in fss2, which is slightly smaller than the recent empirical values $r_R{}^{exp} = 0.474 \pm 0.016$ and 0.465 ± 0.011 [9,10].

In summary, we have upgraded our quark model FSS to fss2, by incorporating the momentum-dependent Bryan-Scott term and the vector-meson exchange potential acting between quarks. With a few phenomenological ingredients, the accuracy of the model in the NN sector has now become almost comparable to that of the OBEP models. The existing data for the YN scattering are well reproduced and the essential feature of the ΛN-ΣN coupling is almost unchanged from our previous models. [1,2] We also calculated NN and YN G-matrices in ordinary nuclear matter, by solving the Bethe-Goldstone equations for the quark-exchange kernel. Similar to our previous models, fss2 predicts a repulsive Σ s.p. potential, the strength of which is about 10 MeV. The repulsive isoscalar part of the Σ s.p. potential is reported to be compatible with recent BNL $(K^-, \pi^{\pm})$ data [11]. The relative ratio of the Scheerbaum factors for Λ to N is about $1/5$ in fss2, due to the strong effect of $LS^{(-)}$ force and the effect of the flavor symmetry breaking. It can be further reduced by many-body effects such as the starting-energy dependence and the density dependence of the G-matrix. This small spin-orbit potential for the Λ might be confirmed in future experiments.

References

1. Y. Fujiwara, C. Nakamoto and Y. Suzuki, Prog. Theor. Phys. **94** (1995) 215, 353.
2. Y. Fujiwara, C. Nakamoto and Y. Suzuki, Phys. Rev. Lett. **76** (1996) 2242; Phys. Rev. **C54** (1996) 2180.
3. T. Fujita, Y. Fujiwara, C. Nakamoto and Y. Suzuki, Prog. Theor. Phys. **100** (1998), 931.
4. M. Kohno, Y. Fujiwara, T. Fujita, C. Nakamoto and Y. Suzuki, Nucl. Phys. **A674** (2000), 229.
5. Y. Fujiwara, M. Kohno, T. Fujita, C. Nakamoto and Y. Suzuki, Nucl. Phys. **A674** (2000), 493.
6. Y. Fujiwara, M. Kohno, C. Nakamoto and Y. Suzuki, Theor. Phys. **103** (2000), 755.
7. Y. Fujiwara, M. Kohno, C. Nakamoto and Y. Suzuki, The electric proceedings of this workshop. http://www-f1.ijs.si/Bled2000.
8. Scattering Analysis Interactive Dial-up (SAID), Virginia Polytechnic Institute, Blacksburg, Virginia R. A. Arndt: Private Communication.
9. V. Hepp and H. Schleich, Z. Phys., **214** (1968), 71.
10. D. Stephen, Ph.D. thesis, Univ. of Massachusetts, 1970 (unpublished)
11. J. Dabrowski: Phys. Rev. **C60** (1999), 025205.

Baryon Structure in the Low Energy Regime of QCD

Leonid Ya. Glozman*

Institute for Theoretical Physics, University of Graz, Universitätsplatz 5, A-8010 Graz, Austria

I review the key problem of light and strange baryon spectroscopy, which suggests a clue for our understanding of underlying dynamics. Then I discuss the spontaneous breaking of chiral symmetry in QCD. In the region of spontaneously broken chiral symmetry, where the Goldstone boson degree of freedom is important, the structure of the elementary excitation of the QCD vacuum can be approximately reproduced by absorption of the scalar interaction between bare (current) quarks into the mass of the quasi particles - i.e. constituent quarks. This implies that in the low-energy regime the proper chiral dynamics is due to the coupling of Goldstone bosons and constituent quarks and that the nucleon should be viewed as a system of confined constituent quarks that interact via the Goldstone boson exchange (GBE) [1]. The GBE interaction contains both the ultraviolet (short range) part, which is independent of pion mass, and the infrared (Yukawa) part. The latter one is important for the long-range nuclear force, but it does not produce any significant effect in baryons because of their small matter radius. The short-range part of the GBE interaction causes a flavor-spin dependent force between quarks and has a range Λ_χ^{-1}. While the infrared (Yukawa) part of the interaction vanishes in the chiral limt, the ultraviolet one - does not [2]. This means that the short-range part of the GBE interaction is "more fundamental" than its Yukawa part. This short-range part of the GBE interaction stems from the γ_5 structure of the vertex and hence is demanded by the Lorentz invariance. At the microscopical level this short range interaction comes from the t-channel iterations of that bare gluonic interaction between quarks that is responsible for chiral symmetry breaking [3]. This is a typical antiscreening behavior; the interaction is represented by a bare gluonic vertex at large momenta, but it blows up at small momenta in the GBE channel due to the (Landau) pole that occures at $q^2 = 0$. I show how this explicitly flavor-dependent short-range part of GBE interaction, when combined with the $SU(6)$ symmetry (that is demanded by large N_c limit in QCD), solves the key problem of baryon spectroscopy and present baryon spectra obtained in a simple analytical calculation [1] as well as in covariant three-body calculations [4]. Finally I show recent lattice results [5–8] and comment on their connection with the present physical picture.

* E-mail: lyg@physik.kfunigraz.ac.at

References

1. L. Ya. Glozman and D. O. Riska, Phys. Rep. **268**, 263 (1996).
2. L. Ya. Glozman, Phys. Lett. **B459** 589 (1999)
3. L. Ya. Glozman and K. Varga, Phys. Rev. **D61**, 074008 (2000)
4. L. Ya. Glozman, W. Plessas, K. Varga, and R. Wagenbrunn, Phys. Rev. **D58** 094030 (1998)
5. K. F. Liu et al, Phys. Rev. **D59** 112001 (1999)
6. S. Sasaki, hep-ph/0004252
7. S. Aoki et al, Phys. Rev. Lett. **82**, 4592 (1999)
8. J. I. Skullerud and A. G. Williams, hep-lat/0007028

Spin polarisabilities of the nucleon at NLO in the chiral expansion[*]

Judith A. McGovern[1][**], Michael C. Birse[1], K. B. Vijaya Kumar[2]

[1] Theoretical Physics Group, Department of Physics and Astronomy, University of Manchester, Manchester, M13 9PL, U.K.
[2] Department of Physics,University of Mangalore, Mangalore 574 199, India

Abstract. We present a calculation of the fourth-order (NLO) contribution to spin-dependent Compton scattering in heavy-baryon chiral perturbation theory, and we give results for the four spin polarisabilities. No low-energy constants, except for the anomalous magnetic moments of the nucleon, enter at this order. The NLO contributions are as large or larger than the LO pieces, making comparison with experimental determinations questionable. We address the issue of whether one-particle reducible graphs in the heavy baryon theory contribute to the polarisabilities.

1 Introduction

The usual notation for the Compton scattering amplitude in the Breit frame is, for incoming real photons of energy ω and momentum $\mathbf{q}$ to outgoing real photons of the same energy energy and momentum $\mathbf{q}'$,

$$
\begin{aligned}
T = {}& \epsilon'^{\mu}\Theta_{\mu\nu}\epsilon^{\nu} \\
= {}& \epsilon' \cdot \epsilon\, A_1(\omega,\theta) + \epsilon' \cdot \hat{\mathbf{q}}\,\epsilon \cdot \hat{\mathbf{q}}'\, A_2(\omega,\theta) \\
& +i\sigma \cdot (\epsilon' \times \epsilon)\, A_3(\omega,\theta) + i\sigma \cdot (\hat{\mathbf{q}}' \times \hat{\mathbf{q}})\,\epsilon' \cdot \epsilon\, A_4(\omega,\theta) \\
& +\Big(i\sigma \cdot (\epsilon' \times \hat{\mathbf{q}})\,\epsilon \cdot \hat{\mathbf{q}}' - i\sigma \cdot (\epsilon \times \hat{\mathbf{q}}')\,\epsilon' \cdot \hat{\mathbf{q}}\Big)\, A_5(\omega,\theta) \\
& +\Big(i\sigma \cdot (\epsilon' \times \hat{\mathbf{q}}')\,\epsilon \cdot \hat{\mathbf{q}}' - i\sigma \cdot (\epsilon \times \hat{\mathbf{q}})\,\epsilon' \cdot \hat{\mathbf{q}}\Big)\, A_6(\omega,\theta),
\end{aligned}
\tag{1}
$$

where hats indicate unit vectors. By crossing symmetry the functions A_i are even in ω for $i = 1, 2$ and odd for $i = 3 - 6$. The leading pieces in an expansion in powers of ω are given by low-energy theorems[1], and the next terms contain the electric and magnetic polarisabilities α and β and the spin polarisabilities γ_i:

$$
A_1(\omega,\theta) = -\frac{Q^2}{m_N} + 4\pi(\alpha + \cos\theta\beta)\omega^2 + \mathcal{O}(\omega^4)
$$

$$
A_2(\omega,\theta) = -4\pi\beta\omega^2 + \mathcal{O}(\omega^4)
$$

$$
A_3(\omega,\theta) = \frac{e^2\omega}{2m_N^2}\Big(Q(Q + 2\kappa) - (Q + \kappa)^2\cos\theta\Big) + 4\pi\omega^3(\gamma_1 + \gamma_5\cos\theta) + \mathcal{O}(\omega^5)
$$

[*] Talk delivered by Judith McGovern
[**] E-mail: judith.mcgovern@man.ac.uk
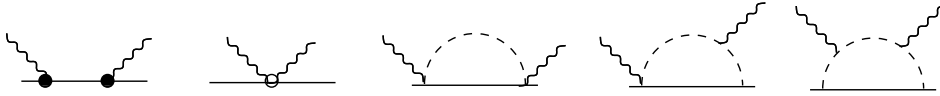
Fig. 1. Diagrams which contribute to spin-dependent Compton scattering in the $\epsilon \cdot v = 0$ gauge at LO. The solid dots are vertices from $\mathcal{L}^{(2)}$ and the open circle is a vertex from $\mathcal{L}^{(3)}$.

$$A_4(\omega, \theta) = -\frac{e^2 \omega}{2m_N^2}(Q + \kappa)^2 + 4\pi\omega^3\gamma_2 + \mathcal{O}(\omega^5)$$

$$A_5(\omega, \theta) = \frac{e^2 \omega}{2m_N^2}(Q + \kappa)^2 + 4\pi\omega^3\gamma_4 + \mathcal{O}(\omega^5)$$

$$A_6(\omega, \theta) = -\frac{e^2 \omega}{2m_N^2}Q(Q + \kappa) + 4\pi\omega^3\gamma_3 + \mathcal{O}(\omega^5) \tag{2}$$

where the charge of nucleon is $Q = (1 + \tau_3)/2$ and its anomalous magnetic moment is $\kappa = (\kappa_s + \kappa_v\tau_3)/2$. Only four of the spin polarisabilities are independent since three are related by $\gamma_5 + \gamma_2 + 2\gamma_4 = 0$. The polarisabilities are isospin dependent.

Compton scattering from the nucleon has recently been the subject of much work, both experimental and theoretical. The unpolarised polarisabilities have been well known for a number of years now, at least for the neutron, but it is only very recently that determinations of the spin polarisabilities have been extracted from fixed-t dispersion analyses of photoproduction data. The forward spin polarisability $\gamma_0 = \gamma_1 + \gamma_5$ has a longer history, with determinations that are in the range of recent values, namely -0.6 to -1.5×10^{-4} fm^4 for the proton.[2–5] Direct measurements of the polarised cross-section at MAMI have been used to obtain a value of -0.8×10^{-4} fm^4, as reported by Pedroni at the GDH200 conference. No direct measurements of polarised Compton scattering have yet been attempted. However the backwards spin polarisability $\gamma_\pi = \gamma_1 - \gamma_5$ has recently been extracted from unpolarised Compton scattering from the proton. The LEGS group[6] obtained -27×10^{-4} fm^4, far from the previously accepted value of -37×10^{-4} fm^4, which is dominated by t-channel pion exchange. In contrast results presented by Wissmann at the GDH2000 conference give a value extracted from TAPS data which is compatible with the old value.

2 Polarisabilities in HBCPT

The non-spin polarisabilities have previously been determined to NLO (fourth order) in heavy baryon chiral perturbation theory (HBCPT). The values are in good agreement with experiment, with the NLO contribution (where LEC's enter) being small compared to the LO part (which comes from pion-nucleon loops). The spin polarisabilities have also been calculated;[7] at lowest order the value $\gamma_0 = \alpha_{em}g_A^2/(24\pi^2 f_\pi^2 m_\pi^2) = 4.51$ is obtained for both proton and neutron, where the entire contribution comes from πN loops.[8] The effect of the Δ enters in counter-terms at fifth order in standard HBCPT, and has been estimated to be
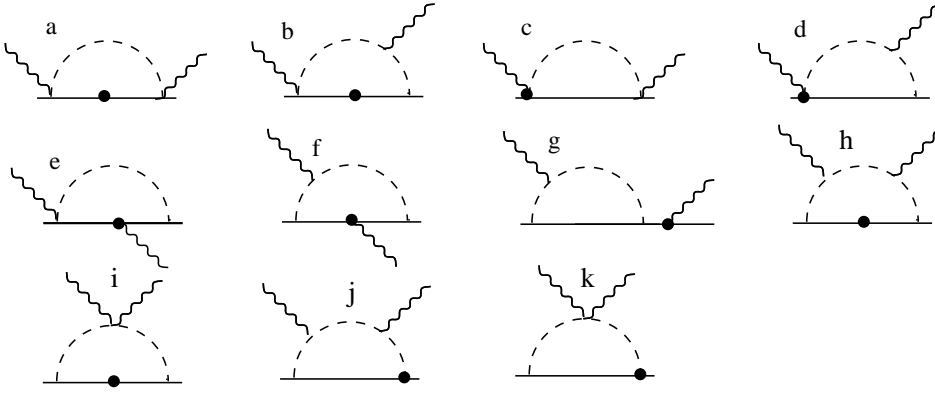
Fig. 2. Diagrams which contribute to spin-dependent forward Compton scattering in the $\epsilon \cdot v = 0$ gauge at NLO. The solid dots are vertices from $\mathcal{L}^{(2)}$.

so large as to change the sign[8]. The calculation has also been done in an extension of HBCPT with an explicit Δ by Hemmert *et al.*[9] They find that the principal effect is from the Δ pole, which contributes -2.4, with the effect of $\pi\Delta$ loops being small, -0.2. Clearly the next most important contribution is likely to be the fourth-order πN piece, and this is the result which is presented here.[10]

Two other groups have also presented fourth order calculations of the spin polarisabilities recently; Ji *et al.* calculated γ_0 and obtained an expression in complete agreement with ours.[11] Gellas *et al.* have also calculated all four polarisabilities.[12] Their calculations agree with ours, but we disagree on what constitutes the polarisabilities; we will say more about this later.

In HBCPT the fixed terms in the amplitudes A_3 to A_6 are reproduced at leading (third) order, by the combination of the Born terms and the seagull diagram. The same terms are produced entirely from Born graphs in the relativistic theory, but integrating out the antinucleons generates a seagull term in the third-order Lagrangian which has a fixed coefficient.[8] This illustrates a point to which we will come back, namely that one cannot determine by inspection which graphs in HBCPT are one-particle reducible. The loop diagrams of Fig. 1 have contributions of order ω which cancel and so do not affect the LET, while the ω^3 terms give the polarisabilities at this order.

At NLO, the diagrams which contribute are given in Fig. 2. In the Breit frame, only diagrams 2a-h contribute, and there can be no seagulls at this order. It follows that there are no undetermined low-energy constants in the final amplitude. When the amplitudes are Taylor expanded, there are contributions at order ω and ω^3. The former do not violate the LETs, however. The third-order contributions to the LETs actually involve the bare values of κ which enter in the second-order Lagrangian. However κ_v has a pion loop contribution at the next order: $\delta\kappa_v = -g_A^2 m_\pi M_N / 4\pi f_\pi^2$. This then contributes to the fourth-order Compton scattering amplitude. Reproducing these terms is one check on our calculations. The order ω^3 pieces give the polarisabilities. The requirement $\gamma_5 + \gamma_2 + 2\gamma_4 = 0$ is satisfied, which provides another non-trivial check on the results.

The loop contributions to the polarisabilities to NLO are

$$\gamma_1 = \frac{\alpha_{em} g_A^2}{24\pi^2 f_\pi^2 m_\pi^2} \left[1 - \frac{\pi m_\pi}{8 M_N} (8 + 5\tau_3) \right]$$

$$\gamma_2 = \frac{\alpha_{em} g_A^2}{48\pi^2 f_\pi^2 m_\pi^2} \left[1 - \frac{\pi m_\pi}{4 M_N} (8 + \kappa_v + 3(1 + \kappa_s)\tau_3) \right]$$

$$\gamma_3 = \frac{\alpha_{em} g_A^2}{96\pi^2 f_\pi^2 m_\pi^2} \left[1 - \frac{\pi m_\pi}{4 M_N} (6 + \tau_3) \right]$$

$$\gamma_4 = \frac{\alpha_{em} g_A^2}{96\pi^2 f_\pi^2 m_\pi^2} \left[-1 + \frac{\pi m_\pi}{4 M_N} (15 + 4\kappa_v + 4(1 + \kappa_s)\tau_3) \right]$$

$$\gamma_0 = \frac{\alpha_{em} g_A^2}{24\pi^2 f_\pi^2 m_\pi^2} \left[1 - \frac{\pi m_\pi}{8 M_N} (15 + 3\kappa_v + (6 + \kappa_s)\tau_3) \right] \tag{3}$$

Although the subleading pieces have a factor of m_π/M_N compared with the leading piece, the numerical coefficients are often large. The anomalous magnetic moments are $\kappa_s = -0.12$ and $\kappa_v = 3.71$; with these values the numerical results for the polarisabilities to fourth order are

$$\gamma_1 = [-21.3\tau_3] + 4.5 - (2.1 + 1.3\tau_3)$$
$$\gamma_2 = 2.3 - (3.1 + 0.7\tau_3)$$
$$\gamma_3 = [10.7\tau_3] + 1.1 - (0.8 + 0.1\tau_3)$$
$$\gamma_4 = [-10.7\tau_3] - 1.1 + (3.9 + 0.5\tau_3)$$
$$\gamma_0 = 4.5 - (6.9 + 1.5\tau_3)$$
$$\gamma_\pi = [-42.7\tau_3] + 4.5 + (2.7 - 1.1\tau_3) \tag{4}$$

The term in square brackets, where it exists, is the third-order t-channel pion exchange contribution. (There is no fourth-order contribution.)

The NLO contributions are disappointingly large, and call the convergence of the expansion into question. While the fifth-order terms have also been estimated to be large,[8] this is due to physics beyond πN loops, namely the contribution of the Δ. Our results show that even in the absence of the Δ, convergence of HBCPT for the polarisabilities has not yet been reached.

3   Comments on the definition of polarisabilities

We now return to the difference between our results and those of the Jülich group, who give expressions for the polarisabilities which are analytically and numerically different from ours. The entire difference comes from the treatment of diagram 2g, which we include in the polarisabilities and they omit. The polarisabilities are not in fact usually defined as in Eq. 2, but as the first term in the expansion of the amplitudes after subtraction of the "Born terms". This removes the LET terms, but, depending on the model used for the Born graphs, also some ω-dependent terms. Gellas *et al.* argue that the contribution of 2g should also be removed by this subtraction.

There are two main objections to this definition. First, it is not model- and representation-dependent, as the one-particle reducible part of 2g beyond the LET piece involves an off-shell "formfunction" or "sideways formfactor", and as stressed by Scherer [13], these cannot be unambiguously defined. Furthermore the procedeure Gellas *et al.* have adopted does not respect Lorentz invariance. At this order there are terms that vanish in the Breit frame which are in fact generated by a lowest-order boost of the third-order (fully irreducible) loop amplitude. (In the centre-of-mass frame these show up as pieces with, apparently, the wrong crossing symmetry: they are even in ω in amplitudes A_3 to A_6, and start at ω^4). However the prescription of Gellas *et al.* discards the contribution of 2g to these pieces, violating the boost invariance of the resulting LO+NLO amplitude. (As Meißner explained in his talk, their prescription is to discard the part of 2g which has the form $f(\omega)/\omega$, where f is analytic. In fact pieces like this also arise from other diagrams, notably 2f, while diagrams 2a-e, though apparently irreducible, contribute LET pieces. The distinction between reducible and irreducible in HBCPT is hidden, as mentioned earlier.)

The other objection to excluding so much from the definition of the polarisability is that, even if it is done consistently, it does not correspond to the definition used in the extraction from fixed-t dispersion relations. There, the polarisabilities are related to the integral of the imaginary part of the amplitudes over the cut, where the amplitudes used have effectively been subtracted at the point where an intermediate nucleon would be on shell.[4] This can at most change the spin polarisabilities by something of order $\alpha_{em} m_{\scriptscriptstyle N}^{-4}$, which is small numerically and is NNLO in HBCPT.

Thus the exclusion of 2g from the "structure constants" such as polarisabilities is neither a consistent definition, nor one that corresponds to dispersion relation determinations.

References

1. F. Low, Phys. Rev. **96** 1428 (1954); M. Gell-Mann and M. Goldberger, Phys. Rev. **96** 1433 (1954).
2. A. M. Sandorfi, C. S. Whisnant and M. Khandaker, Phys. Rev. **D 50** R6681 (1994).
3. D. Drechsel, G. Krein and O. Hanstein, Phys. Lett. **B 420** 248 (1998).
4. D. Babusci, G. Giordano, A. I. L'vov, G. Matone and A. M. Nathan, Phys. Rev. **C 58** 1013 (1998).
5. D. Drechsel, M. Gorchtein, B. Pasquini and M. Vanderhaeghen, Phys. Rev. **C 61** 015204 (2000).
6. J. Tonnison, A. M. Sandorfi, S. Hoblit and A. M. Nathan, Phys. Rev. Lett. 80 4382 (1998).
7. V. Bernard, N. Kaiser and U.-G. Meißner, Int. J. Mod. Phys. E **4** 193 (1995).
8. V. Bernard, N. Kaiser, J. Kambor and U.-G. Meißner, Nucl. Phys. **B 388** 315 (1992).
9. T. R. Hemmert, B. R. Holstein J. Kambor and G. Knöchlein, Phys. Rev. **D 57** 5746 (1998).
10. K. B. V. Kumar, J. A. McGovern and M. C. Birse, `hep-ph/9909442`.
11. X. Ji, C-W. Kao and J. Osborne, Phys. Rev. **D 61** 074003 (2000).
12. G. C. Gellas, T. R. Hemmert and U.-G. Meißner, `nucl-th/0002027`.
13. S. Scherer, *Czech. J. Phys.* **49** 1307 (1999).

The anomalous $\gamma \to \pi^+\pi^0\pi^-$ form factor and the light–quark mass functions at low momenta[⋆]

Dubravko Klabučar[1][⋆⋆], Bojan Bistrović[2]

[1] Physics Department, P.M.F., Zagreb University, Bijenička c. 32, Zagreb, Croatia
[2] Center for Theoretical Physics, Laboratory for Nuclear Science and Department of Physics, Massachusetts Institute of Technology, Cambridge, Massachusetts 02139

Abstract. The $\gamma \to 3\pi$ form factor was calculated in a simple–minded constituent model with a constant quark mass parameter, as well as in the Schwinger-Dyson approach. The comparison of these and various other theoretical results on this anomalous process, as well as the scarce already available data (hopefully to be supplemented by more accurate CEBAF data), seem to favor Schwinger–Dyson modeling which would yield relatively small low–momentum values of the constituent (dynamically dressed) quark mass function.

The Abelian-anomalous $\pi^0 \to \gamma\gamma$ amplitude is exactly [1,2] $T_\pi^{2\gamma}(m_\pi = 0) = e^2 N_c/(12\pi^2 f_\pi)$ in the chiral and soft limit of pions of vanishing mass m_π. On similarly fundamental grounds, the anomalous amplitude for the $\gamma(q) \to \pi^+(p_1) \pi^0(p_2)\pi^-(p_3)$ process, is predicted [3] to be

$$F_\gamma^{3\pi}(0,0,0) = \frac{1}{ef_\pi^2} T_\pi^{2\gamma}(0) = \frac{eN_c}{12\pi^2 f_\pi^3}\,, \tag{1}$$

also in the chiral limit and at the soft point, where the momenta of all three pions vanish: $\{p_1, p_2, p_3\} = \{0, 0, 0\}$. While the chiral and soft limit are an excellent approximation for $\pi^0 \to \gamma\gamma$, the already published [4] and presently planned Primakoff experiments at CERN [5], as well as the current CEBAF measurement [6] of the $\gamma(q) \to \pi^+(p_1)\pi^0(p_2)\pi^-(p_3)$, involve values of energy and momentum transfer which are not negligible compared to typical hadronic scales. This gives a lot of motivation for theoretical predictions of the $\gamma \to 3\pi$ amplitude for non–vanishing $\{p_1, p_2, p_3\}$, *i.e.*, the form factor $F_\gamma^{3\pi}(p_1, p_2, p_3)$. We calculated it as the quark "box"-amplitude (see Fig. 1) in the two related approaches [7,8] sketched below.

In our Ref. [7], the intermediate fermion "box" loop is the one of "simple" constituent quarks with the constant quark mass parameter M. The isospinor $\Psi = (u, d)^\top$ of the light constituent quarks couple to the isovector pions π^a through the pseudoscalar Yukawa coupling $g\gamma_5\tau^a$. Its constant quark-pion coupling

---

[⋆] Talk delivered by Dubravko Klabučar
[⋆⋆] E-mail: klabucar@phy.hr
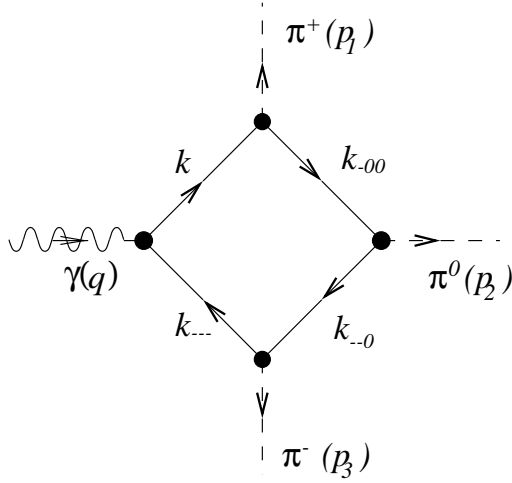
Fig. 1. One of the box diagrams for the process $\gamma(q) \rightarrow \pi^+(p_1)\pi^0(p_2)\pi^-(p_3)$. The other five are obtained from this one by the permutations of the vertices of the three different pions.

strength g is related to the pion decay constant $f_\pi = 92.4$ MeV through the quark-level Goldberger-Treiman (GT) relation $g/M = 1/f_\pi$. The result of this calculation also corresponds to the form factor, in the lowest order in pion interactions, of the sigma-model and of the chiral quark model. In Ref. [7], we give the analytic expression for the form factor in terms of an expansion in the pion momenta up to the order $\mathcal{O}(p^8)$ relative to the soft point result, and also perform its exact numerical evaluation. The latter predictions of this quark loop model [7] are given [normalized to the soft-point amplitude (1)] in Fig. 2 by the long-dashed curve for $M = 330$ MeV, by the line of empty boxes for $M = 400$ MeV, and by the line of crosses for the large value $M = 580$ MeV. Note that in the lowest order in pion interactions, they are also the form factors of the σ-model and of the chiral quark model.

Our second Ref. [8] employs the Schwinger-Dyson (SD) approach [9], which is consistent both with the chiral symmetry constraints in the low-energy domain and with the perturbative QCD in the high-energy domain. In this approach, quarks in the fermion loop do not have free propagators with the simple-minded constant constituent mass M. Instead, the box loop amplitude is evaluated with the dressed quark propagator

$$S(k) = \frac{1}{i\slashed{k}\,A(k^2) + m + B(k^2)} \equiv \frac{Z(k^2)}{i\slashed{k} + \mathcal{M}(k^2)} \tag{2}$$

containing the *momentum-dependent*, mostly dynamically generated quark mass function $\mathcal{M}(k^2)$ following from the SD solution for the dressed quark propagator (2). The explicit chiral symmetry breaking $m(\sim 2$ MeV in the present model choice [10,8]) is two orders of magnitude smaller than the quark mass function *at small momenta*, where it corresponds to the notion of the constituent quark mass. Indeed, in Refs. [10,8] as well as in the model choice reviewed in our Ref. [11],
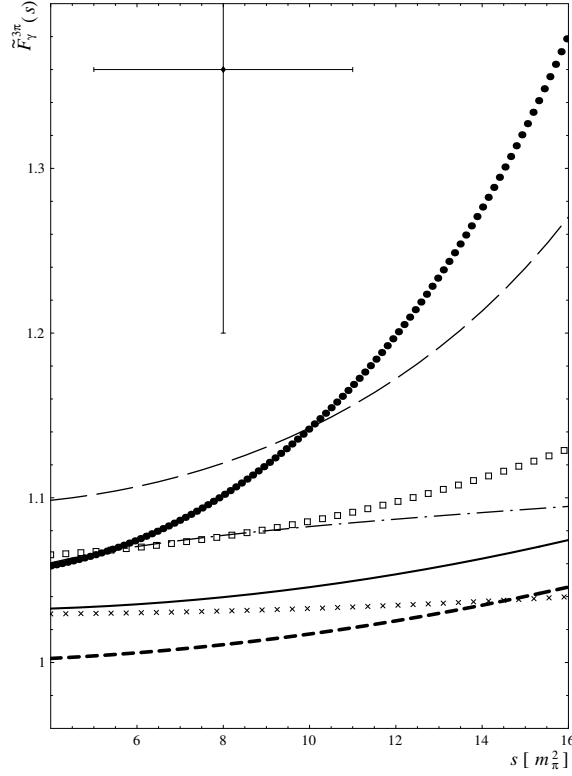
Fig. 2. Various predictions for the dependence of the normalized $\gamma 3\pi$ form factor $\widetilde{F}_\gamma^{3\pi}$ on the Mandelstam variable $s \equiv (p_1 + p_2)^2$. The kinematics is as in the Serpukhov measurement (which provided[4] the shown data point): the photon and all three pions are on shell, $q^2 = 0$ and $p_1^2 = p_2^2 = p_3^2 = m_\pi^2$.

$\mathcal{M}(k^2 \sim 0) \sim 300$ to 400 MeV. On the other hand, since already the present–day SD modeling is well–based [9] on many aspects of QCD, such SD–generated $\mathcal{M}(k^2)$ should be close to the true QCD quark mass function.

SD approach employs the Bethe–Salpeter (BS) bound–state pion–quark–antiquark vertex $\Gamma_{\pi^a}(k, p_{\pi^a})$ (here, in Fig. 1, instead of the aforementioned momentum–independent Yukawa coupling). The propagator (2) is consistent with the solution for the BS solution for $\Gamma_{\pi^a}(k, p_{\pi^a})$, and then, in this approach, the light pseudoscalar mesons are simultaneously the quark-antiquark bound states and the (quasi) Goldstone bosons of dynamical chiral symmetry breaking [9]. Thanks to this, and also to carefully preserving the vector Ward-Takahashi identity in the quark-photon vertex, the *both* fundamental anomalous amplitudes $T_\pi^{2\gamma}(0)$ and $F_\pi^{3\pi}(0,0,0)$ for the respective decays $\pi^0 \to \gamma\gamma$ and $\gamma \to \pi^+\pi^0\pi^-$, are evaluated analytically and exactly in the chiral limit and the soft limit [10]. (Note that reproducing these results even only roughly, let alone analytically, is otherwise quite problematic for bound-state approaches, as discussed in Ref. [11].)

In Fig. 2, the solid curve gives our $\gamma 3\pi$ form factor obtained in the SD approach for the empirical pion mass, $m_\pi = 138.5$ MeV, while the dashed curve

gives it in the chiral limit, $m_\pi = 0 = m$. To understand the relationship between the predictions of these two approaches, one should, besides the curves in Fig. 2, compare also the analytic expressions we derived for the form factors [esp. Eqs. (20)–(21) in Ref. [8] and analogous formulas in Ref. [7]]. This way, one can see, first, why the constant, momentum-independent term is smaller in the SD case, causing the downward shift of the SD form factors with respect to those in the constant constituent mass case. Second, this constant term in the both approaches diminishes with the increase of the pertinent mass scales, namely M in the constant-mass case, and the scale which rules the SD–modeling and which is of course closely related to the resulting scale of the *dynamically generated* constituent mass $\mathcal{M}(k^2 \sim 0)$. Finally, the momentum–dependent terms are similar in the both approaches; notably, the coefficients of the momentum expansions (in powers of $p_i \cdot p_j$) are similarly suppressed by powers of their pertinent scales. This all implies a transparent relationship between $\mathcal{M}(k^2)$ at small k^2 and the $\gamma 3\pi$ form factor, so that the accurate CEBAF data, which hopefully are to appear soon [6], should be able to constrain $\mathcal{M}(k^2)$ at small k^2, and thus the whole infrared SD modeling. Admittedly, we used the Ball–Chiu Ansatz for the dressed quark–photon vertex, but this is adequate since Ref. [12] found that for $-0.4\,\mathrm{GeV}^2 < q^2 < 0.2\,\mathrm{GeV}^2$, the true solution for the dressed vertex is approximated well by this Ansatz plus the vector–meson resonant contributions which however vanish in our case of the real photon, $q^2 = 0$. Therefore, if the experimental form factor is measured with sufficient precision to judge the present SD model results definitely too low, it will be a clear signal that the SD modeling should be reformulated and refitted so that it is governed by a smaller mass scale and smaller values of $\mathcal{M}(k^2 \sim 0)$.

The only already available data, the Serpukhov experimental point [4] (shown in the upper left corner of Fig. 2), is higher than all theoretical predictions and is probably an overestimate. However, the SD predictions are farthest from it. Indeed, in the momentum interval shown in Fig. 2, the SD form factors are lower than those of other theoretical approaches (for reasonable values of their parameters) including vector meson dominance [13] (the dotted curve) and of chiral perturbation theory [14] (the dash-dotted curve). Therefore, even the present experimental and theoretical knowledge indicates that the momentum–dependent mass function in the SD model [10] we adopted [8], may already be too large at small k^2, where its typical value for light u, d quarks is $\mathcal{M}(k^2 \approx 0) \approx 360$ MeV. Note that this value is, at present, probably the lowest in the SD–modeling except for the model reviewed in Ref. [11], which has very similar $\mathcal{M}(k^2)$ at low k^2. (Some other very successful [9] SD models obtain even higher values, $\mathcal{M}(k^2 \approx 0) \approx 600$ MeV and more, which would lead to even lower $\gamma 3\pi$ transition form factors.) It is thus desirable to reformulate SD phenomenology using momentum–dependent mass functions which are smaller at low k^2. This conclusion is in agreement with recent lattice QCD studies of the quark propagator which find [15] $\mathcal{M}(k^2 = 0) = 298 \pm 8$ MeV (for $m = 0$).

ipation at Mini-Workshop Bled 2000: FEW-QUARK PROBLEMS, Bled, Slovenia, 8–15 July 2000.

References

1. S. L. Adler, Phys. Rev. **177**, 2426 (1969).
2. J. S. Bell and R. Jackiw, Nuovo Cim. **A60**, 47 (1969).
3. S. L. Adler *et al.*, Phys. Rev. **D 4** (1971) 3497; M. V. Terent'ev, Phys. Lett. **38B** (1972) 419; R. Aviv and A. Zee, Phys. Rev. **D 5** (1972) 2372.
4. Yu. M. Antipov *et al.*, Phys. Rev. **D 36** (1987) 21.
5. M. A. Moinester *et al.*, e-print `hep-ex/9903017`, and proceedings of 37th International Winter Meeting on Nuclear Physics, Bormio, Italy, 25-29 Jan 1999.
6. R. A. Miskimen, K. Wang and A. Yagneswaran, *Study of the Axial Anomaly using the* $\gamma\pi^+ \to \pi^+\pi^0$ *Reaction ...*, Letter of intent, CEBAF-experiment 94-015.
7. B. Bistrović and D. Klabučar, Phys. Rev. **D 61** (2000) 033006.
8. B. Bistrović and D. Klabučar, Phys. Lett. **B 478** (2000) 127-136.
9. A recent review is: C. D. Roberts, e-print `arXiv:nucl-th/0007054`.
10. R. Alkofer and C. D. Roberts, Phys. Lett. **B 369**, 101 (1996).
11. D. Kekez, B. Bistrović, and D. Klabučar, Int. J. Mod. Phys. **A 14**, (1999) 161.
12. P. Maris and P. Tandy, Phys. Rev. **C 61** (2000) 045202.
13. S. Rudaz, Phys. Lett. **B 145** (1984) 281.
14. B. Holstein, Phys. Rev. **D 53** (1996) 4099.
15. J. I. Skullerud and A. G. Williams, e-print `hep-lat/0007028`.

Nuclear matter and hypernuclear states calculated with the new SU_6 Quark Model Kyoto-Niigata potential[*]

Michio Kohno[1][**], Y. Fujiwara[2], C. Nakamoto[3] and Y. Suzuki[4]

[1] Physics Division, Kyushu Dental College, Kitakyushu 803-8580, Japan
[2] Department of Physics, Kyoto University, Kyoto 606-8502, Japan
[3] Suzuka National College of Technology, Suzuka 510-0294, Japan
[4] Department of Physics, Niigata University, Niigata 950-2181, Japan

Abstract. Nuclear matter saturation curves and hyperon single-particle (s.p.) properties in nuclear matter are presented, using the new version of the SU_6 quark model Kyoto-Niigata potential. The Σ s.p. potential is turned out to be repulsive. The s.p. spin-orbit strength for the Λ becomes small due to the $LS^{(-)}$ component. With these favorable results in view of the experimental data, the extension of the quark model predictions to the strangeness -2 sector is in progress.

The spin-flavor SU_6 quark model provides a unified framework to describe the NN and YN interactions. Because of the scarcity of the experimental information in the strangeness sector it is interesting and valuable to discuss quantitative predictions of the quark model potential. In refs. [1,2] we presented G-matrix calculations for the NN, ΛN and ΣN interactions in nuclear matter, using the Kyoto-Niigata potential FSS [3,4]. As Fujiwara explained in his talk in this workshop, we upgraded the FSS to the new version fss2 to remedy the insufficient description at higher energies by incorporating the momentum dependent Bryan-Scott terms and vector mesons.

Since the quark model potential is defined in a form of RGM kernel, we first define partial wave Born amplitudes in momentum space by numerical angle integration. This amplitude is applied to solve the Bethe-Goldstone equation. Nuclear matter saturation curves with the QTQ and the continuous choices for intermediate spectra are shown in Fig. 1, compared with the results from the Paris [5] and the Bonn-B [6] potentials. The result demonstrates that the quark model potential works as well as the sophisticated OBEP in spite of the different description of the short-ranged repulsive interaction.

The s.p. potentials $U(k)$ of N, Λ and Σ calculated by the G-matrices with the continuous choice for intermediate spectra are shown in Fig. 2. It is noted that the Σ s.p. potential turns out to be repulsive, reflecting the characteristic repulsion in the $^3S_1 + ^3D_1$ channel of the isospin $3/2$, which is in line with the recent analysis [7] of the $(K^-, \pi^\pm)$ experimental spectra.

---

[*] Talk delivered by Michio Kohno
[**] E-mail: kohno@kyu-dent.ac.jp
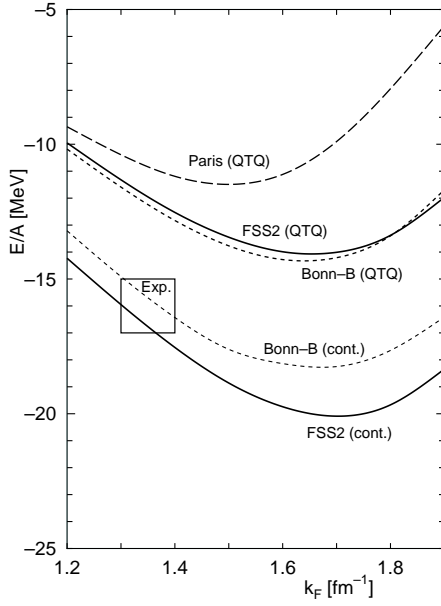
Fig. 1. Nuclear matter saturation curves
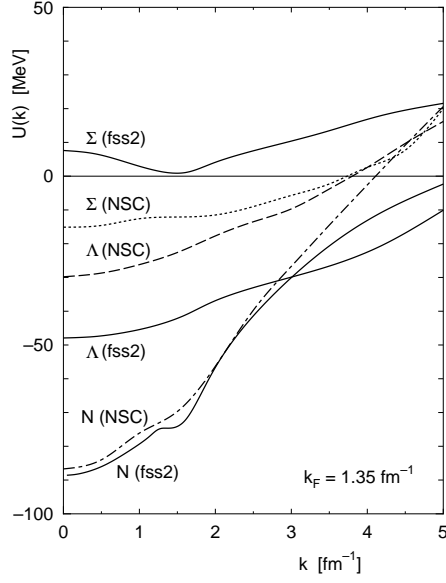
Fig. 2. Nucleon, Λ and Σ s.p. potentials $U(k)$ in nuclear matter with $k_F = 1.35$ fm^{-1}, using the quark model potential fss2. Results by Schulze *et al.* [8] with the Nijmegen NSC potential [9] are also shown.

Another interesting quantity is the strength of the s.p. spin-orbit potential, which is characterized by the strength S_B in the Thomas form:

$$U_B^{\ell s}(r) = -\frac{\pi}{2} S_B \frac{1}{r} \frac{d\rho(r)}{dr} \ell \cdot \sigma \ .$$

The quark model description of the YN interaction contains the antisymmetric spin-orbit ($LS^{(-)}$) component which originates from the Fermi-Breit LS interaction. The large cancellation between the LS and $LS^{(-)}$ contributions in the isospin $I = 1/2$ channel leads to a small s.p. spin-orbit potential for the Λ, $S_\Lambda/S_N \sim 0.26$, which is favourably compared with recent experimental data. The short-range correlation is also found to reduce the S_Λ/S_N. On the other hand $S_\Sigma/S_N \sim 0.54$. Detailed accounts of the s.p. spin-orbit strengths are reported in ref. [2].

Encouraged by these successful predictions of the quark model NN and YN interactions, we are now preparing the studies of the effective interactions in the $\Lambda\Lambda$-$\Sigma\Sigma$-ΞN channel and the multi Λ hyperonic nuclear matter.

References

1. M. Kohno, Y. Fujiwara, T. Fujita, C. Nakamoto and Y. Suzuki, Nucl. Phys. **A674** (2000) 229.
2. Y. Fujiwara, M. Kohno, T. Fujita, C. Nakamoto and Y. Suzuki, Nucl. Phys. **A674** (2000) 493.
3. Y. Fujiwara, C. Nakamoto and Y. Suzuki, Phys. Rev. Lett. **76** (1996) 2242; Phys. Rev. **C54** (1996) 2180.
4. T. Fujita, Y. Fujiwara, C. Nakamoto and Y. Suzuki, Prog. Theor. Phys. **100** (1998) 931.
5. M. Lacombe *et al.*, Phys. Rev. **C21** (1980) 861.
6. R. Machleidt, Adv. Nucl. Phys. **19** (1989) 189.
7. J. Dabrowski, Phys. Rev. **C60** (1999) 025205.
8. H.-J. Schulze *et al.*, Phys. Rev. **C57** (1998) 704.
9. P. Maessen, Th.A. Rijken and J.J.de Swart, Phys. Rev. **C40** (1989) 2226.

Exact treatment of the Pauli operator in nuclear matter[*]

Michio Kohno[1][**], K. Suzuki[2], R. Okamoto[2] and S. Nagata[3]

[1] Physics Division, Kyushu Dental College, Kitakyushu 803-8580, Japan
[2] Department of Physics, Kyushu Institute of Technology, Kitakyushu 804-8550, Japan
[3] Department of Applied Physics, Miyazaki University, Miyazaki 889-2192, Japan

Abstract. Exact formulae are derived for the matrix element of the Pauli operator Q in the Bethe-Goldstone equation and the binding energy per particle in nuclear matter. Numerical calculations are carried out, using the Bonn B potential and the quark model Kyoto-Niigata potential fss2. The exact treatment of the operator Q brings about non-negligible attractive contribution to the binding energy compared with the standard angle average approximation. However the difference is rather small, which quantitatively demonstrates the good quality of the angle average prescription in nuclear matter calculations.

The Pauli principle plays an essential role in the nucleon-nucleon scattering in nuclear medium. It constrains single particle momenta of intermediate two particles to be above the Fermi momentum k_F. The Pauli operator Q is defined as

$$Q = \frac{1}{2} \sum_{\alpha\beta} |\alpha\beta\rangle\langle\alpha\beta| \, \Theta(k_\alpha - k_F) \, \Theta(k_\beta - k_F) \, .$$

The operator Q depends not only on the magnitude of total and relative momenta of scattering two nucleons but also on their relative angles. Properties of this angular dependence, owing to which partial waves with different angular momenta are coupled, were investigated in the early stage of the development of the Brueckner theory. Werner presented explicit coupled equations in 1959 [1]. However, since the numerical calculations are rather involved, the standard angle average approximation has been introduced to avoid the difficulty.

The matrix element of the operator Q between angular-momentum-coupling states is given as

$$\langle \mathbf{K}k(\ell_1 S_1)J_1 M_1 T_1 T_{z1}|Q|\mathbf{K}'k'(\ell_2 S_2)J_2 M_2 T_2 T_{z2}\rangle$$
$$= \delta(\mathbf{K} - \mathbf{K}')\frac{\delta(k - k')}{k^2}\delta_{S_1 S_2}\delta_{T_1 T_2}\delta_{T_{z1} T_{z2}}Q(\ell_1 J_1 M_1, \ell_2 J_2 M_2 : S_1 T_1 k K \theta_K \phi_K) \, .$$

We derived [2] useful analytic expressions for the $Q(\ell_1 J_1 M_1, \ell_2 J_2 M_2 : S_1 T_1 k K \theta_K \phi_K)$ as

$$Q(\ell_1 J_1 M_1, \ell_2 J_2 M_2 : ST k K \theta_K \phi_K)$$

---

[*] Talk delivered by Michio Kohno
[**] E-mail: kohno@kyu-dent.ac.jp

$$= f_{\ell_1 ST}\, f_{\ell_2 ST}\, \{\, \delta_{\ell_1 \ell_2}\delta_{J_1 J_2}\delta_{M_1 M_2}\, x_0 + \sum_{L>0,\,L=\text{even}} (-1)^{S+M_1}\, \frac{\sqrt{4\pi}\,\hat{\ell}_1 \hat{\ell}_2 \hat{J}_1 \hat{J}_2}{\hat{L}^3}$$

$$\times \langle \ell_1 0 \ell_2 0 | L 0\rangle \langle J_1 -M_1 J_2 M_2 | L M\rangle Y_{LM}(\theta_K, \phi_K) W(\ell_1 J_1 \ell_2 J_2; SL)[P_{L+1}(x_0) - P_{L-1}(x_0)]\} \,,$$

where θ_K and ϕ_K are the polar angles of the c.m. momentum $\mathbf{K}$, $\hat{\ell} \equiv \sqrt{2\ell+1}$,

$$f_{\ell ST} \equiv \frac{1-(-1)^{\ell+S+T}}{2} \quad \text{and} \quad x_0 = \begin{cases} 0 & \text{for} \quad k < \sqrt{k_F^2 - K^2/4}, \\ \frac{K^2/4 + k^2 - k_F^2}{Kk} & \text{for} \quad \sqrt{k_F^2 - K^2/4} < k < k_F + K/2, \\ 1 & \text{otherwise.} \end{cases}$$

We also presented practical expressions for the nucleon single particle potential, based on which numerical calculations of the ground state energy were carried out.
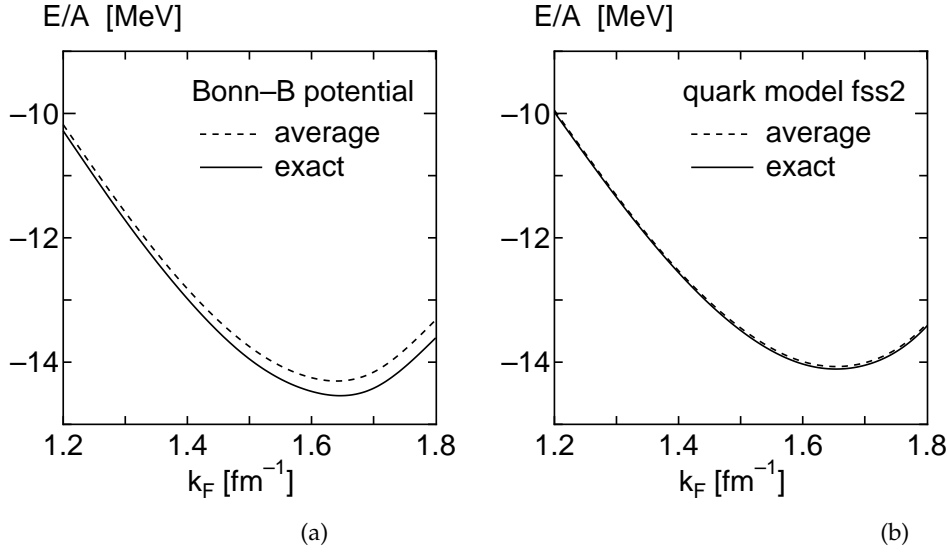
Fig. 1. Energies per nucleon in symmetric nuclear matter as a function of the Fermi momentum k_F: (a) Bonn-B potential [3] and (b) quark model potential fss2 [4].

Calculated saturation curves with the Bonn B potential [3] and the new version of the quark model Kyoto-Niigata potential fss2 [4] are shown in Fig. 1, where results with the exact Pauli operator and the angle averaged one are compared. The exact treatment of the Pauli operator brings about attractive contributions to the binding energy per nucleon at any nuclear densities. However the difference is rather small, although the results somewhat depend on the nucleon-nucleon interaction employed. This quantitatively confirms the good quality of the angle average approximation. The same conclusion was obtained by Schiller, Müther and Czerski [5]. It is suggested that the angle average treatment of the Pauli operator in considering more than three-body correlations is reliable.

References

1. E. Werner, Nucl. Phys. **10** (1959), 688-697.
2. K. Suzuki, R. Okamoto, M. Kohno and S. Nagata, Nucl. Phys. **A665** (2000) 92-104.
3. R. Machleidt, Adv. Nucl. Phys. **19** (1989) 189.
4. Y. Fujiwara, talk given in this workshop.
5. E. Schiller, H. Müther and P. Czerski, Phys. Rev. **C59** (1999) 2934; Phys. Rev. **C60** (1999) 059901.

The new driving mechanism for nuclear force: lessons of the workshop[*]

Vladimir I. Kukulin[**]

Institute of Nuclear Physics, Moscow State University, 119899 Moscow, Russia

Abstract. Instead of the Yukawa mechanism for intermediate- and short-range interaction, some new approach based on formation of the symmetric six-quark bag in the state $|(0s)^6[6]_X, L = 0\rangle$ dressed due to strong coupling to π, σ and ρ fields are suggested. This new mechanism offers both a strong intermediate-range attraction which replaces the effective σ-exchange (or excitation of two isobars in the intermediate state) in traditional force models and also short-range repulsion. Simple illustrative model is developed which demonstrates clearly how well the suggested new mechanism can reproduce NN data. Some important lessons of the workshop discussions have been included in the talk.

It was found in recent years that the traditional models for NN forces, based on the Yukawa concept of one- or two-meson exchanges between free nucleons even at the quark level lead to numerous disagreements with newest precise experimental data for few-nucleon observables (especially for spin-polarised particles) [1–3]. There are also various inner inconsistencies and disagreements between the traditional NN force models and predictions of fundamental theories for meson-baryon interaction (e.g. for meson-nucleon cut-off factors). All these disagreements stimulate strongly new attempts to develop alternative force models based either on chiral perturbation theory or a new quark-meson models.

Our recent studies in the field [1–3] have led us to a principally new mechanism for intermediate- and short-range NN forces – the so called "dressed" bag mechanism which is able to explain the failure of the traditional Yukawa exchange models and also to solve many long-standing puzzles in the field. This mechanism has good resources in explanation of many fundamental difficulties of modern hadronic physics, e.g. the puzzles in baryon spectroscopy (e.g. normal ordering in Λ-sector and inverse ordering in nucleon sector for excited negative and positive parity states), the complicated interplay between NN short-range repulsion and intermediate range attraction, the ABC-puzzle in 2π-production in pp and pd collisions etc.

The new model is based on the important observation [4] that two possible six-quark space symmetries in even NN partial waves (for illustration we consider here the S-wave only), viz. $|s^6[6]L = 0\rangle$ and $|s^4p^2[42]L = 0\rangle$ correspond to the states of different nature. The first states have almost equal projections

---

[*] The respective original work included in the talk was done jointly with Drs. I.T.Obukhovsky, V.N.Pomerantsev and Prof. A. Faessler
[**] E-mail:kukulin@nucl-th.sinp.msu.ru

into the NN, $\Delta\Delta$ and CC channels and thus correspond to bag-like intermediate states while the states of second type are projected mainly onto NN channel and thus can be considered as clusterised NN states with *nodal* NN relative motion wavefunctions. In the present work we develop this picture much further on the quark-meson microscopic basis and derive the microscopic NN transition amplitudes through six-quark $+2\pi$ intermediate states in s-channel (see Fig. 1).

The transition is accompanied by a virtual emission and subsequent absorption of two tightly correlated pions by diquark pairs or, alternatively, by two $1p$-shell quarks when they jump from the $1p$- to the $0s$-shell orbit or vice versa. These two pions can form both the scalar σ and vector ρ mesons which surround the symmetric six-quark bag.
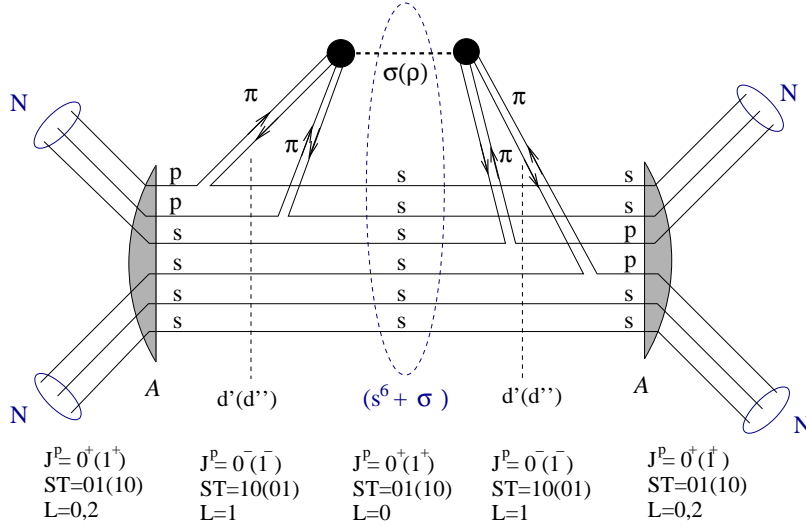
Fig. 1. The graph illustrates two sequential π-meson emissions and absorptions via an intermediate σ- (or ρ-) meson cloud and the generation of a symmetric six-quark bag.

It follows from previous studies (see e.g. [5]) for chiral symmetry restoration effects in multiquark systems or in high density nuclear matter that some phase transition happens when the quark density or the temperature of the system is increased, which leads to a (partial) restoration of the broken chiral symmetry. The consequence of the above restoration is a strengthening of the sigma-meson field in the NN overlap region and reduction of the constituent quark mass. This could be modeled by "dressing" of the most compact six-quark configurations $|s^6[6]_X L = 0\rangle$ and $|s^5 p[51]_X L = 1\rangle$ inside the NN overlap region with an effective sigma-meson field. The resulting scalar- and vector-meson clouds will stabilize the multi-quark bag due to a (partial) chiral symmetry restoration effect in the dense multi-quark system and thus enhance all the contributions of such a type. Thus, the picture of NN interaction emerged from the model can be referred to as the 6q "dressed" bag (DB) model for baryon-baryon interaction [1–3].

The light "σ" or a similar "scalar-isoscalar meson" with mass $m \sim 300$ MeV is assumed to exist only in a high density environment and not in the vacuum, contrary to the π and ρ mesons. This mechanism, being combined with an additional orthogonality requirement[6], can describe both the short-range repulsion and the medium range attraction and can replace the t-channel exchange by σ- and ω-mesons in the conventional Yukawa-type picture of the NN force.

The direct calculation of the multiloop diagram on Fig. 1 [1,2] using quark pair-creation model results for S- and D-partial waves (in NN-channel) in a separable operator of form:

$$
V_E^{L'L}(r',r) = \begin{pmatrix} g_0^2 G_{00}(E)|2s(r')\rangle\langle 2s(r)| & g_0 g_2 G_{02}(E)|2s(r')\rangle\langle 2d(r)| \\ g_2 g_0 G_{20}(E)|2d(r')\rangle\langle 2s(r)| & g_2^2 G_{22}(E)|2d(r')\rangle\langle 2d(r)| \end{pmatrix}, \quad (1)
$$

where the generalised propagators $G_{ll'}(E)$ are related to the DB intermediate state [1,2]. The interaction given by Eq.(1) can be interpreted as an effective NN potential in our model.

In accordance with this, the contribution of mechanism displayed in the diagram in FIG. 1 to the NN interaction in the S and D partial waves can be expressed through the matrix element:

$$
A_{NN \to d_0 + \sigma \to NN}^{L'L} = \int d^3 r' d^3 r \Psi_{NN}^{L'}{}^*(E; \mathbf{r}') V_E^{L'L}(\mathbf{r}', \mathbf{r}) \Psi_{NN}^L(E; \mathbf{r}), \quad (2)
$$

where Ψ_{NN}^L and $\Psi_{NN}^{L'}$ are the "proper" nodal NN scattering wave functions in initial and final state respectively.

The interaction operator (1) mixes S- and D-partial waves in the triplet NN channel and thus it leads to a specific tensor mixing with the range ~ 1 fm (about that of the intermediate DB state). Thus the proposed new mechanism for NN interaction induced by the intermediate dressed six-quark bag $|s^6 + 2\pi\rangle$ results in a specific matrix separable form of interaction with *nodal* (in S- in P-partial waves) form factors and a specific tensor mixing of new type [7].

An important question is arising in this development, what is an interrelation between the new above mechanism and the traditional picture of NN interaction emerged from RGM. Let us to remind that the consistent RGM description (i.e. with no σ-meson exchange between quarks), as was additionally confirmed by Fl. Stancu in this Workshop, leads to purely repulsive NN interaction. The strength of the repulsion is likely of right magnitude because it reproduces well the slope of NN S-wave phase shifts at $E > 200$ MeV. Hence the new mechanism for NN interaction considered here, which leads to a strong intermediate-range attraction, being combined to the above RGM picture, is able to provide full quark-meson microscopic framework for quantitative description of fundamental nuclear force.

Moreover, the proposed model will lead to the appearance of strong 3N and 4N forces mediated by 2π and ρ exchanges [3]. In this Workshop Prof. Moszkowski has suggested to use specific features of 3N force resulted from the new model to explain the saturation properties of nuclear matter. It should emphasized in this connection that the 3N force followed from the new model has a new feature of

"substitution" when the nuclear matter density arises. In this case the enhancement of the attractive 3N force contribution should be accompanied by the respective weakening two-body attractive contributions and vice versa. So by this specific mechanism at the sufficiently high density the nuclear matter dynamics will be governed mainly by three- and four-body nuclear forces rather than two-body contributions. And this specific "substitution" mechanism leads, as is evident, to relativistic Walecka model, in contrast to conventional force models.

The new 3N force includes both central and spin-orbit components. Such a spin-orbit 3N force is extremely desirable to explain the low energy puzzle of the analyzing power A_y in N-d scattering and also the behavior of A_y in the 3N system at higher energies $E_N \simeq 250 \div 350$ MeV at backward angles. The central components of the 3N and 4N forces are expected to be strongly attractive and thus they must contribute to 3N and (may be) 4N binding energies possibly resolving hereby the very old puzzle with the binding energies of the lightest nuclei.

Future studies must show to what degree such expectations can be justified.

References

1. A. Faessler, V. I. Kukulin, I. T. Obukhovsky and V. N. Pomerantsev, E-print:nucl-th/9912074.
2. V. I. Kukulin, I. T. Obukhovsky and V. N. Pomerantsev, A. Faessler, *Phys. Atom. Nucl. in press*.
3. V. I. Kukulin, *Proceeds. of the V Winter School on Theoretical Physics PIYaF, Gatchina, S.-Petersburg, 8 – 14 Febr. 1999.*, p. 142;
4. A. M. Kusainov, V. G. Neudatchin, and I. T. Obukhovsky, Phys.Rev. **C 44**, 2343 (1991).
5. T. Hatsuda and T. Kunihiro, Phys. Rep. **247**, 221 (1994); T. Hatsuda, T. Kunihiro and H. Shimizu, Phys.Rev.Lett. **82**, 2840 (1999).
6. V. I. Kukulin, V. N. Pomerantsev, and A. Faessler, Phys.Rev. **C 59**, 3021 (1999); V.I. Kukulin and V.N. Pomerantsev, Nucl.Phys. **A 631**, 456c (1998).
7. V. I. Kukulin, V. N. Pomerantsev, S. G. Cooper and R. Mackintosh, Few-Body Systems, Suppl. **10**, 439 (1998).

NJL Model and the Nuclear Tightrope

Steve A. Moszkowski*

UCLA, Los Angeles, USA

1 Introduction

Tightrope is balancing act. There are actually two aspects to this:
I. Large two nucleon scattering lengths and
II. Small Nuclear Binding Energies relative to Rest Energy.
Both of these were known since the 1930's. However, the NJL Model can help to get more basic understanding.

2 Large Two Nucleon Scattering Lengths

Large scattering length = small binding (or antibinding).
For T=0, S=1 (d), we get binding = 2.22 MeV, a = 5.4 fm , while for T=1, S=0 (pp), we get antibinding = 0.1 MeV, a = -23 fm. Clearly, it requires only a slight change in the potential to get zero binding.
Splitting (to both sides of tightrope!) is due to spin-dependence. Without it we would not be here! But its role in quark-nuclear physics is unclear. Neglect spin-dependence for now.

3 Scalar Meson Exchange with NJL Model

For a review of the NJL model, see Klevansky [1] and Vogl and Weise [2]. We will not discuss the model here, but only mention two important consequences for the Sigma (Scalar Meson) Exchange Interaction:
1. The mass of the sigma is:

$$m_\sigma = 2\,m_q = 2M/N_c \tag{1}$$

so that the $q - \bar{q}$ forms a state with zero binding relative to the constituent quarks. (This is if we neglect any explicit chiral symmetry breaking, which means that the current quark mass, and thus also the pion mass, is neglected.)
2. The strength of the equivalent Yukawa interaction is:

$$\frac{g^2}{4\pi} \approx \pi N_c, \tag{2}$$

---

* E-mail: stevemos@ucla.edu

(provided the NJL Cutoff is at m_σ)

This is not far from the strength required to get $a = \infty$ and $N_b = \frac{N_c - 1}{2}$ deeply bound states.

Some other points: OPEP (with empirical pion mass) gives only 30 percent of binding.

We need a repulsion to get rid of deeply bound states. Goldstone-Boson exchange can lead to such a repulsion, see Bartz and Stancu [3], though it is not the only possible explanation.

4   Small Nuclear Binding Energies Relative to Rest Energy

4.1   Known Results

BE/A of nuclei ranges up to 8.5 MeV.
BE/A of nuclear matter $\approx$ 16 MeV.
Rest Energy/A = 938 MeV.
Binding energies are only about 1 percent of rest energies!

4.2   NJL Model For Nuclear Matter

We are actually describing quark matter. There is no confinement or quark clustering in the NJL model.

Consider first a toy model in two dimensions.

$$T = \frac{g_c \rho}{2} \qquad \text{for small } \rho \tag{3}$$

$$W = -\frac{(g - g_c)\rho}{2} \tag{4}$$

This expression for W applies for ρ up to the value where $m_q = 0$. g_c is the critical value of g necessary to just give two body binding in 2D.

$$W = c_1 \rho^{1/2} - c_2 + c_3 \rho^{-1} \qquad \text{for larger } \rho \tag{5}$$

We get saturation, but with zero quark mass!

For a more realistic model in three dimensions, the calculations are more complicated, but one still gets saturation with zero quark mass, similar to 2D.

4.3   Generalized NJL Model (With J. da Providencia)

Assume $q - \bar{q}$ coupling gets stronger with density:

$g_s = \frac{g}{[1 - b(g - g_c)^2 \rho^2]}$ This still preserves chiral symmetry (with dependence on ρ^2). Effective scalar coupling $g_s = (b + 1)(g - g_c)$ but we need vector meson with coupl. $g_v = b(g - g_c)$ to get same low ρ result. We (somewhat arbitrarily) identify b with $b = N_b = \frac{N_c - 1}{2}$ We can solve the Generalized NJL model numerically. Note that the correction opposes chiral symmetry restoration.

We can make a low density expansion. For energy per particle and neglecting all kinetic energies:

$$\frac{W}{m} \approx -\frac{g\rho}{2} + bg^2\rho^2 + \dots \tag{6}$$

$$\frac{W}{M} \approx -\frac{g\rho}{2N_c} + \frac{(N_c - 1)g^2\rho^2}{2N_c} + \dots \tag{7}$$

Here m denotes the constituent quark mass and $M = N_c\, m$ the nucleon mass. For the effective mass, which is the ratio of either mass in the medium to that in free space, we have:

$$m^* = 1 - g\rho + \dots \tag{8}$$

$$g\rho_0 = \frac{1}{2(N_c - 1)} = (1 - m^*) \tag{9}$$

Apart from kinetic energies, the saturation energy per nucleon is:

$$\frac{W_0}{M} = -\frac{1}{8N_c(N_c - 1)} \tag{10}$$

For $N_c = 3$, $W_0 = -20 MeV$ (CLOSE to empirical value!)

4.4   Connection with Relativistic Mean Field Theory at Low Density

In the relativistic mean field approach, the nuclear matter energy per particle, (neglecting kinetic energy) is given by:

$$\frac{W(m^*, \hat{\rho})}{M} = m^* - 1 + \frac{B_v\,\hat{\rho}}{2} + \frac{(1 - m^*)^2}{2B_s\hat{\rho}\,m^{*\,\alpha_s}} \tag{11}$$

Here m^* denotes the effective mass in units of the free nucleon mass. The Walecka and Zimanyi-Moszkowski derivative coupling models [4] correspond to $\alpha_s = 0, 2$ respectively. If $B \ll 1$, then $B_v \approx B_s \approx B$. We then obtain, for small densities:

$$m^* = 1 - B\hat{\rho} + \dots \tag{12}$$

$$\frac{W}{M} = \frac{\alpha_s B^2}{2}(-2\hat{\rho} + \hat{\rho}^2) + \dots \tag{13}$$

Comparing the effective mass, with that from the generalized NJL model, we see that:

$$B = \frac{1}{2(N_c - 1)} \tag{14}$$

$$W_0 = -M\frac{\alpha_s B^2}{2} = -M\frac{\alpha_s}{8(N_c - 1)^2} \tag{15}$$

For $\alpha_s = 1$, we reproduce the results of the generalized NJL model, at least for large N_c. This is intermediate between the original Walecka model and the derivative coupling model and is close to the hybrid model used by Glendenning, Weber and S.M. [5]. Of course, the mean field models, unlike the generalized NJL model, lead to finite energies at all densities, but the GNJL is slightly less phenomenological.

5 Open Problems

NJL is like a quark shell model, see Petry et. al. [6] and Talmi [7]. How to include effect of quark clustering, without losing NJL simplifications?
Relation of Effective Vector repulsion to short range correlations?
Can Goldstone Boson Exchange do the job, or do we need non-localities, as in Moscow potential?
Where does the density dependence of g_s come from?

References

1. S. P. Klevansky, Rev. Mod. Phys. **64** (1992) 649.
2. U. Vogl, W. Weise, Prog. Part. Nucl. Phys. **27** (1991) 195.
3. D.Bartz, Fl. Stancu, Phys. Rev. C **59** (1999) 1756.
4. J. Zimanyi, S. A. Moszkowski, Phys. Rev. C **42** (1990) 1416.
5. N. K. Glendenning, F. Weber, S. A. Moszkowski, Phys. Rev. C **45** (1992) 844.
6. H. R. Petry et al., Phys. Lett. B **159** (1985) 363.
7. I. Talmi, Phys. Lett. B **205** (1988) 140.

Treatment of three-quark problems in Faddeev theory[*]

Zoltan Papp[1,2][**], A. Krassnigg[2], and W. Plessas[2]

[1] Institute of Nuclear Research of the Hungarian Academy of Sciences, H–4001 Debrecen, Hungary
[2] Institute for Theoretical Physics, University of Graz, A–8010 Graz, Austria

We propose a method that allows for the efficient solution of the three-body Faddeev equations in the presence of infinitely rising confinement interactions. Such a method is useful in calculations of nonrelativistic and especially semirelativistic constituent quark models. The convergence of the partial wave series is accelerated and possible spurious contributions in the Faddeev components are avoided.

We start from the total Hamiltonian of a nonrelativistic or a semirelativistic three-quark system, which can be written as

$$H = H^0 + \nu_\alpha + \nu_\beta + \nu_\gamma, \tag{1}$$

where H^0 is the three-body kinetic-energy operator and $\nu_\delta = \nu_\delta^c + \nu_\delta^{hf}$ represents the mutual quark-quark interactions containing both the confinement (ν_δ^c) and hyperfine (ν_δ^{hf}) potentials in the subsystems $\delta = \alpha, \beta, \gamma$

In the nonrelativistic case we may express the kinetic-energy operator by four equivalent forms

$$H^0 = \frac{p_\alpha^2}{2\mu_\alpha} + \frac{q_\alpha^2}{2M_\alpha} = \frac{p_\beta^2}{2\mu_\beta} + \frac{q_\beta^2}{2M_\beta} = \frac{p_\gamma^2}{2\mu_\gamma} + \frac{q_\gamma^2}{2M_\gamma} = \sum_{i=1}^{3} \frac{k_i^2}{2m_i}, \tag{2}$$

i.e. either through individual particle momenta k_i in the center-of-mass system or in terms of relative momenta p_δ and q_δ conjugate to the usual Jacobi coordinates x_δ and y_δ, respectively ($\delta = \alpha, \beta, \gamma$). In Eq. (2), m_i denotes the individual particle mass, μ_δ the reduced mass in the two-body subsystem δ, and M_δ the reduced mass of this subsystem with the third particle δ. In the semirelativistic case the kinetic-energy operator takes the form

$$H^0 = \sum_{i=1}^{3} \sqrt{k_i^2 + m_i^2}, \tag{3}$$

where again k_i are the individual particle three-momenta in the frame with total three-momentum $\mathbf{P} = \sum_{i=1}^{3} k_i = 0$. We note that a Hamiltonian as in Eq. (1) together with the relativistic kinetic-energy operator (3) represents an allowed mass

---

[*] Talk delivered by Zoltan Papp
[**] E-mail: zpapp@physics.csulb.edu

operator in the point-form formalism of Poincaré-invariant quantum mechanics, irrespective of the dynamical origin of the interactions.

Strictly speaking the standard Faddeev scheme applies only for potentials falling of fast enough at large distances. This makes it necessary to modify the Faddeev formalism. Otherwise one risks unpleasant properties in the Faddeev components. In particular, for infinitely rising potentials spurious contributions are picked up and also the partial-wave series becomes slowly convergent.

One can circumvent these difficulties by performing the Faddeev decomposition in such a way that all the long-range potentials are included in a modified channel Green's operator. Specifically, in our case at least the long-range parts of the confinement interactions in all subsystems α, β, and γ should be included in the modified channel resolvent. One can attain this goal by adopting a different splitting of the total Hamiltonian into

$$H = H^c + \tilde{v}_\alpha + \tilde{v}_\beta + \tilde{v}_\gamma, \tag{4}$$

where

$$H^c = H^0 + \tilde{v}_\alpha^c + \tilde{v}_\beta^c + \tilde{v}_\gamma^c \tag{5}$$

contains, besides the kinetic energy, the long-range parts $\tilde{v}_\delta^c$ of the confining interactions v_δ^c in all subsystems. The potentials $\tilde{v}_\delta$ are the residual interactions containing the hyperfine potentials and the short-range parts of the confinement.

Based on Eqs. (4) and (5) we now decompose the total wave function into

$$|\Psi\rangle = |\tilde{\Psi}_\alpha\rangle + |\tilde{\Psi}_\beta\rangle + |\tilde{\Psi}_\gamma\rangle, \tag{6}$$

where the modified Faddeev components are defined as

$$|\tilde{\Psi}_\alpha\rangle = G^c(E)\tilde{v}_\alpha|\Psi\rangle \tag{7}$$

with

$$G^c(E) = (E - H^c)^{-1}. \tag{8}$$

They fulfill the integral equations

$$|\tilde{\Psi}_\alpha\rangle = G_\alpha^c(E)\tilde{v}_\alpha(|\tilde{\Psi}_\beta\rangle + |\tilde{\Psi}_\gamma\rangle), \tag{9}$$

with α, β, γ again a cyclic permutation. The new channel resolvent is given by

$$G_\alpha^c(E) = (E - H^c - \tilde{v}_\alpha)^{-1}. \tag{10}$$

It exhibits just the desired property of including the long-range confining interactions in all subsystems α, β, γ. Only the short-range potential $\tilde{v}_\alpha$ remains in the modified Faddeev equations (9). Specifically, since now G_α^c contains also the long-range parts $\tilde{v}_\beta^c + \tilde{v}_\gamma^c$ of the confinement interactions in channels β and γ, the dependence of the component $|\tilde{\Psi}_\alpha\rangle$ on the Jacobi coordinate y_δ can never become a free motion. Rather the proper confinement-type asymptotic conditions are imposed on $|\tilde{\Psi}_\alpha\rangle$. As a result, spurious contributions are avoided in the individual Faddeev components, and at the same time the partial-wave expansion converges much faster.

The splitting of the interactions in Eqs. (4) and (5) has to be done with care. In general, the interaction parts put into H^c must not produce any bound state. Otherwise the proper behavior of the Faddeev components $|\tilde{\psi}_\alpha\rangle$ would again be spoiled. Suppose the potentials contained in H^c would produce bound states. Then at the corresponding energies, the resolvent $G^c(E)$ would become singular. Consequently, according to Eq. (7), any large Faddeev component $|\tilde{\psi}_\alpha\rangle$ could be generated even if the full solution $|\Psi\rangle$ remains infinitesimally small. Therefore, besides the true physical solutions of the Hamiltonian H, Eqs. (9) would also produce spurious solutions associated with the discrete eigenstates of the Hamiltonian H^c. These spurious solutions would occur for any $\tilde{v}_\alpha$, thus having no bearing for the physical spectrum of H. Of course, when adding up the three individual Faddeev components these spurious solutions would cancel out. However, they would cause numerical instabilities in the practical calculations. Therefore they should be avoided by not allowing H^c to produce any bound states.

In the case of confinement interactions the above requirement cannot strictly be met, since even the longest-range parts of the infinitely rising potential generate bound states. However, there is a practical way out: one needs to eliminate the bound states generated by H^c only in the region of physical interest. Outside that domain, i.e. reasonably far above the physical spectrum, they do not matter. In practice, upon splitting the interactions in the Hamiltonian (4) an auxiliary short-range potential is introduced with no effect on the physically interesting states. It only serves the purpose of cutting off the confinement interaction at short and intermediate distances thus avoiding low-lying bound states of H^c.

We solve Eqs. (9) along the Coulomb-Sturmian (CS) separable expansion approach. The further details of the method and the demonstration of its power in the example of the Goldstone-boson-exchange chiral quark model for baryons is given in Refs. [1] and [2].

References

1. Z. Papp, Few-Body Systems **26**, 99 (1999)
2. Z. Papp, A. Krassnigg, and W. Plessas, Phys. Rev. C **62**, 044004 (2000).

News from the Goldstone-Boson-Exchange Chiral Quark Model

Willibald Plessas⋆

Institute for Theoretical Physics, University of Graz, Universitätsplatz 5, A-8010 Graz, Austria

The chiral constituent quark model based on Goldstone-boson-exchange as the effective hyperfine interaction between constituent quarks has performed well for the description of the spectroscopy of all light and strange baryons [1]. Originally the model was constructed with the spin-spin component of the pseudoscalar exchange only [2]. Recently it has been extended to include all force components (central, tensor, spin-orbit) and furthermore vector and scalar exchanges [3,4]. Also, rigorous semirelativistic solutions of the three-quark problem have been provided [5]. We discuss the present status of the development of the Goldstone-boson-exchange chiral quark model.

The model, in different variants, has already been applied (by several groups) to various problems beyond baryon spectroscopy. One has thus obtained valuable insight into its performance more generally in low- and intermediate-energy hadron processes. We summarize the corresponding results and discuss them in comparison to other constituent quark models and/or (effective) approaches to low-energy QCD.

References

1. L.Ya. Glozman, Z. Papp, W. Plessas, K. Varga, and R.F. Wagenbrunn: *Effective Q-Q interactions in constituent quark models*, Phys. Rev. **C 57**, 3406 (1998).
2. L.Ya. Glozman, W. Plessas, K. Varga, and R.F. Wagenbrunn: *Unified description of light- and strange-baryon spectra*, Phys. Rev **D 58**, 094030 (1998).
3. R.F. Wagenbrunn, L.Ya. Glozman, W. Plessas, and K. Varga: *Goldstone-boson-exchange dynamics in the constituent-quark model for baryons*, Few-Body Systems Suppl. 10, 387 (1999).
4. R.F. Wagenbrunn, L.Ya. Glozman, W. Plessas, and K. Varga: *Semirelativistic constituent-quark model with Goldstone-boson-exchange hyperfine interactions*, Few-Body Systems Suppl. 11, 25 (1999).
5. Z. Papp, A. Krassnigg, and W. Plessas: *Faddeev approach to confined three-quark problems*, Preprint nucl-th/0002006.

⋆ E-mail: plessas@bkfug.kfunigraz.ac.at

Few-body problems inspired by hadron spectroscopy

Jean-Marc Richard[*]

Institut des Sciences Nucléaires Université Joseph Fourier – CNRS-IN2P3 53, avenue des Martyrs, F-38026 Grenoble Cedex, France

Abstract. I discuss some results derived in very simplified models of hadron spectroscopy, where a static potential is associated with non-relativistic kinematics. Several regularity patterns of the experimental spectrum are explained in such simple models. It is underlined that some methods developed for hadronic physics have applications in other fields, in particular atomic physics. A few results can be extended to cases involving spin-dependent forces or relativistic kinematics.

1   Introduction

As discussed in several contributions at this nice workshop, the dynamics of light quarks is far from being simple, with non-perturbative effects even at short distances, and highly-relativistic motion of the constituents inside hadrons. Nevertheless, it is interesting to consider a fictitious world, with the hadron spectrum governed by a simple Hamiltonian where a non-relativistic kinematics is supplemented by a static, flavour-independent potential. The regularities derived from the properties of the Schrödinger equation are similar to these observed in the actual spectrum. This suggests that the actual QCD theory of quark confinement should exhibit similar regularities.

One should also notice that several results derived in the context of quark models of hadrons have been successfully applied to other few-body problems, in particular in atomic physics.

Another challenge consists of extending theorems on level order, convexity, etc., to less naive Hamiltonians with spin-dependent forces and relativistic kinematics. Some of the first results will be mentioned.

2   Results on mesons

The discovery of Ψ and Υ resonances and their excitations has stimulated many studies in the quark model. In particular, the successful description of these spectra by the same potential has motivated investigations on the consequences of flavour independence. The rigorous results have been summarized in the reviews by Quigg and Rosner and by Martin and Grosse. A few examples are given below, dealing with energy levels.

---

[*] E-mail: jmrichar@isn.in2p3.fr

All potentials models reproduce the observed pattern of quarkonium that $E(1P) < E(2S)$. Note the notation adopted here, (n, ℓ), in terms of which the principal quantum number of atomic physics is $n + \ell$. It has been proved that $E(n + 1, \ell) > E(n, \ell + 1)$ if $\Delta V > 0$, and the reverse if $\Delta V < 0$. The Coulomb degeneracy is recovered as a limiting case. The sign of Δ reflects whether the charge $Q(r)$ seen at distance r grows (asymptotic freedom), decreases or remains constant (Gauss theorem).

This "Coulomb theorem" can be applied successfully to muonic atoms, which are sensitive to the size of the nucleus ($Q(r) \nearrow$), and to alkaline atoms whose last electron penetrates the inner electron shells ($Q(r) \searrow$).

Another theorem describes how the harmonic oscillator (h.o.) degeneracy $E(n + 1, \ell) = E(n, \ell + 2)$ is broken. A strict inequality is obtained if the sign of V'' is constant.

In both the complete Hamiltonian $\mathbf{p}_1^2/(2m_1) + \mathbf{p}_2^2/(2m_2) + V(r_{12})$ or its reduced version $\mathbf{p}^2/(2\mu) + V(r)$, the individual inverse masses m_i or the inverse reduced mass enter through a positive operator $\mathbf{p}^2$, and linearly. It results that each energy level is an increasing function of this inverse mass m_i^{-1} or μ^{-1}, and that the ground-state energy (or the sum of first levels) is a concave function of this variable. There are many applications. For instance, for the ground-state of the meson with charm and beauty,

$$(b\bar{s}) + (c\bar{c}) - (c\bar{s}) < (b\bar{c}) < (b\bar{b} + c\bar{c})/2. \tag{1}$$

3   Level order of baryon spectra

For many years, the only widespread knowledge of the 3-body problem was the harmonic oscillator. This remains true outside the few-body community. The discussion on baryon excitations is thus often restricted to situations where $V = \sum v(r_{ij})$, with $v(r) = Kr^2 + \delta v$, and δv treated as a correction.

First-order perturbation theory is usually excellent, especially if the oscillator strength K is variationally adjusted to minimise the magnitude of the corrections. However, when first-order perturbation is shown (or claimed) to produce a crossing of levels, one is reasonably worried about higher-order terms, and a more rigorous treatment of the energy spectrum becomes desirable.

A decomposition better than $V = \sum Kr_{ij}^2 + \delta v$ is provided by the generalised partial-wave expansion

$$V = V_0(\rho) + \delta V, \tag{2}$$

where $\rho \propto (r_{12}^2 + r_{23}^2 + r_{31}^2)^{1/2}$ is the hyperradius. The last term δV gives a very small correction to the first levels. With the hyperscalar potential V_0 only, the wave function reads $\Psi = \rho^{-5/2}u(\rho)P_{[L]}(\Omega)$, where the last factor contains the "grand-angular" part. The energy and the hyperradial part are governed by

$$u''(\rho) - \frac{\ell(\ell + 1)}{\rho^2}u(\rho) + m[E - V_0(\rho)]u(\rho) = 0, \tag{3}$$

very similar to the usual radial equations of the 2-body problem, except that the effective angular momentum is now $\ell = 3/2$ for the ground-state and its radial

excitations and $\ell = 5/2$ for the first orbital excitation with negative parity. The Coulomb theorem holds for non-integer ℓ. If $\Delta V > 0$, then $E(2S) > E(1P)$, i.e., the Roper comes above the orbital excitation. Note that a three-body potential cannot be distinguished from a simple pairwise interaction once it is reduced to its hyperscalar component V_0 by suitable angular integration. It also results from numerical tests that relativistic kinematics does not change significantly the *relative* magnitude of orbital vs. radial excitation energies.

The splitting of levels in the nearly hyperscalar potential (2) is very similar to the famous pattern of the $N = 2$ h.o. multiplet, except that the Roper is disentangled. A similar result is found for higher negative-parity excitation: the split $N = 3$ levels of the nearly harmonic model are separated into a radially excited $L = 1$ and a set of split $L = 3$ levels.

4 Tests of flavour independence for baryons

The analogue for baryons of the inequality between $b\bar{b}$, $c\bar{c}$ and $b\bar{c}$ reads.

$$(QQq) + (Q'Q'q) \leq 2(QQ'q). \tag{4}$$

Unlike the meson case, it requires mild restrictions on the potentials.

For instance, the equal spacing rule $\Omega^- - \Xi^* = \Xi^* - \Sigma^* = \Sigma^* - \Delta$ is understood as follows: the central force gives a concave behaviour, with for instance $\Omega^- - \Xi^* < \Xi^* - \Sigma^*$, but a quasi perfect linearity is restored by the spin–spin interaction which acts more strongly on light quarks. A similar scenario holds for the Gell-Mann–Okubo formula.

Inequalities can also be written for baryons with heavy flavour, some of them being more accessible than others to experimental checks in the near future. Examples are

$$3(bcs) \geq (bbb) + (ccc) + (sss), \tag{5}$$
$$2(bcq) \geq (bbq) + (ccq), \qquad 2(cqq) \geq (ccq) + (qqq).$$

5 Baryons with two heavy flavours

There is a renewed interest in this subject. The recent observation of the $(b\bar{c})$ mesons demonstrates our ability to reconstruct hadrons with two heavy quarks from their decay products.

Baryons with two heavy quarks $(QQ'q)$ are rather fascinating: they combine the adiabatic motion of two heavy quarks as in J/Ψ and Υ mesons with the highly relativistic motion of a light quark as in flavoured mesons D or B.

The wave function of (QQq) exhibits a clear diquark clustering with $r(QQ) \ll r(Qq)$ for the average distances. This does not necessarily mean that for a given potential model, a naive two-step calculation is justified. Here I mean: estimate first the (QQ) mass using the direct potential $v(QQ)$ only, and then solve the $[(QQ)-q]$ 2-body problem using a point-like diquark. If v is harmonic, one would

miss a factor $3/2$ in the effective spring constant of the (QQ) system, and thus a factor $(3/2)^{1/2}$ in its excitation energy.

On the other hand, it has been checked that the Born–Oppenheimer approximation works extremely well for these (QQq) systems, even when the quark mass ratio Q/q is not very large. This system is the analogue of H_2^+ in atomic physics.

6   The search of multiquarks

A concept of "order" or "disorder" might be introduce to study multiquark stability. This is related to the breaking of permutation symmetry. Consider for instance

$$
\begin{aligned}
H_4(x) &= \sum_{i=1}^{4} \frac{\mathbf{p}_i^2}{2m} + (1 - 2x)(V_{12} + V_{34}) + (1 + x)(V_{13} + V_{14} + V_{23} + V_{24}) \\
&= H_S + x H_{MS},
\end{aligned}
\tag{6}
$$

where the parameter x measures the departure from a fully symmetric interaction. From the variational principle, the ground-state energy $E(x)$ is maximal at $x = 0$. In most cases, $E(x)$ will be approximately parabolic, so the amount of binding below $E(0)$ is measured by $|x|$.

In simple colour models of multiquark confinement, the analogue of $|x|$ is larger for the threshold (two mesons) that for a $(\bar{q}\bar{q}qq)$ composite. So a stable multiquark is unlikely.

For the $(\bar{Q}\bar{Q}qq)$ systems presented by our slovenian hosts, and discussed earlier by Ader et al., Stancu and Brink, and others, there is another asymmetry, in the kinetic energy, which now favours multiquark binding. So there is a competition with the colour-dependent potential.

The methods developed for quark studies has been applied for systematic investigations of the stability of three-charge and four-charge systems in atomic physics.

Bibliography

A more comprehensive account of these considerations, including references to original papers or to recent review articles will be found in the Proceedings of the Few-Body Conference held at Evora, Portugal, in September 2000 (to appear as a special issue of Nuclear Physics A). I would like to thank again the organizers of this Workshop for the very pleasant and stimulating environment.

Vacuum properties in the presence of quantum fluctuations of the quark condensate

Georges Ripka *

Service de Physique Théorique, Centre d'Etudes de Saclay
F-91191 Gif-sur-Yvette Cedex, France

Abstract. The quantum fluctuations of the quark condensate are calculated using a regulated Nambu Jona-Lasinio model. The corresponding quantum fluctuations of the chiral fields are compared to those which are predicted by an "equivalent" sigma model. They are found to be large and comparable in size but they do not restore chiral symmetry. The restoration of chiral symmetry is prevented by an "exchange term" of the pion field which does not appear in the equivalent sigma model. A vacuum instability is found to be dangerously close when the model is regulated with a sharp 4-momentum cut-off.

1 Introduction.

This lecture discusses the modifications of vacuum properties which could arise due to quantum fluctuations of the chiral field, more specifically, due to the quantum fluctuations of the quark condensate. The latter is found to be surprisingly large, the root mean square deviation of the quark condensate attaining and exceeding 50% of the condensate itself. We shall discuss two distinct modifications of the vacuum: restoration of chiral symmetry due to quantum fluctuations of the chiral field, as heralded by Kleinert and Van den Boosche [1], and a vacuum instability not related to chiral symmetry restoration [2].

2 Chiral symmetry restoration due to quantum fluctuations of the chiral field.

2.1 The linear sigma model argument.

The physical vacuum with a spontaneously broken chiral symmetry is often described by the linear sigma model, which, in the chiral limit $(m_\pi = 0)$, has a euclidean action of the form:

$$I = \int d_4 x \left(\frac{1}{2} \left(\partial_\mu \sigma \right)^2 + \frac{1}{2} \left(\partial_\mu \pi_i \right)^2 + \frac{\kappa^2}{8} \left(\sigma^2 + \pi_i^2 - f_\pi^2 \right)^2 \right) \tag{1}$$

---

* E-mail: ripka@cea.fr

Classically, we have (for translationally invariant fields):

$$\sigma^2 + \pi_i^2 = f_\pi^2 \tag{2}$$

and the vacuum stationary point is:

$$\sigma = f_\pi \qquad \pi_i = 0 \tag{3}$$

We assume that κ^2 is large enough (and the σ-meson is heavy enough) not to have to worry about the quantum fluctuations of the σ field. So we quantize the pion field while the σ field remains classical. We may then say that: $\sigma^2 = f_\pi^2 - \langle \pi_i^2 \rangle$. Classically, $\langle \pi_i^2 \rangle = 0$ but the quantum fluctuations of the pion field make $\langle \pi_i^2 \rangle > 0$ and therefore $\sigma^2 < f_\pi^2$.

Let us estimate the fluctuation $\langle \pi_i^2 \rangle$ of the pion field. A system of free pions of mass m_π is described by the partition function:

$$Z = \int D(\pi) \, e^{-\frac{1}{2} \int d_4 x \, \pi_i \left(-\partial_\mu^2 + m_\pi^2 \right) \pi_i} = e^{-\frac{1}{2} \operatorname{tr} \ln \left(-\partial_\mu^2 + m_\pi^2 \right)} \tag{4}$$

It follows that:

$$\frac{1}{2} \int d_4 x \, \langle \pi_i^2(x) \rangle = -\frac{\partial \ln Z}{\partial m_\pi^2} = \frac{\partial}{\partial m_\pi^2} \frac{1}{2} \operatorname{tr} \ln \left(-\partial_\mu^2 + m_\pi^2 \right) = \frac{1}{2} \Omega \left(N_f^2 - 1 \right) \sum_{k < \Lambda} \frac{1}{k^2 + m_\pi^2} \tag{5}$$

where the sum is regularized using a 4-momentum cut-off and where $\Omega = \int d_4 x$ is the euclidean space-time volume. In the chiral limit $m_\pi = 0$, we have:

$$\langle \pi_i^2(x) \rangle = \frac{1}{2\Omega} \left(N_f^2 - 1 \right) \sum_{k < \Lambda} \frac{1}{k^2} = \left(N_f^2 - 1 \right) \frac{\Lambda^2}{16\pi^2} \tag{6}$$

so that:

$$\sigma^2 = f_\pi^2 - \left(N_f^2 - 1 \right) \frac{\Lambda^2}{16\pi^2} \tag{7}$$

If we had evaluated this quantity with a 3-momentum cut-off, we would have obtained $\langle \pi_i^2 \rangle = \left(N_f^2 - 1 \right) \frac{\Lambda^2}{8\pi^2}$. Let us pursue with a 4-momentum cut-off. We have:

$$\frac{\langle \pi_i^2 \rangle}{f_\pi^2} = \left(N_f^2 - 1 \right) \frac{\Lambda^2}{16\pi^2 f_\pi^2} \tag{8}$$

We deduce that chiral symmetry restoration will occur when $\sigma = 0$, that is, when $\frac{\langle \pi_i^2 \rangle}{f_\pi^2} > 1$:

$$\frac{\langle \pi_i^2 \rangle}{f_\pi^2} = \left(N_f^2 - 1 \right) \frac{\Lambda^2}{16\pi^2 f_\pi^2} > 1 \tag{9}$$

With $f_\pi = 93$ MeV and with $N_f^2 - 1 = 3$ pions, the condition reads:

$$\Lambda^2 > \frac{1}{2.20 \times 10^{-6}} \qquad \Lambda > 674 \; MeV \tag{10}$$

In most calculations which use the Nambu Jona-Lasinio model, this condition is fulfilled. We conclude that the quantum fluctuations of the pion do indeed restore chiral symmetry. If we had used a 3-momentum cut-off, chiral symmetry would be restored when $\Lambda > 477$ MeV.

2.2   The non-linear sigma model argument.

We now argue that this is precisely what is claimed by Kleinert and Van den Boosche [1], although it is said in a considerably different language. They argue as follows. If κ^2 (and therefore the σ mass) is large enough, the action can be thought of as the action of the non-linear sigma model, which in turn can be viewed as an action with N_f^2 fields, namely (σ, π_i), subject to the constraint:

$$\sigma^2 + \pi_i^2 = f_\pi^2 \tag{11}$$

The way to treat the non-linear sigma model is in the textbooks [3]. We work with the action:

$$I_\lambda(\sigma, \pi) = \int d_4 x \left(\frac{1}{2}(\partial_\mu \sigma)^2 + \frac{1}{2}(\partial_\mu \pi_i)^2 + \lambda \left(\sigma^2 + \pi_i^2 - f_\pi^2 \right) \right) \tag{12}$$

in which we add a constraining parameter λ. The action is made stationary with respect to variations of λ. We integrate out the π field, to get the effective action:

$$I_\lambda(\sigma) = \int d_4 x \left(\frac{1}{2}(\partial_\mu \sigma)^2 + \lambda \left(\sigma^2 - f_\pi^2 \right) \right) + \frac{1}{2} \operatorname{tr} \ln \left(-\partial_\mu^2 + \lambda \right) \tag{13}$$

The action is stationary with respect to variations of λ and σ if:

$$\lambda \sigma = 0 \qquad \sigma^2 = f_\pi^2 - \frac{1}{2}\left(N_f^2 - 1 \right) \sum_k \frac{1}{k^2 + \lambda} \tag{14}$$

So either $\lambda = 0$ and $\sigma \neq 0$, in which case we have:

$$\sigma^2 = f_\pi^2 - \frac{1}{2}\left(N_f^2 - 1 \right) \sum_k \frac{1}{k^2} \tag{15}$$

or $\lambda \neq 0$ and $\sigma = 0$.

The condition (15) is exactly the same as the condition (7). Thus, the "stiffness factor", discussed in Ref.[1], is nothing but a measure of $\frac{\langle \pi_i^2 \rangle}{f_\pi^2}$.

3   Quantum fluctuations of the quark condensate calculated in the Nambu Jona-Lasinio model.

We now show that the quantum fluctuations of the chiral field are indeed large in the Nambu Jona-Lasinio model, but that chiral symmetry is far from being restored. The regularized Nambu Jona-Lasinio model is defined in section 4. We begin by giving some results.

In the Nambu Jona-Lasinio model, the chiral field is composed of a scalar field S and $N_f^2 - 1$ pseudoscalar fields P_i. They are related to the quark bilinears:

$$S = V\left(\bar{\psi}\psi \right) \qquad P_i = V\left(\bar{\psi}i\gamma_5 \tau_i \psi \right) \tag{16}$$

where $V = -\frac{g^2}{N_c}$ is the 4-quark interaction strength. The quark propagator in the vacuum is:

$$\frac{1}{k_\mu \gamma_\mu + M_0 r_k^2} \tag{17}$$

and the model is regularized using either a sharp 4-momentum cut-off or a soft gaussian cut-off function:

$$r_k = 1 \text{ if } k^2 < \Lambda^2 \quad r_k = 0 \text{ if } k > \Lambda \quad \text{(sharp cut-off)} \tag{18}$$

$$r_k = e^{-\frac{k^2}{2\Lambda^2}} \quad \text{(gaussian regulator)}.$$

Let $\varphi_0 = M_0$ be the strength of the scalar field in the physical vacuum. We shall show results obtained with typical parameters. If we choose $M_0 = 300\ MeV$ and $\Lambda = 750\ MeV$, then $\frac{M_0}{\Lambda} = 0.4$. We then obtain $f_\pi = 94.6\ MeV$ with a sharp cut-off and $f_\pi = 92.4\ MeV$ with a gaussian cut-off (in the chiral limit). The interaction strengths are:

$$V = -9.53\ \Lambda^{-2} \text{ (sharp cut-off)} \quad V = -18.4\ \Lambda^{-2} \text{ (gaussian cut-off)} \tag{19}$$

and the squared pseudo-scalar field has the expectation value

$$\langle P_i^2 \rangle = V^2 \left\langle \left(\bar\psi i \gamma_5 \tau_i \psi \right)^2 \right\rangle \tag{20}$$

At low q we identify the pion field as:

$$\pi_i = \sqrt{Z_\pi} P_i \qquad f_\pi = \sqrt{Z_\pi} M_0 \tag{21}$$

so that, in the Nambu Jona-Lasinio model:

$$\frac{\langle \pi_i^2 \rangle}{f_\pi^2} = \frac{V^2 \left\langle \left(\bar\psi i \gamma_5 \tau_i \psi \right)^2 \right\rangle}{M_0^2} \tag{22}$$

where $\left\langle \left(\bar\psi i \gamma_5 \tau_i \psi \right)^2 \right\rangle$ is the pion contribution to the squared condensate.

3.1   Results obtained for the quark condensate and for the quantum fluctuations of the chiral field.

Let us examine the values of the quark condensates and of the quantum fluctuations of the chiral field calculated in the chiral limit.

- The quark condensate calculated with a sharp cut off is:

$$\langle \bar\psi\psi \rangle^{\frac{1}{3}} = -0.352 \times \Lambda = 263\ MeV \quad \text{(sharp cut-off)} \tag{23}$$

is about 25 % smaller when it is calculated with a soft gaussian regulator:

$$\langle \bar\psi\psi \rangle^{\frac{1}{2}} = -0.280 \times \Lambda = 210\ MeV \quad \text{(gaussian regulator)} \tag{24}$$

$\langle\bar\psi\psi\rangle$	σ-contribution	π-contribution	total
classical	-0.04187	0	-0.04187
exchange term	0.00158	-0.00475	-0.00317
ring graphs	0.00014	0.00134	0.00148
total contribution	-0.04015	-0.00341	-0.04356

Table 1. Various contributions to the quark condensate calculated with a sharp 4-momentum cut-off and with $M_0/\Lambda = 0.4$. The quark condensate is expressed in units of Λ^3.

$\langle\bar\psi\psi\rangle$	σ-contribution	π-contribution	total
classical	-0.02178	0	-0.02178
exchange term	0.00162	-0.00486	-0.00324
ring graphs	0.00077	0.00228	0.00305
total contribution	-0.0193	-0.00258	-0.02197

Table 2. Various contributions to the quark condensate calculated with a gaussian cut-off function and with $M_0/\Lambda = 0.4$. The quark condensate is expressed in units of Λ^3.

- The magnitude of the quantum fluctuations of the pion field can be measured by the mean square deviation Δ^2 of the condensate from its classical value:

$$\Delta^2 = \left\langle\left(\bar\psi\Gamma_a\psi\right)^2\right\rangle - \left\langle\bar\psi\psi\right\rangle^2 \tag{25}$$

The relative root mean square fluctuation of the condensate Δ is:

$$\frac{\Delta}{\left|\langle\bar\psi\psi\rangle\right|} = 0.41 \quad \text{(sharp cut-off)} \qquad \frac{\Delta}{\langle\bar\psi\psi\rangle} = 0.77 \quad \text{(gaussian regulator)} \tag{26}$$

These are surprisingly large numbers, certainly larger than $1/N_c$. The linear sigma model estimate did give us a fair warning that this might occur.

- This feature also applies to the ratio $\dfrac{\langle\pi_i^2\rangle}{f_\pi^2} = \dfrac{V^2\left\langle\left(\bar\psi i\gamma_5\tau_i\psi\right)^2\right\rangle}{M_0^2}$ which was so crucial for the linear sigma model estimate of the restoration of chiral symmetry. We find:

$$\frac{\langle\pi_i^2\rangle}{f_\pi^2} = 0.38 \quad \text{(sharp cut-off)} \qquad \frac{\langle\pi_i^2\rangle}{f_\pi^2} = 0.85 \quad \text{(gaussian regulator)} \tag{27}$$

- In spite of these large quantum fluctuations of the chiral field, the quark condensates change by barely a few percent. This is shown in tables 1 and 2 where various contributions to the quark condensate are given in units of Λ^3. The change in the quark condensate is much smaller than $1/N_c$.

3.2   The effect and meaning of the exchange terms.

The tables 1 and 2 show that, among the $1/N_c$ corrections, the exchange terms dominate. The exchange and ring graphs are illustrated on figures 1 and 2. The

way in which they arise is explained in section 4.1. The exchange graphs contribute 2-3 times more than the remaining ring graphs. Furthermore, the pion contributes about three times more to the condensate than the sigma, so that the sigma field contributes about as much to the exchange term as any one of the pions. However, the exchange term in the pion channel enhances the quark condensate instead of reducing it. As a result of this there is a very strong cancellation between the exchange terms and the ring graphs. This is why the sigma and pion loops contribute so little to the quark condensate. They increase the condensate by 4% when a sharp cut-off is used, and by 1% when a gaussian regulator is used. This is about ten times less than $1/N_c$.

The ring graphs reduce the condensate (in absolute value) in both the sigma and pion channels. This can be expected. Indeed, the ring graphs promote quarks from the Dirac sea negative energy orbits (which contribute negative values to the condensate) to the positive energy orbits (which contribute positive values to the condensate). The net result is a positive contribution to the condensate which reduces the negative classical value.

What then is the meaning of the exchange terms? The exchange terms have the special feature of belonging to first order perturbation theory (see figures 1 and 2). Their contribution to the energy is not due to a modification of the Dirac sea. It is simply the exchange term arising in the expectation value of the quark-quark interaction in the Dirac sea.

However, the contribution of the exchange term to the quark condensate does involve $q\bar{q}$ excitations. These excitations are due to a modification of the constituent quark mass which is expressed in terms of quark-antiquark excitations of the Dirac sea. The exchange term is modifying (increasing in fact) the constituent quark mass and therefore the value of f_π.

These results suggest that, in order to reduce the Nambu Jona-Lasinio model to an equivalent sigma model, it might be better to include the exchange term in the constituent quark mass, which is another way of saying that, in spite of the $1/N_c$ counting rule, it may be better to do Hartree-Fock theory than Hartree theory. The exchange (Fock) term should be included in the gap equation. The direct (Hartree) term is, of course, included in the classical bosonized action.

In the equivalent sigma model, f_π is proportional to the constituent quark mass. Failure to notice that that the constituent quark mass is altered by the exchange term is what lead Kleinert and Van den Boosche to conclude erroneously in Ref.[1] that chiral symmetry would be restored in the Nambu Jona-Lasinio model. They were right however in expecting large quantum fluctuations of the quark condensate.

4   The regularized Nambu Jona-Lasinio model.

The condensates quoted in section 3.1 were calculated with a regularized Nambu Jona-Lasinio model which is defined by the euclidean action:

$$I_m\left(q,\bar{q}\right) = \int d_4x \; \left[\bar{q}\left(-i\partial_\mu\gamma_\mu\right)q + m\bar{\psi}\psi - \left(\frac{g^2}{2N_c}+j\right)\left(\bar{\psi}\Gamma_a\psi\right)^2\right] \qquad (28)$$

The euclidean Dirac matrices are $\gamma_\mu = \gamma^\mu = (i\beta, \boldsymbol{\gamma})$. The matrices $\Gamma_a = (1, i\gamma_5\boldsymbol{\tau})$ are defined in terms of the $N_f^2 - 1$ generators $\boldsymbol{\tau}$ of flavor rotations. Results are given for $N_f = 2$ flavors. The coupling constant $\frac{g^2}{N_c}$ is taken to be inversely proportional to N_c in order to reproduce the N_c counting rules. The current quark mass m is introduced as a source term used to calculate the regularized quark condensate $\langle\bar\psi\psi\rangle$. We have also introduced a source term $\frac{1}{2}j\left(\bar\psi\Gamma_a\psi\right)^2$ which is used to calculate the squared quark condensate $\left\langle\left(\bar\psi\Gamma_a\psi\right)^2\right\rangle$.

The quark field is $q(x)$ and the $\psi(x)$ fields are *delocalized* quark fields, which are defined in terms of a *regulator* r as follows:

$$\psi(x) = \int d_4x \ \langle x|r|y\rangle \ q(y) \tag{29}$$

The regulator r is diagonal in k-space: $\langle k|r|k'\rangle = \delta_{kk'}r(k)$ and its explicit form in given in Eq.(18). The use of a sharp cut-off function is tantamount to the calculation of Feynman graphs in which the quark propagators are cut off at a 4-momentum Λ - a most usual practice. The regulator r, introduced by the delocalized fields, makes all the Feynman graphs converge. A regularization of this type results when quarks propagate in a vacuum described by in the instanton liquid model of the QCD (see Ref.[4] and further references therein). A Nambu Jona-Lasinio model regulated in this manner with a gaussian regulator was first used in Ref.[5], and further elaborated and applied in both the meson and the soliton sectors [5],[6],[7],[8], [9],[2]. Its properties are also discussed in [10].

With one exception. In this work, as in Ref.[2], the regulator multiplies the current quark mass. The introduction of the regulator in the current quark mass term $m\bar\psi\psi = m\bar q r^2 q$ requires some explanation. The current quark mass m is used as a source term to calculate the quark condensate $\langle\bar\psi\psi\rangle$ which, admittedly, would be finite (by reason of symmetry) even in the absence of a regulator - and, indeed, values of quark condensates are usually calculated with an unregularized source term in the Nambu Jona-Lasinio action. However, when we calculate the *fluctuation* $\left\langle\left(\bar\psi\Gamma_a\psi\right)^2\right\rangle - \langle\bar\psi\psi\rangle^2$ of the quark condensate, the expectation value $\left\langle\left(\bar\psi\Gamma_a\psi\right)^2\right\rangle$ diverges. It would be inconsistent and difficult to interpret the fluctuation $\left\langle\left(\bar\psi\Gamma_a\psi\right)^2\right\rangle - \langle\bar\psi\psi\rangle^2$ if $\langle\bar\psi\psi\rangle$ were evaluated using a bare source term and $\left\langle\left(\bar\psi\Gamma_a\psi\right)^2\right\rangle$ using a regulator. When a regularized source term $m\bar\psi\psi = m\bar q r^2 q$ is used, the current quark mass m can no longer be identified with the current quark mass term appearing in the QCD lagrangian. Of course, when a sharp cut-off is used, it makes no difference if the current quark mass term is multiplied by the regulator or not. We have seen in section 3.1 that the leading order contribution to the quark condensate $\langle\bar\psi\psi\rangle^{1/3}$ diminishes by only 20% when the sharp cut-off is replaced by a gaussian regulator. (This statement may be misleading because when the sharp cut-off is replaced by a gaussian regulator, the interaction strength V is also modified so as to fit f_π. If we use a gaussian regulator, the quark condensate calculated with a regulated source term mr^2 is $\langle\bar\psi\psi\rangle = -0.0218\,\Lambda^3$ whereas the quark condensate calculated with a bare source term m is $\langle\bar\psi\psi\rangle = -0.0505\,\Lambda^3$.)

The way in which the current quark mass of the QCD lagrangian appears in the low energy effective theory is model dependent and it has been studied in some detail in Ref.[11] within the instanton liquid model of the QCD vacuum [12],[13],[4].

An equivalent bosonized form of the Nambu Jona-Lasinio action (28) is:

$$I_{j,m}(\varphi) = -\text{Tr}\ln(-i\partial_\mu\gamma_\mu + r\varphi_a\Gamma_a r) - \frac{1}{2}(\varphi - m)(V - j)^{-1}(\varphi - m) \qquad (30)$$

The first term is the quark loop expressed in terms of the chiral field φ, which is a chiral 4-vector $\varphi_a = (S, P_i)$ so that $\varphi_a\Gamma_a = S + i\gamma_5\tau_i P_i$. In the second term, the chiral 4-vector $m_a \equiv (m, 0, 0, 0)$ is the current quark mass and V is the local interaction:

$$\langle xa|V|yb\rangle = -\frac{g^2}{N_c}\delta_{ab}\delta(x - y) \qquad (31)$$

The partition function of the system, in the presence of the sources j and m is given by the expression:

$$e^{-W(j,m)} = \int D(\varphi)\, e^{-I_{j,m}(\varphi) - \frac{1}{2}\text{tr}\ln(V - j)} \qquad (32)$$

The quark condensate $\langle\bar\psi\psi\rangle$ and the squared quark condensates $\left\langle\left(\bar\psi\Gamma_a\psi\right)^2\right\rangle$ can be calculated from the partition function $W(j, m)$ using the expressions:

$$\langle\bar\psi\psi\rangle = \frac{1}{\Omega}\frac{\partial W(j,m)}{\partial m} \qquad \frac{1}{2}\left\langle\left(\bar\psi\Gamma_a\psi\right)^2\right\rangle = -\frac{1}{\Omega}\frac{\partial W(j,m)}{\partial j} \qquad (33)$$

where Ω is the space-time volume $\int d_4 x = \Omega$.

The stationary point $\varphi_a = (M, 0, 0, 0)$ of the action is given by the gap equation:

$$(V - j)^{-1} = -4N_c N_f\frac{M}{M - m}g_M \qquad (34)$$

This equation relates the constituent quark mass M to the interaction strength $V - j$.

4.1 The exchange and ring contributions.

The second order expansion of the action $I_{jm}(\varphi)$ around the stationary point reads:

$$I_{jm}(\varphi) = I_{jm}(M) + \frac{1}{2}\varphi\left(\Pi + (V - j)^{-1}\right)\varphi \qquad (35)$$

where $I_{jm}(M)$ is the action calculated at the stationary point $\varphi = (M, 0, 0, 0)$ and where Π is the polarization function (often referred to as the Lindhardt function):

$$\langle xa|\Pi|yb\rangle = -\frac{\delta}{\delta\varphi_a(x)\,\delta\varphi_b(y)}\text{Tr}\ln(-i\partial_\mu\gamma_\mu + r\varphi_a\Gamma_a r) \qquad (36)$$

Substituting this expansion into the partition function (32), we can calculate the partition function $W(j, m)$ using gaussian integration with the result:

$$W(j, m) = I_{jm}(M) + \frac{1}{2}\text{tr}\ln(1 - \Pi(V - j)) \qquad (37)$$

The first term of the action (37) is what we refer to as the "classical" action. The values labelled "classical" in the tables displayed in section 3.1 are obtained by calculating the condensates (33) while retaining only the term I_{jm} in the partition function (37). The logarithm in (37) is what we refer to as the loop contribution. The expansion of the logarithm expresses the loop contribution in terms of the Feynman graphs shown on figure 1.
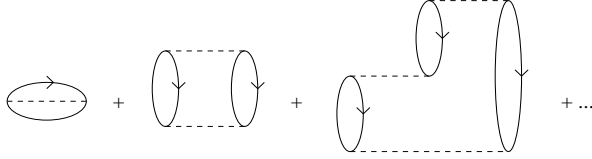
Fig. 1. The Feynman graphs which represent the meson loop contribution to the partition function. The first graph is the exchange graph and the remaining graphs are the ring graphs.

The first term of the loop expansion is what we call the "exchange term", also referred to as the Fock term:[1]

$$W_{exch} = -\frac{1}{2}\mathrm{tr}\Pi\,(V - j)$$
(38)

The remaining terms are what we call the ring graphs.
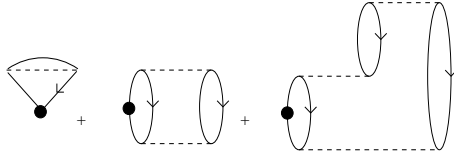
Fig. 2. The contribution to the quark condensate of the Feynman graphs shown on figure 1. The black blob represents the operator $\bar{\psi}\psi$. The first graph (which is the dominating contribution) is the contribution of the exchange term. It represents $q\bar{q}$ excitations which describe a change in mass of the Dirac sea quarks. This exchange graph would not appear in a Hartree-Fock approximation, which would include the exchange graph in the gap equation.

It is simple to show that the inverse meson propagators are given by:

$$K^{-1} = \Pi + (V - j)^{-1}$$
(39)

They are diagonal in momentum and flavor space: $\langle q a\,|K^{-1}|\,k'q\rangle = \delta_{ab}\delta_{kk'}K_a\,(q)$ and a straightforward calculation yields the following explicit expressions for the S (sigma) and P (pion) inverse propagators:

---

[1] The direct (Hartree) term is included in the "classical" action $I_{j,m}$.
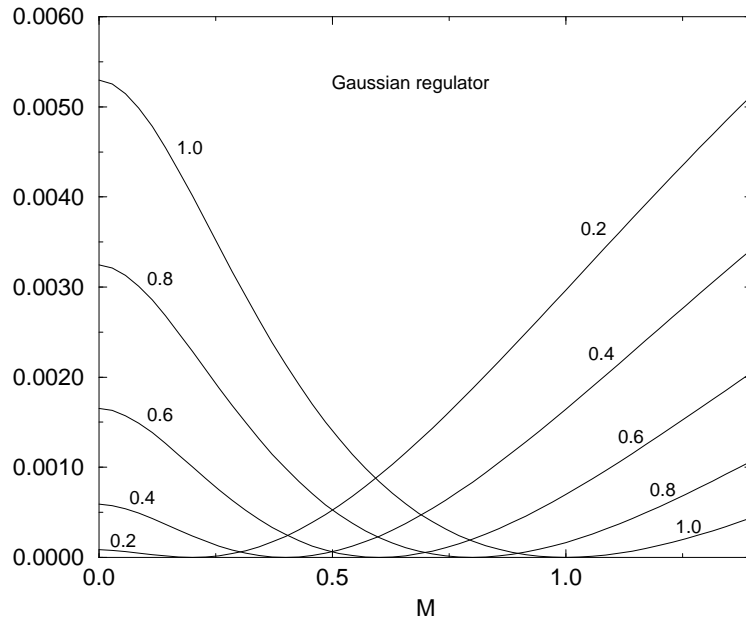
Fig. 3. The effective potential plotted against M when a soft gaussian cut-off function is used. The potential is expressed units of Λ^4.

$$K_S^{-1}(q) = 4N_c N_f \left(\frac{1}{2}q^2 f_M^{22}(q) + M^2 \left(f_M^{26}(q) + f_M^{44}(q) \right) - g_M(q) + \frac{M}{M-m}g_M \right)$$
(40)

$$K_P^{-1}(q) = 4N_c N_f \left(\frac{1}{2}q^2 f_M^{22}(q) + M^2 \left(f_M^{26}(q) - f_M^{44}(q) \right) - g_M(q) + \frac{M}{M-m}g_M \right)$$

where the loop integrals are:

$$f_M^{np}(q) = \frac{1}{\Omega} \sum_k \frac{r_{k-\frac{q}{2}}^n r_{k+\frac{q}{2}}^p}{\left(\left(k-\frac{q}{2}\right)^2 + r_{k-\frac{q}{2}}^4 M^2 \right) \left(\left(k+\frac{q}{2}\right)^2 + r_{k+\frac{q}{2}}^4 M^2 \right)}$$
(41)

and:

$$g_M(q) = \frac{1}{\Omega} \sum_k \frac{r_{k-\frac{q}{2}}^2}{\left(k-\frac{q}{2}\right)^2 + r_{k-\frac{q}{2}}^4 M^2} r_{k+\frac{q}{2}}^2 \qquad g_M \equiv g_M(q=0)$$
(42)

These are the expressions which are obtained from the second order expansion of the action (30) retaining the regulators from the outset and throughout.

Innumerable papers have been published (including some of my own) in which the meson propagators are derived from the unregulated Nambu Jona-Lasinio action:

$$I_{j,m}(\varphi) = -\text{Tr} \ln \left(-i\partial_\mu \gamma_\mu + \varphi_a \Gamma_a\right) - \frac{1}{2}(\varphi - m)(V - j)^{-1}(\varphi - m)$$
(43)
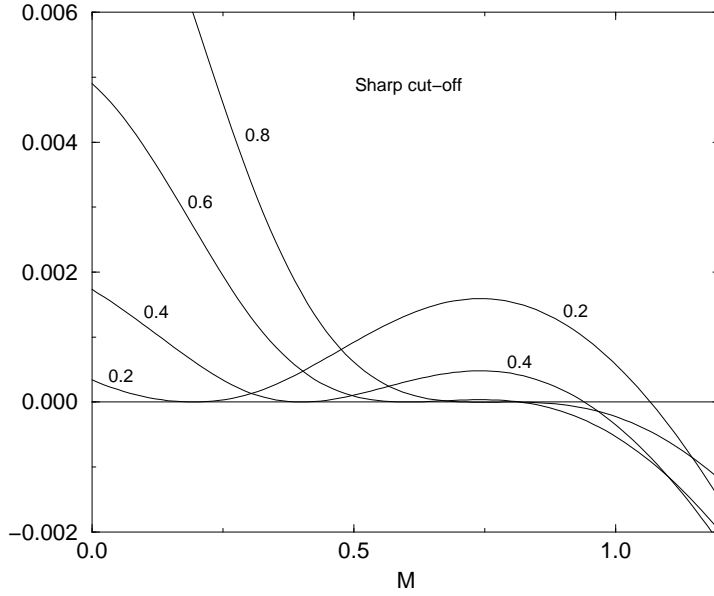
Fig. 4. The effective potential plotted against M when a sharp cut-off is used. The effective potential is expressed in units of Λ^4.

The expressions obtained for the propagators are then:

$$K_S^{-1}(q) = 4N_c N_f \left(\frac{1}{2} \left(q^2 + 4M^2 \right) f_M(q) + \frac{m}{M-m} g_M \right) \qquad (44)$$

$$K_P^{-1}(q) = 4N_c N_f \left(\frac{1}{2} q^2 f_M(q) + \frac{m}{M-m} g_M \right)$$

where the loop integrals are:

$$f_M(q) = \frac{1}{\Omega} \sum_{k<\Lambda} \frac{1}{\left(\left(k - \frac{q}{2} \right)^2 + M^2 \right) \left(\left(k + \frac{q}{2} \right)^2 + M^2 \right)} \qquad (45)$$

and:

$$g_M = \frac{1}{\Omega} \sum_{k<\Lambda} \frac{1}{\left(k - \frac{q}{2} \right)^2 + M^2} \qquad (46)$$

The table 3 shows the low q behaviour of the S and P inverse propagators in various approximations. They are calculated in the chiral limit.

5   An instability of the vacuum.

The partition function (37) can also be used to calculate the effective potential:

$$\Gamma = W(j, m) - j \frac{\partial W(j, m)}{\partial j} = W(j, m) + \frac{1}{2} j \left\langle \left(\bar{\psi} \Gamma_a \psi \right)^2 \right\rangle \qquad (47)$$
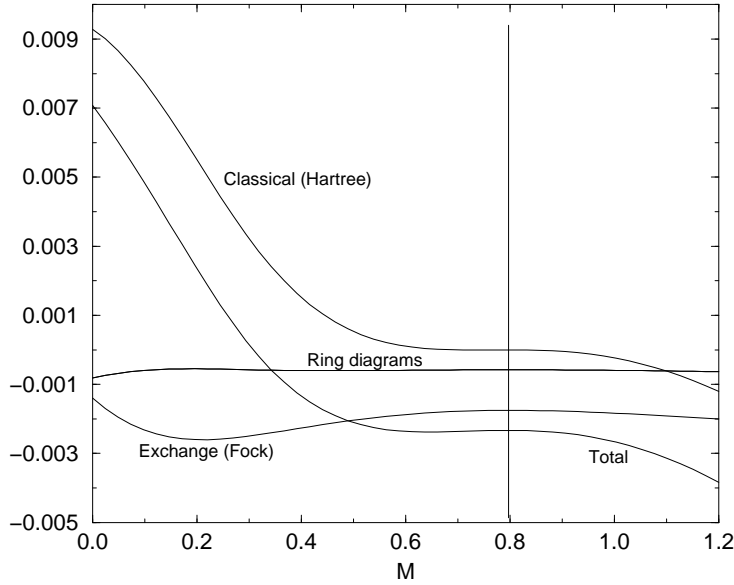
Fig. 5. Various contributions to the effective potential calculated with a sharp cut-off and $M_0/\Lambda = 0.8$. The contributions are expressed in units of Λ^4.

inverse propagators	$K_P^{-1}\,(q=0)$	$Z_\pi = \left.\dfrac{d\,K_P^{-1}}{d\,q^2}\right|_{q=0}$	$K_S^{-1}\,(q=0)$	$\left.\dfrac{d\,K_S^{-1}}{d\,q^2}\right|_{q=0}$
regulated action	0	0.0995	0.0546	0.0592
regulated $f\,(q)$	0	0.0850	0.0544	0.0448
$f\,(q) = f\,(0)$	0	0.0850	0.0544	0.0850

Table 3. Three approximations to the inverse S and P propagators, calculated with a sharp 4-momentum cut-off and with $M_0/\Lambda = 0.4$. The first row gives the values obtained from an regularized action (30). The second row gives the values obtained from a unregularized action and by subsequently regularizing the loop integrals. The last row gives the results obtained by neglecting the q dependence of the loop integral $f\,(q)$. The inverse quark propagators are given in units of Λ^2 and $\frac{d\,K^{-1}}{d\,q^2}$ is dimensionless.

As we vary j, the squared condensate $\left\langle \left(\bar{\psi}\Gamma_a\psi\right)^2 \right\rangle$ changes. Thus, when we plot the effective potential against j, we discover how the energy of the system varies when the system is forced to modify the squared condensate $\left\langle \left(\bar{\psi}\Gamma_a\psi\right)^2 \right\rangle$. The effective potential has a stationary point at $j = 0$, that is, in the absence of a constraint. If the stationary point of the effective potential is a minimum, the system is (at least locally) stable against fluctuations of $\left\langle \left(\bar{\psi}\Gamma_a\psi\right)^2 \right\rangle$. If it is an inflection point, it is unstable and we shall indeed find that this can easily occur when a sharp cut-off is used.

When j is varied, the constituent quark mass M also changes, according to the gap equation (34). One finds that M is a monotonically increasing function of j so that the effective potential can be plotted against M equally well. The vacuum constituent quark mass is the mass M_0 obtained with $j = 0$. The contribution
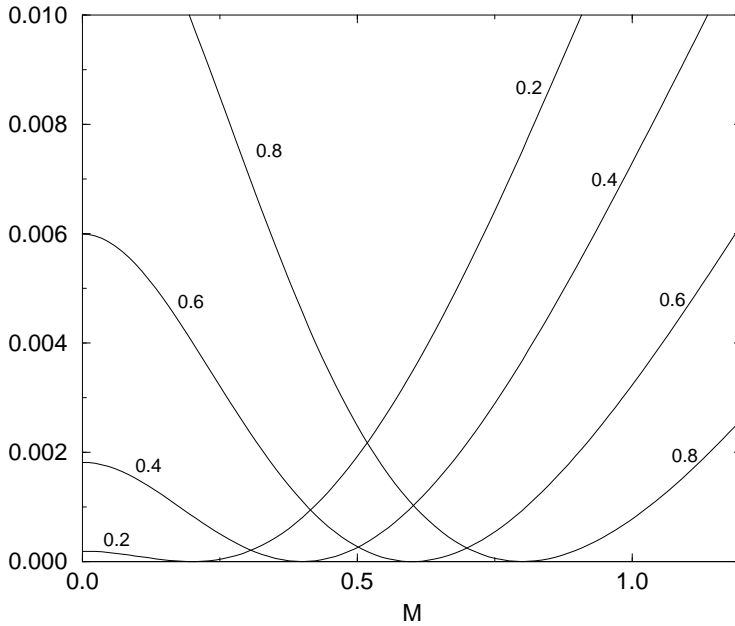
Fig. 6. The effective potential calculated with a sharp 3-momentum cut-off plotted against M. It is expressed in units of Λ^4.

of each Feynman graph to the effective potential is stationary at the point $M = M_0$ and this is why plots of the the effective potential against M are nicer to look at than plots against j. The vacuum constituent quark mass M_0 is a measure of the interaction strength V, to which it is related by the gap equation. For a given shape of the regulator, the occurrence of an instability depends on only one parameter, namely M_0/Λ.

Figure 3 shows the effective potential calculated with a gaussian cut-off for various values of M_0/Λ. The ground state appears to be stable within the range of reasonable values of M_0/Λ.

Figure 4 shows the effective potential plotted against M when a sharp cut-off is used. When $M_0/\Lambda > 0.74$ the ground state develops an instability with respect to increasing values of M. This instability is not related to the restoration of chiral symmetry and, indeed, the pion remains a Goldstone boson for all values of M. As shown on Fig.5, the instability is due to the classical action and the meson loop contributions do not modify it.

Figure 6 shows the effective potential calculated with a sharp 3-momentum cut-off. No instability appears. This provides a clue as to the cause of the instability which arises when a sharp 4-momentum cut-off is used. Indeed, when a 3-momentum cut-off is used, the Nambu Jona-Lasinio model defines a time-independent hamiltonian and the 3-momentum cut-off simply restricts the Hilbert space available to the quarks. This allows a quantum mechanical interpretation of the results. If H is the Nambu Jona-Lasinio hamiltonian, then the ground state

wavefunction $|j\rangle$ is calculated with the hamiltonian

$$\bar{H}_j = H - j \int d_3x \ \left(\bar{\psi}\Gamma_a\psi\right)^2 \tag{48}$$

containing the constraint proportional to j. The effective potential Γ is then equal to the energy $E(j) = \langle j|H|j\rangle$ of the system and it displays a stationary point when $j = 0$ or, equivalently, when $M = M_0$. The Nambu Jona-Lasinio model, regularized with a 3-momentum cut-off, has been used in Refs.[14] and [15] for example.

The use of a 3-momentum cut-off has another important feature. The meson propagators have only poles on the imaginary axis where they should. When a 4-momentum cut-off is used, unphysical poles appear in the complex energy plane, as they do when proper-time regularization is used for the quark loop [16].

The fact that the instability occurs when the model is regularized with a 4-momentum cut-off and not when a 3-momentum cut-off is used, strongly suggests that the instability is due to the unphysical poles introduced by the regulator. This conclusion is corroborated by the observation that the instability also occurs when a gaussian cut-off is used, but at the much higher values $M_0/\Lambda \geq 2.93$ where the cut-off is too small to be physically meaningful. With a gaussian regulator and in the relevant range of parameters $0.4 < M_0/\Lambda < 0.8$, one needs to probe the system with values as high as $M/\Lambda > 4$ before it becomes apparent that the energy is not bounded from below. The instability is an unpleasant feature of effective theories which use relatively low cut-offs. However, the low value of the cut-off is dictated by the vacuum properties and we need to learn to work with it. Further details are found in Ref.[2].

We conclude from this analysis that it is much safer to use a soft regulator, such as a gaussian, than a sharp cut-off.

References

1. H. Kleinert and B. Van Den Boosche, *Phys.Lett. B474*, page 336, 2000.
2. G.Ripka, *Quantum fluctuations of the quark condensate*, hep-ph/0003201, 2000.
3. J.Zinn-Justin, *Quantum Field Theory and Critical Phenomena*, Clarendon Press, Oxford, 1989.
4. C. Weiss D.I. Diakonov, M.V. Polyakov, *Nucl. Phys. B461*, page 539, 1996.
5. R.D.Bowler and M.C.Birse, *Nucl.Phys. A582*, page 655, 1995.
6. R.S.Plant and M.C.Birse, *Nucl.Phys. A628*, page 607, 1998.
7. W.Broniowski B.Golli and G.Ripka, *Phys.Lett. B437*, page 24, 1998.
8. Wojciech Broniowski, *Mesons in non-local chiral quark models*, hep-ph/9911204, 1999.
9. B.Szczerebinska and W.Broniowski, *Acta Polonica 31*, page 835, 2000.
10. Georges Ripka, *Quarks Bound by Chiral Fields*, Oxford University Press, Oxford, 1997.
11. M.Musakhanov, *Europ.Phys.Journal C9*, page 235, 1999.
12. E.Shuryak, *Nucl.Phys. B203*, pages 93,116,140, 1982.
13. D.I.Diakonov and V.Y.Petrov, *Nucl.Phys. B272*, page 457, 1986.
14. D.Blaschke S.Schmidt and Y.Kalinovsky. *Phys.Rev. C50*, page 435, 1994.
15. S.P. Klevansky Y.B. He, J. Hfner and P. Rehberg, *Nucl. Phys. A630*, page 719, 1998.
16. E.N.Nikolov W.Broniowski, G.Ripka and K.Goeke, *Zeit.Phys. A354*, page 421, 1996.

Nucleon-Nucleon Scattering in a Chiral Constituent Quark Model

Floarea Stancu*

Institute of Physics, B.5, University of Liege, Sart Tilman, B-4000 Liege 1, Belgium

Abstract. We study the nucleon-nucleon interaction in the chiral constituent quark model of Refs. [1,2] by using the resonating group method, convenient for treating the interaction between composite particles. The calculated phase shifts for the $^3S_1$ and $^1S_0$ channels show the presence of a strong repulsive core due to the combined effect of the quark interchange and the spin-flavour structure of the effective quark-quark interaction. Such a structure stems from the pseudoscalar meson exchange between quarks and is a consequence of the spontaneous breaking of the chiral symmetry. We perform single and coupled channel calculations and show the role of coupling of the $\Delta\Delta$ and hidden colour CC channels on the behaviour of the phase shifts. The addition of a σ-meson exchange quark-quark interaction brings the $^1S_0$ phase shift closer to the experimental data. We intend to include a tensor quark-quark interaction to improve the description of the $^3S_1$ phase shift.

In this talk I shall mainly present results obtained in collaboration with Daniel Bartz [3,4] for the nucleon-nucleon (NN) scattering phase shifts calculated in the resonating group method.

The study of the NN interaction in the framework of quark models has already some history. Twenty years ago Oka and Yazaki [5] published the first L = 0 phase shifts with the resonating group method. Those results were obtained from models based on one-gluon exchange (OGE) interaction between quarks. Based on such models one could explain the short-range repulsion of the NN interaction potential as due to the chromomagnetic spin-spin interaction, combined with quark interchanges between 3q clusters. In order to describe the data, long- and medium-range interactions were added at the nucleon level. During the same period, using a cluster model basis as well, Harvey [6] gave a classification of the six-quark states including the orbital symmetries $[6]_O$ and $[42]_O$. Mitja Rosina, Bojan Golli and collaborators [7] discussed the relation between the resonating group method and the generator coordinate method and introduced effective local NN potentials.

Here we employ a constituent quark model where the short-range quark-quark interaction is entirely due to pseudoscalar meson exchange, instead of one-gluon exchange. This is the chiral constituent quark model of Ref. [1], parametrized in a nonrelativistic version in Ref. [2]. The origin of this model is thought to lie in the spontaneous breaking of chiral symmetry in QCD which implies the existence of Goldstone bosons (pseudoscalar mesons) and constituent quarks

---

* E-mail: fstancu@ulg.ac.be

with dynamical mass. If a quark-pseudoscalar meson coupling is assumed this generates a pseudoscalar meson exchange between quarks which is spin and flavour dependent. The spin-flavour structure is crucial in reproducing the correct order of the baryon spectra [1,2]. The present status of this model is presented by L. Glozman and W. Plessas at this workshop. Hereafter this model will be called the Goldstone boson exchange (GBE) model.

It is important to correctly describe both the baryon spectra and the baryon-baryon interaction with the same model. The model [1,2] gives a good description of the baryon spectra and in particular the correct order of positive and negative parity states, both in nonstrange and strange baryons, in contrast to the OGE model. In fact the pseudoscalar exchange interaction has two parts : a repulsive Yukawa potential tail and an attractive contact δ-interaction. When regularized, the latter generates the short-range part of the quark-quark interaction. This dominates over the Yukawa part in the description of baryon spectra. The whole interaction contains the main ingredients required in the calculation of the NN potential, and it is thus natural to study the NN problem within the GBE model. In addition, the two-meson exchange interaction between constituent quarks reinforces the effect of the flavour-spin part of the one-meson exchange and also provides a contribution of a σ-meson exchange type [8] required to describe the middle-range attraction.

Preliminary studies of the NN interaction with the GBE model have been made in Refs. [9–11]. They showed that the GBE interaction induces a short-range repulsion in the NN potential. In Refs. [9,10] this is concluded from studies at zero separation between clusters and in [11] an adiabatic potential is calculated explicitly. Here we report on dynamical calculations of the NN interaction obtained in the framework of the GBE model and based on the resonation group method [3,4]. In Ref. [3] the $^3S_1$ and $^1S_0$ phase shifts have been derived in single and three coupled channels calculations. It was found that the coupling to the $\Delta\Delta$ and CC (hidden colour) channels contribute very little to the NN phase shift. These studies show that the GBE model can explain the short-range repulsion, as due to the flavour-spin quark-quark interaction and to the quark interchange between clusters.

However, to describe the scattering data and the deuteron properties, intermediate- and long-range attraction potentials are necessary. In Ref. [4] a σ-meson exchange interaction has been added at the quark level to the six-quark Hamiltonian. This interaction has the form

$$V_\sigma = -\frac{g_{\sigma q}^2}{4\pi} \left(\frac{e^{-\mu_\sigma r}}{r} - \frac{e^{-\Lambda_\sigma r}}{r} \right),$$
(1)

An optimal set of values of the parametres entering this potential has been found to be

$$\frac{g_{\sigma q}^2}{4\pi} = \frac{g_{\pi q}^2}{4\pi} = 1.24, \quad \mu_\sigma = 0.60 \, \text{GeV}, \quad \Lambda_\sigma = 0.83 \, \text{GeV}.$$
(2)

As one can see from Fig. 1, with these values the theoretical phase shift for $^1S_0$ gets quite close to the experimental points without altering the good short-range behaviour, and in particular the change of sign of the phase shift at $E_{lab} \approx 260$
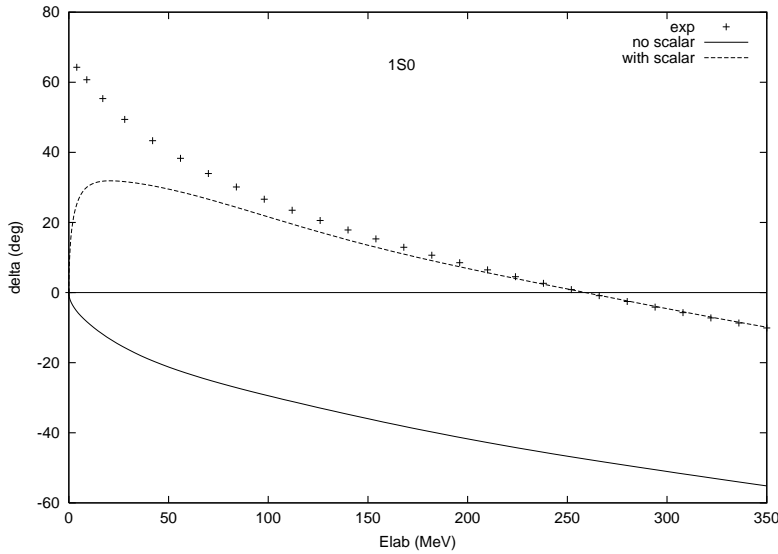
Fig. 1. The $^1S_0$ NN scattering phase shift obtained in the GBE model as a function of E_{lab}. The solid line is without and the dashed line with the σ-meson exchange potential between quarks with $\mu_\sigma = 0.60$ GeV and $\Lambda_\sigma = 0.83$ GeV. Experimental data are from Ref. [12].

MeV. Thus the addition of a σ-meson exchange interaction alone leads to a good description of the phase shift in a large energy interval. One can argue that the still existing discrepancy at low energies could possibly be removed by the coupling of the $^5D_0$ N-Δ channel. To achieve this coupling, as well as to describe the $^3S_1$ phase shift, the introduction of a tensor interaction is necessary.

References

1. L.Ya. Glozman and D.O. Riska, Phys. Rep. **268**, 263 (1996)
2. L.Ya. Glozman, Z. Papp, W. Plessas, K. Varga and R. Wagenbrunn, Nucl.Phys. **A623** (1997) 90c
3. D. Bartz and Fl. Stancu, e-print nucl-th/0009010
4. D. Bartz and Fl. Stancu, e-print hep-ph/0006012
5. M. Oka and K. Yazaki, Phys. Lett. **90B** 41 (1980); Progr. Theor. Phys **66** 556 (1981); ibid **66** 572 (1981).
6. M. Harvey, Nucl. Phys. **A352** (1981) 301; **A481** (1988) 834.
7. M. Cvetic, B. Golli, N. Mankoc-Borstnik and M. Rosina, Nucl. Phys. **A395** (1983) 349
8. D. O. Riska and G. E. Brown, Nucl. Phys. **A653** (1999) 251
9. Fl. Stancu, S. Pepin and L. Ya. Glozman, Phys. Rev. **C56** (1997) 2779; **C59** (1999) 1219 (erratum).
10. D. Bartz, Fl. Stancu, Phys. Rev. **C59** (1999) 1756.
11. D. Bartz and Fl. Stancu, Phys. Rev. **C60** (1999) 055207
12. V. G. J. Stoks, R. A. M. Klomp, M. C. M. Rentmeester and J. J. de Swart, Phys. Rev. **C48** (1993) 792; V. G. J. Stoks, R. A. M. Klomp, C. P. F. Terheggen and J. J. de Swart, Phys. Rev. **C49** (1994) 2950.

Description of nucleon excitations as decaying states

Bojan Golli[*]

Faculty of Education, University of Ljubljana, and J. Stefan Institute, Ljubljana, Slovenia

Abstract. Two methods to describe excited states of baryons as decaying states are presented: the Analytic Continuation in Coupling Constant and the Kohn variational principle for the K-matrix. The methods are applied to a simple model of the Δ resonance consisting of the pion coupled to three valence quarks.

The work has been done in collaboration with Vladimir Kukulin and Simon Širca.

1 Motivation

Baryons are usually computed as bound states neglecting possible decay channels. The inclusion of strongly decaying channels may considerably influence the position of the state as well as some other properties. The aim of the present work is to estimate this effect in a simplified model and to discuss two possible approaches to describe decaying states. The methods determine the position and the width of the resonance, and furthermore, provide a suitable tool to calculate new observables, which cannot be obtained in a bound state calculation, such as non-resonant contributions to production amplitudes. In this work we shall focus on the decay of the Δ resonance.

2 The model

The decay of the Δ resonance into the nucleon and the pion is most naturally described in models with chiral symmetry, such as the linear σ model (LSM), the chromodielectric model (CDM), the cloudy bag model CBM, etc. Here we use a simplified model which contains the main features of these models. It assumes frozen quark profiles and neglects meson-self interaction. Furthermore, it does not take into account additional scalar fields (sigma mesons in the LSM, chromodielectric field and sigma mesons in the CDM, or the bag potential in the CBM) since their main role is to fix the quark profiles and generate a constant energy shift for all baryons. In the present calculation, the quarks profiles are taken over from the ground state calculation in the LSM[1]. We know that the profiles do not change considerably from one model to the other, so this is not a very severe restriction. The inclusion of meson self-interaction may, however, more importantly alter the results.

---

[*] E-mail: Bojan.Golli@ijs.si

For the quark-pion interaction we assume the usual pseudoscalar form:

$$H_{quark-meson} = ig \int dr^3 \, \bar{q} \boldsymbol{\tau} \cdot \hat{\boldsymbol{\pi}} \gamma_5 q \ . \tag{1}$$

In models with spontaneous symmetry breaking, such as the LSM, the parameter g is related to the 'constituent' quark mass by $M_q = g f_\pi$. From 350 MeV$<$ $M_q <$450 MeV we estimate that physically sensible values for g are $4 < g < 5$.

The model is usually solved at the mean field level. We interpret the solution as a coherent state of pions around the three quark core, and generate physical N and Δ states by the Peierls Yoccoz projection of good spin and isospin. The resulting states are interpreted as a superposition of 3 bare quarks plus 3 quarks with one or more pions coupled, respectively, to nucleon or Δ quantum numbers:

$$\begin{aligned}
|\Phi_N\rangle &= P^{J=\frac{1}{2}, T=\frac{1}{2}}|\Phi\rangle \\
&= (3q)_N + [(3q)_N \pi]^{J=\frac{1}{2}, T=\frac{1}{2}} + [(3q)_\Delta \pi]^{\frac{1}{2}, \frac{1}{2}} + [(3q)_N \pi\pi]^{\frac{1}{2}, \frac{1}{2}} + \ldots \quad (2)
\end{aligned}$$
$$\begin{aligned}
|\Phi_\Delta\rangle &= P^{J=\frac{3}{2}, T=\frac{3}{2}}|\Phi\rangle \\
&= (3q)_\Delta + [(3q)_N \pi]^{J=\frac{3}{2}, T=\frac{3}{2}} + [(3q)_\Delta \pi]^{\frac{3}{2}, \frac{3}{2}} + [(3q)_N \pi\pi]^{\frac{3}{2}, \frac{3}{2}} + \ldots \quad (3)
\end{aligned}$$

In the Δ channel, the probability of finding one or more pions is higher than in the N channel; as a consequence the Δ lies higher then the nucleon. In the simplified model we obtain $E_\Delta - E_N = 84$ MeV and 126 MeV for $g = 4.3$ and 5 respectively; including meson self interaction and performing self-consistent calculation increases the splitting by some 40 MeV. Hence, the ΔN splitting due to pions is only roughly one half of the experimental one; an additional hyperfine interaction is needed to bring $E_\Delta - E_N$ to the experimental value (293 MeV). In our simple model we therefore introduce a *phenomenological* form of the interaction:

$$H' = \varepsilon P_{(3q)_\Delta} \tag{4}$$

where $P_{(3q)_\Delta}$ is the projector onto components containing 3 quarks coupled to Δ quantum numbers. Using $\varepsilon = 262$ MeV and 235 MeV for $g = 4.3$ and 5 respectively, increases the splitting to the desired value.

3   The Kohn variational principle for the phase shift

The ansatz for the Δ resonance is taken in the form

$$|\Psi_\Delta\rangle = c\,|\Phi_\Delta\rangle + \int dk\,\eta(k_0, k) \left[a^\dagger_{mt}(k)|\Phi_N\rangle \right]^{J=\frac{3}{2}, T=\frac{3}{2}}$$

where $a^\dagger_{mt}(k)$ creates a p-wave pion, m, t are the third components of its spin and isospin, k_0 denotes the pion momentum, while $|\Phi_N\rangle$ and $|\Phi_\Delta\rangle$ correspond to the nucleon and the Δ bound states ((2) and (3)), respectively. Asymptotically, the pion state behaves as

$$\eta(k_0, r) = k_0 j_1(k_0 r) - \tan\delta \, k_0 y_1(k_0 r) \ , \quad r \to \infty \ .$$

Here we use standing waves to describe the pion rather than outgoing (and incoming) waves. In k-space this leads to

$$\eta(k_0, k) = \sqrt{\frac{\pi}{2}}\, \delta(k - k_0) + \frac{\chi(k_0, k)}{\omega_k - \omega_0}\ , \quad \tan\delta = \sqrt{2\pi}\,\frac{\omega_0}{k_0}\,\chi(k_0, k_0)$$

The variational principle requires that the Kohn functional[2]

$$\mathcal{F}_K = \tan\delta - \frac{2\omega_0}{k_0\langle\Phi_N|\Phi_N\rangle}\,\langle\Psi_\Delta|H - E|\Psi_\Delta\rangle$$

remains stationary with respect to variation of c and $\chi(k_0, k)$, as well as to variation of the intrinsic pion profile in $|\Psi_\Delta\rangle$.

In the above form only one channel is assumed; if more than one channel is open, $\tan\delta$ is replaced by the K matrix.

Typical results for the phase shift are displayed in Fig. 1 and compared to the experimental values. By varying ε it is possible to reproduce the experimental position of the resonance; using $g = 4.3$ ($\varepsilon = 273$ MeV) the width (i.e. the slope of the curve) is well reproduced while for $g = 5$ ($\varepsilon = 252$ MeV) the width is too large. These results are obtain by optimizing $|\Psi_\Delta\rangle$; if we do not vary the intrinsic pion profile but take it over from the bound state calculation the results change only very slightly provided the value of ε is changed by a few MeV. Hence, the properties of the Δ do not change significantly when the decay channel is open; the main effect is that the energy drops by some 10 MeV (10 MeV for $g = 4.3$ and 13 MeV for $g = 5$).

4   The Analytic Continuation in Coupling Constant

Consider the scattering of a non-relativistic particle on an attractive potential $V(r)$ which possesses a quasi bound state in the continuum. Introduce a parameter (coupling constant) λ:

$$H = H_{kin} + \lambda V(r)\ .$$

For sufficiently large λ, $\lambda > 1$ the state becomes bound. Let's denote the threshold value as λ_{th}. The method [3] is based on the fact that it much easier to solve the bound state problem than the continuum case. It consists of the following steps:

- Determine λ_{th} and calculate E as a function of λ for $\lambda > \lambda_{th}$.
- Introduce a variable $x = \sqrt{\lambda - \lambda_{th}}$; calculate $k(x) = i\sqrt{-2mE}$ in the bound state region.
- Fit $k(x)$ by a polynomial:

$$k(x) = i(c_0 + c_1 x + c_2 x^2 + \ldots + c_{2M} x^{2M})\ .$$

- Construct a Padé approximant:

$$k(x) = i\,\frac{a_0 + a_1 x + \ldots + a_M x^M}{1 + b_1 x + \ldots + b_M x^M}\ . \tag{5}$$
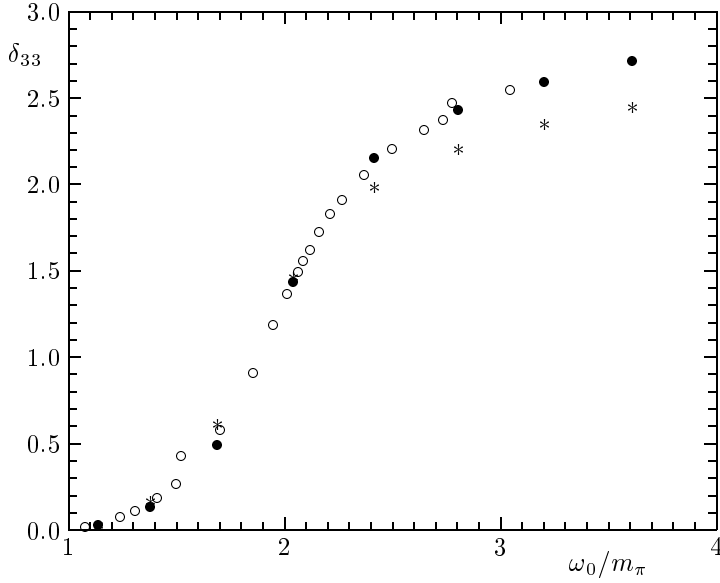
Fig. 1. The phase shift in the P33 channel: ○ are the experimental values, • values from the variational calculation using $g = 4.3$ and $\varepsilon = 273$ MeV, and * those for $g = 5$ and $\varepsilon = 253$ MeV.

- Analytically continue $k(x)$ to the region $\lambda < \lambda_{th}$ (i.e. to imaginary x) where $k(x)$ becomes complex.
- Determine the position and the width of the resonance as analytic continuation in λ:

$$E_r = \frac{1}{2m} \operatorname{Re} \operatorname{cont}_{\lambda \to 1} k^2 , \qquad \Gamma = -2 \frac{1}{2m} \operatorname{Im} \operatorname{cont}_{\lambda \to 1} k^2 . \qquad (6)$$

This method does not provide only the position and the width of the resonance; the matrix element of an operator $\mathcal{O}$ between the resonant state $|\Psi_r\rangle$ and a bound state $|\Phi\rangle$ can be calculated as

$$\langle \Psi_r | \mathcal{O} | \Phi \rangle = \operatorname{cont}_{\lambda \to 1} \langle \Psi_b(\lambda) | \mathcal{O} | \Phi \rangle .$$

In our implementation of the method, we relate the coupling constant λ to the parameter of the phenomenological hyperfine interaction:

$$\lambda V(r) \to \varepsilon P_{(3q)_\Delta} , \qquad x = \sqrt{\varepsilon_{th} - \varepsilon} \qquad (7)$$

where ε_{th} is the value of ε at the threshold: $E_\Delta(\varepsilon_{th}) - E_N = m_\pi$. For sufficiently high ε, the real part of the energy eventually reaches the experimental position of the resonance; this value of ε then corresponds to $\lambda = 1$ of the original formulation of the method.

In our very preliminary calculation we treat the pion non-relativistically. For $\varepsilon < \varepsilon_{th}$ we calculate

$$k(x) = i\sqrt{2m_\pi(E_{th} - E)}, \quad E = E_\Delta(x) - E_N ,$$

fit $k(x)$ using a Padé approximant (5) and continue $k(x)$ to the resonance region. The energy difference, $E_\Delta - E_N$, and the width of the resonance are then obtained by (6). The 'physical value' of x (and ε from (7)) is determined as $\mathrm{Re}E (= E_\Delta - E_N)$ reaches the experimental value 293 MeV. The corresponding value of $\mathrm{Im}E (= \Gamma)$ then predicts the width of Δ and is to be compared with the experimental value ~ 120 MeV.

Fig. 2 shows the behaviour of $E_\Delta - E_N$ and Γ as functions of x for two vales of g. For higher order of the Padé approximant, $M \geq 3$, the method becomes numerically instable and the determination of E and Γ is no more reliable. For $g = 4.3$ and $M = 1$ and 2, the experimental splitting is reached for $x^2 \approx 230$ MeV (and corresponding $\varepsilon = 300$ MeV). This yields $\Gamma \approx 60$ MeV which is only half of the experimental value, most probably due to the non-relativistic treatment. For $g = 5$ the value of Γ is larger (in accordance with Fig. 1) but its determination is less reliable.

In order to be able predict reliable results it is necessary formulate the approach relativistically and to understand the origin of numerical instabilities for higher M.
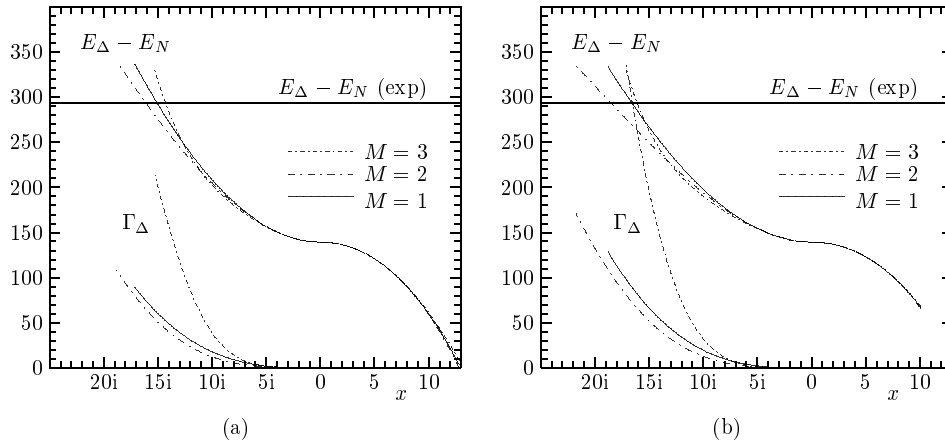
Fig. 2. ΔN splitting and Δ width (in MeV) as functions of x (in units $\sqrt{\mathrm{MeV}}$) for $g = 4.3$ (a), and $g = 5$ (b).

References

1. B. Golli and M. Rosina, Phys. Lett. B 165 (1985) 347; M. C. Birse, Phys. Rev. D 33 (1986) 1934.
2. B. Golli, M. Rosina, J. da Providência, Nucl. Phys. **A436** (1985) 733
3. V.M. Krasnopolsky and V.I.Kukulin, *Phys. Lett*, **69A** (1978) 251, V.M. Krasnopolsky and V.I.Kukulin, *Phys. Lett*, **96B** (1980) 4, N. Tanaka et al. *Phys. Rev.* **C59** (1999) 1391

Will dimesons discriminate between meson-exchange and gluon-exchange effective quark-quark interaction?

Damjan Janc and Mitja Rosina[*]

Faculty of Mathematics and Physics, University of Ljubljana, Jadranska 19, P.O. Box 2964, 1001 Ljubljana, Slovenia, and J. Stefan Institute, Ljubljana, Slovenia

Abstract. A phenomenological estimate is derived such that the binding energies of heavy dimesons are expressed as combinations of masses of different mesons and baryons. We get $\bar{b}\bar{b}qq$ (I=0, J=1) bound by about 100 MeV and $\bar{c}\bar{c}qq$ unbound. The result is almost model independent and should come out similar in any model which reproduces Λ_b and Λ_c correctly. Therefore it does not discriminate between meson-exchange and gluon-exchange interaction of the two light quarks.

1   Introduction

The constituent quark model has been rather successful in describing the properties of individual hadrons [1–3]. The extrapolation to two-hadron systems is, however, still rather uncertain. Much can be learned by studying heavy two-meson systems which decay only weakly. Although difficult to detect because of a low production cross section, they are interesting theoretically, to confront different models. The detailed calculations in the literature [4,5] rely on particular quark models, therefore we attempt an almost model-independent phenomenological estimate.

Our estimate of the binding energy [6] is based on the assumption that the wave functions of the two light quarks around the heavy quark in Λ_c, Λ_b and around the antidiquark in the $\bar{c}\bar{c}qq$ and $\bar{b}\bar{b}qq$ dimesons are very similar. This assumption implies that the heavy antidiquark in a colour triplet state acts just like a very heavy quark and that the $1/m$ corrections are neglected [7]. We show by means of a detailed calculation [8,6] that the deviations from both assumptions lead only to minor corrections.

2   The phenomenological relation for the binding energy of dimesons

We call the u and d quarks q and the dimesons (tetraquarks) $(\bar{b}\bar{b}qq) = T_{bb}$, $(\bar{c}\bar{c}qq) = T_{cc}$. The masses of particles are denoted just by their names, and the tilde denotes a hyperfine average (e.g. $\tilde{D} = \frac{1}{4}D + \frac{3}{4}D^*$).

---

[*] E-mail: mitja.rosina@ijs.si

The binding energies $E_{b\bar{b}}$ of a quark and antiquark in a meson is a function of the reduced mass only, e.g. $\Upsilon = b + b + E_{b\bar{b}}$, $E_{b\bar{b}} = F(m = b/2)$. For the diquark bb the Schrödinger equation is similar as for the $b\bar{b}$ meson with twice weaker interaction

$$\left[\frac{p^2}{2(b/2)} + V_{bb}\right]\psi = \frac{1}{2}\left[\frac{p^2}{2(b/4)} + V_{b\bar{b}}\right]\psi = E_{bb}\psi, \qquad E_{bb} = \frac{1}{2}F(b/4).$$

Now we compare the following hadrons (and analogous for charm)

$$T_{bb} = 2b + 2q + E_{bb} + E_{qqQ}, \qquad \Upsilon = 2b + E_{b\bar{b}}, \qquad \Lambda_b = b + 2q + E_{qqQ},$$

where $E_{qqQ} \approx E_{qq(\bar{b}\bar{b})} \approx E_{qqb}$ is the potential plus kinetic energy contribution of the two light quarks in the field of a "heavy quark". We obtain the phenomenological relations

$$T_{bb} = \Lambda_b + \tfrac{1}{2}\Upsilon + \delta E_{bb}, \qquad \delta E_{bb} = \tfrac{1}{2}[F(b/4) - F(b/2)].$$

$$T_{cc} = \Lambda_c + \tfrac{1}{2}J/\psi + \delta E_{cc}, \qquad \delta E_{cc} = \tfrac{1}{2}[F(c/4) - F(c/2)].$$

The binding of the $(I = 0, J = 1)$ dimesons is expressed with respect to the corresponding thresholds

$$\triangle T_{bb} = \Lambda_b + \tfrac{1}{2}\Upsilon - B - B^* + \delta E_{bb} = -250\,\text{MeV} + \delta E_{bb},$$
$$\triangle T_{cc} = \Lambda_c + \tfrac{1}{2}J/\psi - D - D^* + \delta E_{cc} = -42\,\text{MeV} + \delta E_{cc}.$$

Now comes an important idea how to obtain phenomenologically the "corrections" δE. In Fig.(2) we interpolate between the phenomenological binding energies obtained from experimental meson masses and from a popular sets of quark masses [9], (b=5259 MeV, c=1870 MeV, s=600 MeV). The tilde denotes hyperfine averages between 0^- and 1^- states.

$$\tfrac{1}{2}F(\tfrac{1}{4}b) = -407\,\text{MeV}, \qquad \delta E_{bb} = +122\,\text{MeV}, \qquad \triangle T_{bb} = -128\,\text{MeV}$$

$$\tfrac{1}{2}F(\tfrac{1}{4}c) \approx -197\,\text{MeV}, \qquad \delta E_{cc} = +139\,\text{MeV}, \qquad \triangle T_{cc} = +97\,\text{MeV}.$$

These values are very close to the result $\triangle T_{bb} = -131\,\text{MeV}$ (and T_{cc} unbound) of a detailed 4-body calculation [4].

Now we make several corrections to our assumptions and approximations, based on detailed calculations [8,6].

Table 1. Corrections to the binding energy of $T_{bb} = BB^*$

Spin-spin interaction	+5 MeV
Centre-of-mass motion	-15 MeV
Finite size of $\bar{b}\bar{b}$	+18 MeV
Mixing of colour (6)–(6) configurations	-25 MeV
Total:	-17 MeV
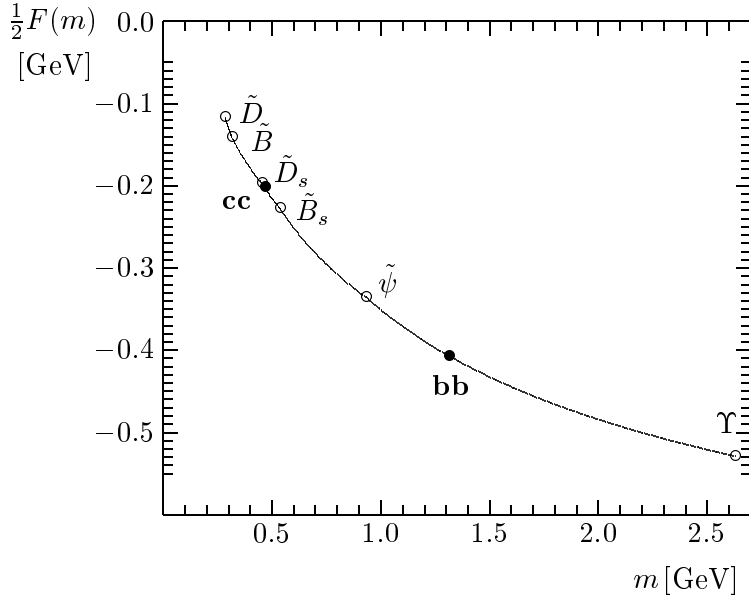
We have also performed a search for a two-cluster configuration ("molecule" BB*). At short distance, the colour triplet configurations give a Coulomb-like attraction while the colour sextet configurations give repulsion. At intermediate distances one can gain energy with a strong mixing between triplet and sextet configurations. Detailed calculations [8] with the Born-Oppenheimer wave function (Resonating Group Method) gave no bound states with a two-cluster ("molecular" or "covalent") structure.

3   Conclusion

It has been hypothesized that the binding energy of heavy dimesons $B + B^*$ and $D + D^*$ might discriminate between constituent quark models using gluon-exchange or meson-exchange spin-spin interaction, or both. It was expected that models with meson-exchange interaction would give an additional strong attraction when the two light quarks meet in I+S=0 state.

The argument was wrong. The two light quarks in the dimesons feel the heavy antidiquark similarly as they feel the heavy quark in Λ_b and Λ_c baryons. Any interaction (OGE, OGBE or combination of both) which fits Λ_b and Λ_c will give similar results for dimeson binding energy and one cannot discriminate. Calculations which simply added OGBE to OGE gave strong binding of dimesons, but were irrelevant since they would overbind heavy baryons.

References

1. Silvestre-Brac, B., Gignoux, C.: Phys. Rev. **D32**, 743 (1985); Richard, J.M.: Phys. Rep. **212**, 1 (1992)
2. Silvestre-Brac, B.: Few-Body Systems **20**, 1 (1996)
3. Glozman, L.Ya., Papp, Z., Plessas, W.: Phys. Lett **B 381**, 311 (1996)
4. Silvestre-Brac, B., Semay, C.: Z. Phys. **C57**, 273 (1993); **C59**, 457 (1993)
5. Brink D. M., Stancu, Fl.: Phys. Rev. **D57**, 6778 (1998)
6. Janc, D., Rosina, M.: preprint hep-ph/0007024 v2, 5 Jul 2000
7. Lichtenberg, D.B., Roncaglia, R., Predazzi, E.: J. Phys. G **23**, 865 (1997)
8. Janc, D.: Diploma Thesis, University of Ljubljana, Ljubljana 1999
9. Bhaduri, R.K., Cohler, L.E., Nogami, Y.: Nuovo Cim. **A65**,376 (1981)